ADDIS ABABA UNIVERSITY
SCHOOL OF GRADUATES STUDIES
PHYICS DEPARTMENT

TROPICAL OCEANS THERMODYNAMIC AND ATMOSPHERIC MODULATIONS OVER SOUTHERN ETHIOPIAN CLIMATE, WATER RESOURCE AND VEGETATION VARIABILITY

BY
MESFIN TADEWOS

A THESIS SUBMITTED TO THE GRADUATE STUDIES ADDIS ABABA UNIVERSITY IN PARTIAL FULFILLMENTOF THE REQUIREMENTS FOR THE DEGREE OF MASTER OF SCIENCE IN PHYSICS DEPARTMENT

ADVISOR: ABEBE YESHANEW (PHD)
CO-ADVISOR: GIZAW MENGISTU (PHD)

ADDIS ABABA UNIVERSITY
AUGUST 2007

Addis Ababa University
Faculty of Science
Department of Physics

The undersigned hereby certify that they have read and recommended to the Faculty of science school of Graduate studies for acceptance a thesis entitled “Tropical Oceans thermodynamic and atmospheric modulation over southern Ethiopia climate, water resource and vegetation variability” by Mesfin Tadewos in partial fulfillment of the requirements for the degree of Master of Science in Physics.

Name	**Signature**
Dr. Abebe Yeshanew, Advisor	_____
Dr. Gizaw Mengistu, Co-Advisor	_____
Dr. Dagnachew Legess,Examiner	_____
Dr. Esayas Belay, Examiner	_____

Acknowledgment

First and for most, I would like to thank, Almighty God, who has helped me in everything. I did and do .No achievement in life without God could be true. Besides I owe any measure of success to the array of input from so many. And any endeavor of this kind could be successful only when it is accomplished by the good will and cooperation of many individuals. Of these, Dr.Abebe Yeshanew, my talented and excellent advisor whose relentless pursuit of and patience with me during preparation and delivery of this thesis was a tremendous source of motivation and encouragement. To my co-advisor, Dr. Gezaw Mengistu .I am greatly grateful for his great deal of help during this painstaking research. To my wife, parents, brothers and sisters for their unwavering support. To Michael Bell, from NOAA research center, who allowed me the privilege of sharing NDVI data in this research.

My thanks and gratitude goes to workers of water resource authority for helping me in providing information regarding to hydrology that enabled me to pursue my thesis. To Towers consult, Ato Dawit Tadewos and his staff who have helped me tremendously for the accomplishment of the thesis. I thank at last but by no means least, Ato Melaku Delelegne, the General Manager of Vision Academy and staff members for their support and continuous encouragement.

To Lord Jesus Christ

Table of contents

Chapter One Introduction

1.1 General Introduction ……..…….1

1.2 The current scientific gaps in the area…….1

1.3 Statement of the problem……..2

1.4 Contribution of the study……..3

1.5 Objective of the Study……..……3

Chapter Two Background and Literature Review

2.1Structures of Ocean……...4

2.1.1 Ocean Density profile …….4

2.1.2 Ocean Temperature profile……..……5

2.1.2.1 Sea Surface Temperature ……..5

2.1.2.2 Heat Content ……11

2.1.4 Ocean Circulation……..……...13

2.1.5 Oceans and climate system……...14

2.1.6 Tropical oceans sea surface temperature and climate variability……...14

2.1.6.1 Tropical Indian Ocean and climate variability…….15

2.1.6.2 Tropical Pacific Ocean and climate variability……20

2.1.6.3 Tropical Atlantic Ocean and climate variability……..26

2.2 Atmospheric Circulation ……....29

2.2.1. Hadley Cell…….……29

2.2.2 Walker Circulation …… …….30

2.3 Description of Ethiopia and its Rivers …….....31

2.3.1. Rivers Basins of Ethiopia…… 31

2.3.2. Rainfall Regimes of Ethiopia…… 31

2.3.3. Atmospheric Dynamic over Ethiopia ……..……..……33

Chapter Three Data and Methods

3.1 Data…….……...34
3.1.1 Ocean Data…….……34
3.1.2 Climate Data…….……..35
3.1.3 Normalized Difference Vegetation Index Data……..35
3.1.4 Hydrological Data…….……..36
3.2 Methods…….……36
3.2.1 Singular Value Decomposition……..36
3.2.2 Correlation…….……38
3.2.3 Regression…….39
3.2.4 Atmospheric Analysis…….……...39

Chapter Four Results and Discussion

4.1 Space-time modes of physical variability……....42
4.1.1 Tropical oceans sea surface temperature modes …….42
4.1.2 Tropical Oceans heat content modes …….……49
4.2 Ethiopian Rainfall modes…….……...55
4.3 Ethiopian Vegetation modes …….……..57

4.4. Association between Tropical Oceans and Ethiopian climate, hydrology and vegetation …… 59
4.5 Contributions of Tropical Oceans to Climate hydrology and NDVI variability …71
4.6 Atmospheric dynamics and Tropical oceans modulation to Ethiopian climate, hydrology and vegetation…….80

Chapter Five Conclusions and Recommendation

5.1Conclusions of the study……94
5.2 Recommendation ……..…96

References……..97

List of Acronyms

1. SSA Sub-Saharan Africa (SSA)
2. GHA Greater Horn of Africa (GHA)
3. IRI International Research Institute for climate System
4. SST Sea Surface Temperature
5. ITCZ Inter Tropical Convergence Zone
6. ENSO El Nino/Southern Oscillation
7. NMA National Metrological Agency
8. DPPC Disaster Prevention and Preparedness Commission
9. ENA Ethiopian News Agency
10. NOAA National Oceanic and Atmospheric Administration
11. SNNPR Southern Nation Nationality People Region
12. AVHRR The advanced Very High Resolution Radiometers
13. ATSR Along Track Scanning Radiometers
14. NWR National Water Resource
15. IOD Indian Ocean Dipole
16. IOZM Indian Ocean Zonal Mode
17. FRGC Frontier Research Center for Global Change
18. TOGA Tropical Ocean-Global Atmosphere
19. WCRP World Climate Research Program
20. NDVI Normalized Difference Vegetation Indices
21. OLR Outgoing Long wave Radiation
22. ERBE Earth Radiation Budget Experiment
23. TOA Top of the Atmosphere

Abstract

Singular value decomposition, correlation and composite analyses were used to investigate the tropical oceans thermodynamic and atmospheric modulations over the southern Ethiopian climate, water resource and vegetation variability. Significant association is found between them using the 50 years ocean and climate dataset from 1951 to 2000 and vegetation data that range from 1981 to 2000.Both climate and vegetation dataset are obtained from international centers. River discharge flow and water level dataset are obtained from the Ethiopian Water Resource. The study reveals the strong association between Tropical oceans thermodynamic and atmospheric circulation and climate, hydrology and vegetation over Southern Ethiopia. The tropical oceans sea surface temperature anomalies contribute 50% to the short rain season (SON) of rainfall over Ethiopia but a very small contribution to the long rain season (MAM) of the rainfall variability over the area. These tropical oceans also have contributions for the vegetation variability to 51.6% during the SON and 44.8% during the MAM seasons and for the water level variability to a 53% and 58% during the short and long rainfall seasons of the southern Ethiopia, respectively. The Tropical oceans heat content contributions also revealed with its 85.6% during the September through December season but with a very small contribution during the March through May season. The wet minus dry composite patterns of sea surface temperature and atmospheric analyses explain during the regional and global atmospheric dynamics together with the Tropical oceans modulation cause the climate, hydrology and vegetation variability. The correlation explains that tropical Indian Ocean is strongly correlated with the short rains of Ethiopia having a 99% confidence level and r=0.640 correlation coefficient. A 90-99% confidence level association except the MAM season is demonstrated by the Atlantic ocean and also the tropical pacific ocean is seen correlated more strongly than the other tropical oceans, particularly the December through February SST anomaly has a strong association with the short rains over Ethiopia.

Chapter One

Introduction

1.1 General Introduction

Two very thin skins of fluid cover the surface of our planet: a low density layer consisting mainly gases (Our atmosphere), and a higher density layer consisting mainly of water (Our oceans).However, the two layers are completely distinct, exchanges of water, gases, particulate matter, heat and momentum are continually taking place across the interface between them. These exchanges have a profound effect on the development of our weather system, and in the long term, the progress of climate variability changes. The role of the Ocean in the climate variability results from its large capacity to store and distribution heat. While the ocean is 4000-m deep on average, the upper 10m has the same as the entire atmosphere and the upper 4-m has a similar to store heat. Although the atmosphere drives the ocean, the atmosphere can also respond to ocean surface condition, particularly sea surface temperature (SST). Direct thermal circulation in which most air rises over warm SSTs and descends over cool SSTs is most prevalent in the tropics. The resulting atmosphere circulation cells influence the pattern of form the Ocean. Thus, the ocean and atmosphere form a coupled system, where sometimes it is difficult to distinguish forcing from response .Because water has a heat capacity and density nearly three orders of magnitude larger than air, the Ocean has thermal and mechanical inertia relation to the atmosphere. The Ocean thus acts as a memory for the coupled-atmosphere system (Bigg, Jickells, Liss and Osborn, 2003; Latif et al 2000).

Tropical Oceans play major roles in the natural variability of the world climate. Anomalous coupled ocean-atmosphere phenomena generated in the tropical oceans produce global atmosphere and oceanic circulation changes that influence regional climate conditions even in remote regions. On the inter annual time scale, the El Niño/Southern Oscillation (ENSO) of the tropical pacific ocean, the Indian ocean Dipole (IOD) and so on are typical examples of such phenomena (Yamagata, Behera, Luo, Masson, Jury, and Rao, 2004; Indejeetal.,2000; Philander,1990; Latif and Dommenget,1999; Webster, Moore, Loshnigg , Leben and Black,(2003)

1.2 The current scientific gaps in the area

The interplay of tropical ocean modulation to southern Ethiopian resources is not documented in scientific journal and literatures. This research bridges the exiting scientific gaps for the first time. It addresses how the global and regional tropical oceans modulate the climate, water and

vegetations in the area in points. It further documents space-time mode of variability of these resource within this area.

1.3 Statement of the problem

Widespread poverty and the dependence of much of the population on rain-fed agriculture make East Africa particularly vulnerable to the effects of climate variability (Black, 2003). Climate variability is the crucial factor to many African countries including Ethiopia and has a major impact on sensitive activities like agriculture water resource, hydroelectric power supply among many others (Yeshanew and Jury, 2006; Anyah and Semazzi, 2005; Ogallo, 1988; Nicholson, 1996; Indeje et al, 2000; Saji et al, 1999; Goddard and Graham, 1999; among others). More than 88% of Ethiopia's 60 million people are engaged in agricultural and pastoral activities for their walks of life and Ethiopia depends on rain fed agriculture with limited use of irrigation. Climatic factors such as droughts or floods significantly impact agricultural out put. Drought is the dominant climate-related disaster in Ethiopia. Droughts in Ethiopia have killed many people and animals in 1957-58, 1964-65, 1972-73 and 1983-84.Though not as pronounced as drought in their impact and publicity, floods and fires have increasingly caused disasters in Ethiopia (Wolde-Georgis, 1997). This makes Ethiopia vulnerable to climate variability.

Fig.1.1. The two impacts of extremes of climate variability, drought (above) and Flood (below) (Image: there and Mutai, 2002: DMCN)

1.4 Contribution of the study

On the basis of the above knowledge, this research ventures to unlock the modes of sea surface temperature and heat content variability of tropical oceans towards the deeper and improved understanding and linking to southern Ethiopian climate, water (including lake levels) and Vegetation distributions.

This research brings a lot of contribution to a better understanding of the events that are common in Ethiopia such as drought and flood. In addition, it aims to identify the important elements that are used to develop prediction scheme that reduces the impacts of extremes on human life, property, and economy in the coming new Ethiopian millennium.

The society at large, environmental, hydrological and atmospheric institutes like hydroelectric power station, water resource, and grain marketing research among others will be benefited from the research. The appropriate use of the result obtained from the research findings will alleviate the impacts of extreme variability such as drought and flood in the area in point.

1.5 Objective of the study

The central objective of this study is to understand the modulations of tropical oceans thermal variability and atmospheric circulation on southern Ethiopia climate, hydrology and vegetation variability. In order to do this, first the special-temporal modes of variability of tropical oceans in space and time will be unraveled in terms of the thermodynamic parameters such as sea surface temperature (SST) and heat content. Secondly, the association of the sea surface temperature (SST) and heat content of the oceans with the variability of climate and hydrology on the southern part of Ethiopian climate/hydrology will be uncovered using simple correlation and regression methods. Thirdly, the tropical atmospheric circulation role in the variability of southern Ethiopia climate, hydrology and vegetation will be revealed.

The paper has six sections. A brief description of theoretical background and review literature is brought in section 2.Data and methods of analysis are given in section 3.Results and discussions are presented in section 4 and 5 while summary and conclusions are given in section 6.

Chapter Two

Background and Literature Review

2.1 Structures of Ocean

Oceans are saline waters that cover almost three quarters (71%) of the surface of the Earth. The area of the oceans is 361 million sq. km., and nearly half of the world's marine waters are over 3,000 meters (9,800 ft) deep. The average salinity of the Earth's oceans is around 35 parts per thousand (ppt), and nearly all seawater falls in the range of 31 to 38 ppt.

2.1.1 Ocean density profile

The ocean waters can be divided into three layers, depending on their densities. Less dense waters form a top layer called the **surface mixed zone**. The temperature and salinity of this layer can change often because it is in direct contact with the air. For example, water evaporation could cause an increase in salinity, and a cold front could cause a drop in temperature. The next layer is the **pycnocline**, or transition zone. The density here does not change very much. This transition zone is a barrier between the surface zone and a bottom layer, allowing little water movement between the two zones. The bottom layer is the **deep zone**, where the water remains cold and dense. The Polar Regions are the only places where deep waters are ever exposed to the atmosphere because the pycnocline is not always present.

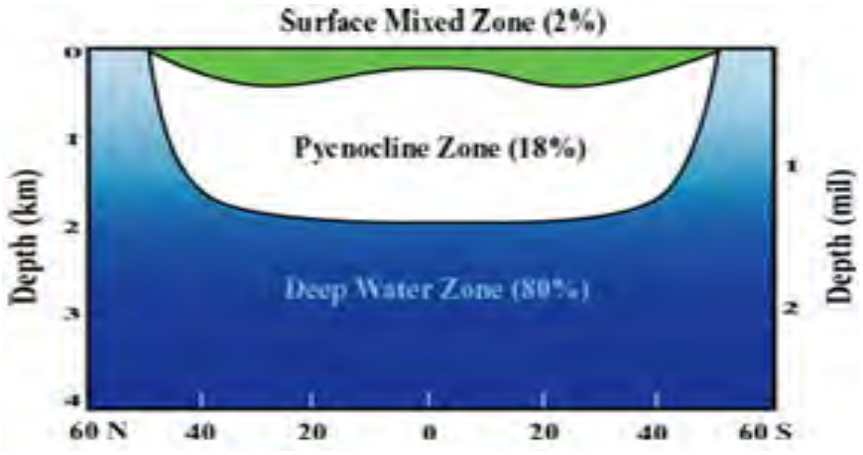

Fig 2.1 Layers of water depending on densities (http://www.onr.navy.mil/Focus/ocean/water/density1.htm)

2.1.2 Ocean Temperature profile

The ocean can be divided into three vertical zones, depending on temperature. The top layer is the **surface layer**, or mixed layer. This layer is the most easily influenced with solar energy (the sun's heat), wind and rain. The next layer is the **thermocline**. Here the water temperature drops as the depth increases. The last layer is the **deep-water layer**. Water temperature in this zone decreases slowly as depth increases. Water temperature in the deepest parts of the ocean is averages about 36°F (2°C).

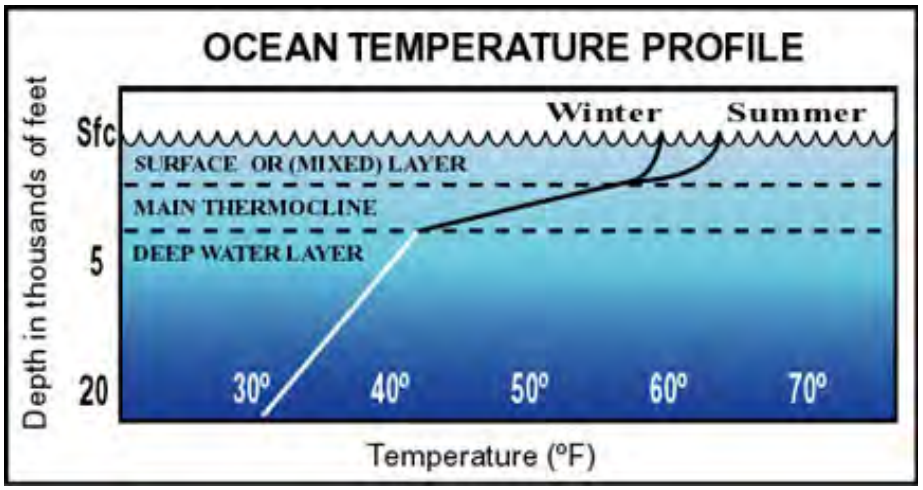

Fig 2.2 Ocean temperature profile (http://www.onr.navy.mil/Focus/cybermail/mailCheck.htm)

2.1.2.1 Sea Surface Temperature (SST)

The temperature structure of the upper ocean is quite complex and depends on various processes acting at the surface and on the first meters of water column. The air-sea interface is affected by process responsible for the heat transfer between the ocean and the atmosphere: the net long wave radiation, the heat convection between the air and the sea and the heating or cooling due to moisture transfer. With in the ocean, the heat is redistributed by molecular diffusivity and tabulated diffusivity. The heating related to the light absorption is another process modifying temperature of warm column. All this processes acting at different depths and depth ranges complicate the definition of the Sea Surface temperature (SST) and the inter comparison with different instruments and models. Every SST observation depends on the measurement technique and sensor that is used, the vertical position of the measurement with in the water column, the local history of all component heat flux conditions, and the time of day the measurement was obtained (Donlon, 2002).

The general definition of sea surface temperature (SST) is that it is the water temperature at the surface (or at 1meter below the sea surface).However, the exacting meaning of 'surface' will vary according to the measurement method used because different things are actually being measured.

2.1.2.1.1. Vertical structure of SST

The vertical structure of SST can be generally classified as follows:

a. The interface SST, SST_{int}

The *interface SST, SST_{int}* is the temperature of an infinitely thin layer at the exact air-sea interface. It represents the temperature at the top of the SST_{skin} layer (and hence the top of the temperature gradient in that layer) and cannot be measured using current technology.

b. The skin SST, SST_{skin}

The *skin SST, $SST_{skin,}$* is a temperature measured by a radiometer at depth. Within a thin layer (~500μm) at the water side of the air-sea interface where conductive and diffusive heat transfer process dominate (where the molecular diffusion and heat conductivity dominate).

The temperature gradient within this layer is given by the ocean atmospheric heat fluxes. The skin temperature is measured by radiometers operating in the spectral region of 3.7 to 12μm (thermal infrared).

The advanced Very High Resolution Radiometers (AVHRR) and Along Track Scanning Radiometers (ATSR) are sensors measuring in the thermal infrared (Wick, 2002). The signal of these sensors potential is approximately 10μm into the water column.

A short temperature gradient characteristically maintained in this thin layer shows SST_{skin} varies according to depth within the layer and because the penetration depth of the emitted radiation is a function of the wave length of the radiation, the value of SST_{skin} varies dependant on the wavelength used to for measurement. This is the basis of measuring the skin temperature gradient using infrared interferometer at wave lengths shorter than 5μm. Consequently, SST_{skin} should always be quoted at specific wavelengths in the water column, for example, $SST_{skin10.5\mu m}$. However, over the parts of the infrared spectrum used to make the measurements of SST_{skin} presented in this study, the variation in penetration depth is very small, and the values of SST_{skin} measured by ideal infrared radiometers and expected to vary by less than 0.01k, and wavelength dependence of $SST_{skin\ can}$ be ignored.

c. The sub-skin SST, $SST_{subskin}$

The *sub_{skin} SST, $SST_{subskin}$* represents the temperature at the base of the skin layer. Beyond the skin layer, the temperature is affected by turbulent mixing and insolation. It varies on a

time scale of minutes and may be influenced by solar warming. Its depth of the sub-skin is of the order of 1mm.Sensor working a low frequency (6-10GHz) with microwave measure the sub-skin SST.

d. The bulk SST or SST_{depth}

The bulk SST or SST_{depth} is the temperature of the water column under the skin layer at a depth completely immersed in the turbulent ocean. This temperature is observed by in situ buoys, CTD and XBT measurements.

e. The constant temperature layer SST, SST_{CTL}

The *constant temperature layer SST, SST_{CTL}* is the sea temperature at a depth where the temperature is not significantly affected by the solar radiation. The diurnal variations are less than 0.2^0c .The effective position of this constant temperature layer can therefore vary from one location to another.

2.1.2.1.2. Sea temperature with the time and space

Since the solar radiation is an important process, the night heat distribution in the upper ocean is different from the day temperature profile. Due to this time and space variation, the SST should be given as a temperature measurement at a specified depth and ideally at a time of day. Several satellite swaths have been combined by taking the maximum temperature. Also day time images have been used, which reduces the information for the subsurface layers. The sea surface temperature was assimilated at 14:00 GMT. The model sea surface temperature reaches its maximum on this diurnal cycle at this time.

The initial resolution of the SST is 1km.Despite the load of the SST is linear with respect to the number of observations; there is no interest to assimilate this huge resolution temperature in the coarse resolution model. The resolution was degraded to 10km where the high resolution information in the SST is not expected to have a significant impact on the Ligurian sea model. The SST data is therefore split into a 1km resolution SST covering mainly the provinçial-basis and a 10km resolution SST of the rest of the Mediterranean.

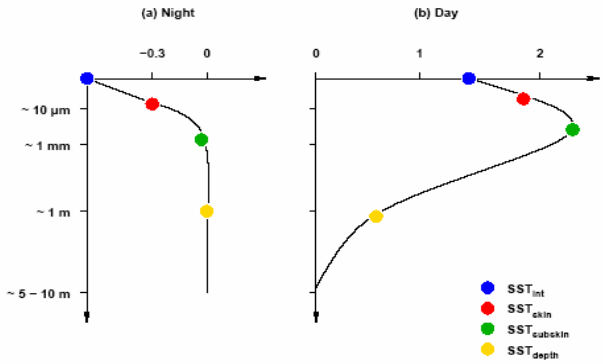

Fig 2.3 The difference between the pre-dawn temperature at 1-5m depths and temperature at varies depths during night (a) and during day (b).Adapted from Donlon(2002)

2.1.2.1.3 Techniques for Measuring SST

a. Earliest Technique

A thermometer was dipped into a bucket of water manually drawn from the sea surface.

b. First automated technique

This was done by measuring the temperature of water intake port of large ships. This is not always consistent. The depth of the water intake as well as exactly where the temperature is taken can vary from vessel to vessel.

c. Fixed buoys

A thermometer attached to a moored or drifting buoy in the ocean would measure the temperature as a specific depth (example the top 1m below the sea surface).It is the most exact and repeatable measurements and the depth of water temperature is exactly 1m.

d. Satellite

Since 1980s satellites have been increasingly utilized to measure SST and have provided an enormous leap in our ability to view the spatial and temporal variation in SST. A satellite infrared radiometer measure the temperature of a very thin layer (about 10micrometer,thick)or skin of the ocean(leading to the phrase skin temperature)representing the top millimeter.

Satellite measurements of SST are far more consistent and in some cases, accurate that the in situ temperature measurements described above.

The satellite measurement is made by sensing the ocean in two or more wavelength in the infrared part of the electromagnetic spectrum, which can then be empirically related to SST.

These wavelengths are chosen because they are,

1. With in the peak of the black body radiation expected from the Earth and
2. Able to transmit well through the atmosphere

The satellite measure SST provides both a synoptic view of the ocean and a high frequency of repeat views, allowing the examination of basin-wide upper ocean dynamics not possible ships or buoys. For example, a ship traveling at 10knots (20km/hr) would require 10years to cover the same area a satellite covers in two minutes.

Difficulties with satellite based absolute SST,

1. Because all the radiation emanates from the top “skin” of the ocean, approximately the top 0.01mm or less, it may not represent the bulk temperature of the upper meter of the ocean due primarily to effects of solar surface heating in the day time, and back radiation and sensible heat loss at night as well as from the effects of surface evaporation.

2. The satellite cannot look through clouds creating a fair weather bias in the long term trends of SST. Nonetheless, these difficulties are small compared to the benefits in understanding gained from satellite SST estimates.

2.1.2.1.3 Sea Surface Temperature Determination

In the infrared, the emissivity of the earth's sea and land surface is near unity. As a result, in the absence of cloud or atmospheric attenuation, the brightness temperature observed with a space-borne window radiometer is equal to surface skin temperature. However, cloud and water vapor absorption usually prohibit direct interpretation of the window channel data so that algorithm needs to be applied to the data to alleviate the influence.

The algorithms and instrumental approach have evolved from the use of a single window channel on a polar orbiting satellite to the use of multispectral radiometer observation from both polar orbiting and geostationary satellites.

A sun synchronous polar orbiting satellite passes a given geographical location and similar local times each days, normally shortly afternoon and midnight, to measure SST.In the presence of SST diurnal variation, if clouds at a location tend to appear at one of these times (say afternoon), the climatology will be biased towards the other time (night SST). If clouds tend to appear at both times, the SST climatology must be estimated from other data. If the cloud diurnal variation varies seasonal, say clouds tend to appear in the afternoon in summer but not in winter, the SST will be biased towards the nighttime SST in summer but not in winter.

2.1.2.1.4 Radiative Transfer equation for sea surface temperature

Radiative Transfer equation in 8-13• m and 3-4• m atmospheric windows

Radiative Transfer Theory (RTT) describes interaction between matters and electromagnetic radiation. If there is no influence of the atmosphere and the surface is assumed to be Lambertia, T can be derived by inverting equation

$$T = \frac{C_2}{l \ln[\frac{e(l)C_1}{p l^5 R} + 1]} \qquad (2.1)$$

Spectral radiance R (•, T) emitted at wavelength • (• m) from a non-black body at temperature T (k) is given by the product of spectral emissivity • (•) and plank's radiation function B (•, T):

$$R(l,T) = e(l)B(l) = e(l)\frac{C_1 l^{-5}}{p[\exp(\frac{C_2}{lT}) - 1]} \qquad (2.2)$$

The TOA channel radiances in the two atmospheric windows, *i.e.* W_2 and in W_1 (only for night time), are given by the radiative transfer equation (RTE):

$$L_K^{TOA} = \varepsilon_K \tau_K(\theta) B_K T_S + L_K^{\uparrow}(\theta) + [1-\varepsilon_K]\tau_K(\theta) L_K^{\downarrow} \qquad (2.3)$$

Where $k=i,j,r$; i,j are channels in W_1 (for AVHRR i,$j=4,5,r=3$, L_K^{TOA} is TOA channel radiance, $B_k(T_s)$ is Planck's function for channel radiance, T_s is surface temperature, $L_k^{\uparrow}(\theta)$ is atmospheric upwelling channel radiance (path radiance), θ is satellite zenith angle, $L_k^{\downarrow}$ is down welling atmospheric channel radiance (hemispherical irradiance divided by $\bullet$), τ_k is atmospheric transmissivity, and ε_k is channel surface emissivity.

The first expression in equation (2.3) denotes the surface-emission attenuated along the upward path, the second term represents the path-radiance (atmospheric contribution in upward direction), and the third term constitutes the atmospheric irradiance reflected from the surface and attenuated along the upward path. For daytime measurements in W_1, also, the reflection and scattering of solar irradiance and the diffused downward solar irradiance have to be considered:

$$L_K^{TOA} = \varepsilon_r \tau_r(\theta) B_r T_S + L_r^{\uparrow}(\theta) + [1-\varepsilon_r]\tau_r(\theta) L_r^{\downarrow} + \tau_r(\theta_{sun}) E_{sun}^{TOA} \cos(\theta_{sun}) \frac{1-\varepsilon_r}{\pi} F_r(\theta,\theta_{sun},\phi)\tau_r(\theta) \qquad (2.4)$$
$$+ \tau_r(\theta,\theta_{sun},\phi) E_{sun}^{d}(\theta,\theta_{sun},\phi) \frac{1-\varepsilon_r}{\pi} F_r(\theta,\theta_{sun},\phi)\tau_r(\theta) + E_{sun}^{s}(\theta,\theta_{sun},\phi)$$

where E_{sun}^{TOA} is TOA solar spectral irradiance for channel r, θ_{sun} is local sun zenith, $\tau_r(\theta_{sun})$ is channel transmissivity along the path of sunlight, $F_r(\theta,\theta_{sun},\phi)$ is angular form factor or the surface, ϕ is difference between satellite and sun azimuth angles , $E_{sun}^{d}(\theta,\theta_{sun},\phi)$ is scattered path solar radiance.

The sea surface emissivity in the infrared region is determined on the basis of data analyses. Net radiation, surface irradiance and other oceanographically and meteorological variables are measured throughout most of the year at the oceanographically observatory tower in Tanabe Bay, Japan. It is found that 0.984±0.004 is a reliable emissivity value from the night time data. Surface emission radiates not from the subsurface water but from the sea surface. The thermal skin layer on the sea surface, however, is disturbed and disappears under high wind speed over 5 m/s through the analyses of the radiation observation using the emissivity value of 0.984. Under low wind speed, the sea surface can be cooler or warmer than the subsurface due to overlying thermal conditions and the skin layer can be neutral as the transient process between them. By using an emissivity value of 0.984, the temperature difference between the sea surface temperature and the temperature determined from surface irradiance that has been reported in the satellite data analyses is found to be reduced by half.

$$SST_{night}=a_0+a_1T_4+a_2\,(T_3-T_5)+a_3\,(T_3-T_5)\,(\sec(\theta_{zen})-1) \quad (2.5)$$

$$SST_{day}=b_0+b_1\,T_4+b_2\,(T_4-T_5)\,(\sec(\theta_{zen})-1) \quad (2.6)$$

Where, T_3, T_4, and T_5 are the three channels of the AVHRR Sensor. θ_{zen} is the satellite zenith angle, a_0 to a_3 nightly and b_0 to b_3 daily regression coefficients.

2.1.2.2 Heat Content

Heat content is a thermodynamic quantity equal to internal energy of a system plus the product of its volume and pressure. Ocean heat content is a major component of earth's energy budget and the heat content of the global ocean plays a critical role in the Earth's heat balance for the climatologically annual cycle (Ellis et al., 1978) and for inter-annual to decadal scales (Levites et al., 2001).To estimate heat content is important to verify Atmosphere-Ocean general Circulations Models that tries to simulate the earth's climate system.

2.1.2.2.1 Heat Flux

The rate at which heat is transported is called the ***heat flux***. It is measured in joules of energy per unit area per unit time (J/m^2s). The net surface heat flux entering the ocean (Q_o) includes net short wave (or solar) radiation (Q_{sw}), net long wave (or bulk) radiation (Q_{lw}),net heat flux due to evaporation (Q_{lat}), and sensible heat flux due to air and water having different surface temperature (Q_{sen}).

The surface heat flux Q is calculated using the formula

$$Q=Q_{sw}\downarrow-Q_{sw}\uparrow+Q_{lw}\downarrow-Q_{lw}\uparrow-Q_{sensible}-Q_{latent} \quad (2.7)$$

Where $Q_{sw}\downarrow$, $Q_{sw}\uparrow$, $Q_{lw}\downarrow$, $Q_{lw}\uparrow$, $Q_{sensible}$,and Q_{latent} are surface downward and upward short wave radiation, surface down ward and upward long wave radiation, sensible heat flux, and latent heat flux respectively. $Q_{sw}\downarrow$, $Q_{sw}\uparrow$ and $Q_{lw}\downarrow$ are derived from NCEP/NCAR reanalysis data. Upward long wave radiation is computed as

$$Q_{lw}\uparrow=\sigma T_{SST}^4 \quad (2.8)$$

Where σ is Stefan Boltzmann constant and T_{SST} is the model SST.The sensible and latent heat fluxes are estimated by

$$Q_{sensible}=\rho C_P C_h/V/(T_a-T_{SST}) \quad (2.9)$$

$$Q_{latent}=\rho_a L C_h/V/(q_a-q_{SST}) \quad (2.10)$$

Where ρ_a is air density, V is wind speed at 10m, T_a is surface air temperature, q_a is surface air humidity, and q_{SST} is saturation humidity at the model SST(Vinayachandran,Iizuuka and Yamagata , 2002).

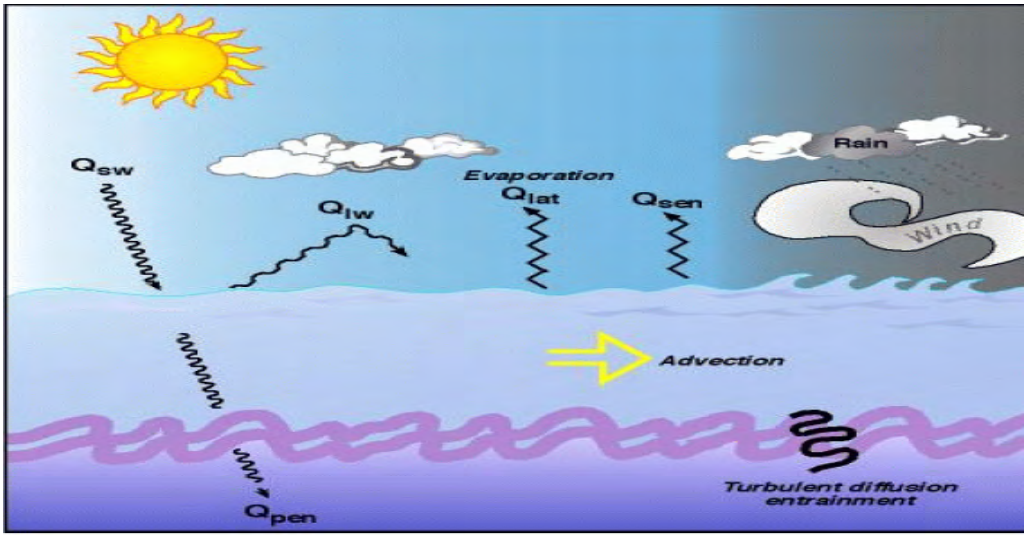

Fig 2.4. Wind and buoyancy forces acting on the upper ocean mixed layer. Solar radiation (Q_{sw}), net long wave radiation (Q_{lw}), latent heat flux (Q_{lat}), and sensible heat flux (Q_{sen}) combined to form the net surface heat flux(Q_o).$Q_{pen}$is the solar radiation penetrating the base of the mixed layer(Academic Presss,2001)

2.1.2.3 Air-Sea heat flux and Sea Surface Temperature (SST)

If oceanic processes are not considered, the change of SST is related to the net heat flux (Q_{net}) by

$$dSST = dt.Q_{net} / \rho c_p h \qquad (2.11)$$

Where h is the mixed layer depth and $dSST$ represents the increment in SST with in one month (dt). $dSST$ is calculated as the mean difference between the last five days and the first five days of month.

Over tropical Atlantic Q_{net} $dSST$ correlates highly with Q_{net} (>0.9.significant at 99% confidence level), except two belt refers, one is ITCZ belt and the other in the central and eastern equatorial cold tongue. If these two regions ocean dynamics processes are known to play a key role and so it is not surprise that the correlation between $dSST$ and Q_{net} is law.

2.4Ocean Circulation

Energy from the Sun doesn't fall equally all over the Earth. Most of the Sun's energy enters the Earth at the equator. This leads to large temperature gradients between the equator and the Poles. Movement of both the air and the oceans is controlled by these temperature differences and the result is a transfer of heat from the equator to the poles. Oceans transport about half the heat around the planet so the oceans are extremely important for the Earth's climate control system. If ocean circulation is changed by global warming, major changes in climate are therefore likely. Ocean circulation also transports oxygen from the air into the ocean making marine life possible.

Seawater continuously moves around the globe as if it is on a huge conveyor belt, moving from the surface to the deep waters and back. Because the distance the water has to travel is so large, it takes about 1000 years for seawater to go all the way around the Earth.

The movement of water around the oceans has two parts, which are strongly linked:

1. A density driven circulation, which is driven by the differences in the density of seawater at different locations. The density of seawater depends on its temperature and how salty it is. As a result, this movement is known as the **thermohaline circulation** (thermo - heat, haline - salt).

2. A **wind driven circulation** which results in huge surface currents like the Gulf Stream.

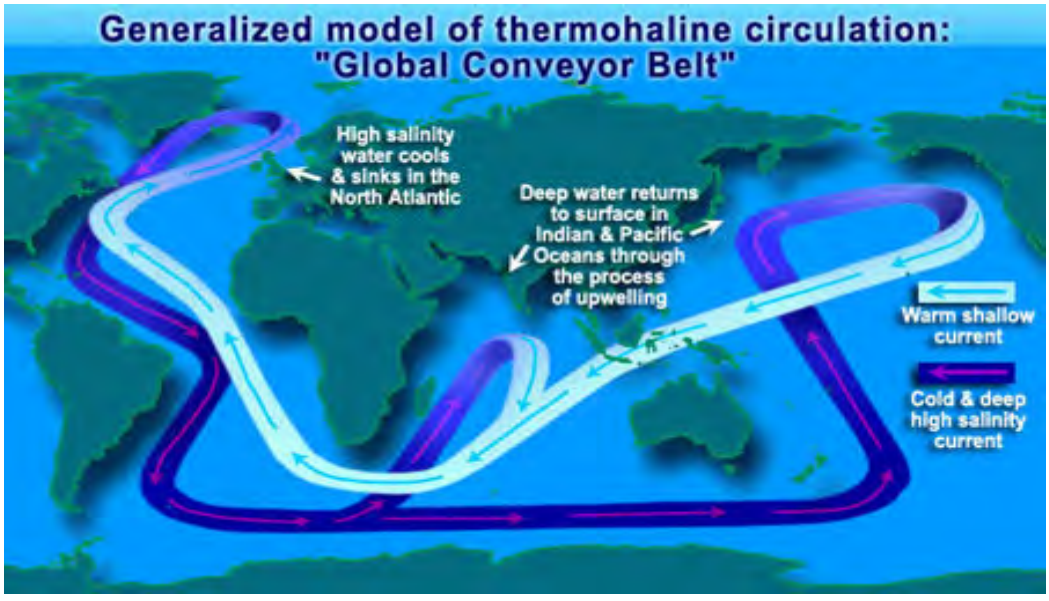

Fig 2.5. The general model of thermohaline circulation: Global Conveyer Belt .The light colored path shows the general movement of the surface waters and the dark colored path shows the movement of water at depth.

(http://www.nasa.gov/centers/goddard/images/content/95552main_0625oceanbehavior_conveyer.jp)

Water has amazing properties, which help to control our climate and make life on Earth possible. Although we call our planet Earth, only 29% of its area is actually land; the rest is covered by water and almost all of this water is in the oceans. Ocean waters continuously move around the globe as if they were on a huge conveyor belt, moving from the surface waters to the deep and back again. Wind, the saltiness of the water and temperature all control this movement. This ocean circulation helps to spread the heat from the Sun throughout the Earth.

The oceans also take up huge amounts of carbon dioxide from the atmosphere. Around a quarter of the carbon dioxide, we humans produce by burning fossil fuels ends up being stored in the oceans. In some ocean areas, this carbon can be stored for centuries, helping to reduce the effects of global warming.

2.1.5 The Oceans and Climate system

The Ocean is an important component of the climate system. It provides the surface temperature boundary over 70% of the globe. It absorbs over 97% of solar radiation incident on it from zenith angles less than 50^0.It provides 85% of the water vapor in the atmosphere. It exchanges, absorbs and emits a host of radioactively important gases. It is a major natural source of atmospheric aerosols. Thus, a static ocean would significantly influence the climate. However, the ocean is dynamic and its surface properties will vary on all time scales, allowing great scope for feedbacks between the ocean and atmosphere which is also known as Ocean-atmosphere coupling. (Bigg, Jickells, Liss and Osborn, 2003)

Climate is commonly defined as the average weather, with an averaging period long enough to smooth out the variability of synoptic systems. The climate of a location refers to more than just the long-term average of the annual cycles of temperature and precipitation. It includes other quantities, such as winds, humidity, and cloudiness. It includes places other surface, such as the upper atmosphere and the oceans. It includes other surface conditions, such as the presence of snow and ice (glaciers and sea ice), soil moisture, and vegetationcover.Furthermore,climate information now includes the variability of all these conditions, such as the frequency of storms, the range and frequency of extreme conditions, and variations from year to year.

2.1.6 Tropical Oceans Sea Surface Temperature and Climate Variability

Tropical Oceans play major roles in the natural variability of the world climate. Anomalous coupled ocean-atmosphere phenomena generated in the tropical oceans produce global atmosphere and oceanic circulation changes that influence regional climate conditions even in remote regions.

On the inter annual time scale, the El Niño/Southern Oscillation (ENSO) of the tropical pacific ocean, the Indian ocean Dipole (IOD) and so on are typical examples of such phenomena (Yamagata, Behera, Luo,Masson,Jury,and Rao ,2004;Ogallo,1998;Yeshanew and Jury,2006;Indeje et al. 2000;Philander 1990;LatifandDommenget,1999;Webster,Moore,Loshnigg,Leben;1999;Saji and Yamagata,1999;Emily,2003)

2.1.6.1 Tropical Indian Ocean and Climate variability

(*Tropical Indian Ocean: Lat.30^{0}S-30^{0}N, Lon.40^{0}E-120^{0}E*)

The inter-annual climate variability originated in the tropical ocean got attention by a number of researchers (Nicholas 1989; Makarau and Jury 1997; Arp et al, 1998; Latif and Dommenget, 1999 and Yamagata, Behera, Luo, Masson, Jury and Rao, 2004 among others) .In contrast to the pacific, the response to Tropical Indian Ocean SST anomalies had not been paid much attention, this was mainly because the variability in the basin is overwhelmed by seasonal winds. The southern monsoon winds that dominate the annual cycle produce strong upwelling along the Somalia coast of the western Indian Ocean weakening of these winds during the boreal fall after the summer monsoon period gives rise to warmer SST mainly owing to weakened upwelling. During this time, the equatorial westerly winds become stronger and generate the strong equatorial currents known as Yoshida-wyriki jet, which transports the warm waters to the east. In some years such as 1994 however, the Yoshida-wyriki jet did not evolve in such a normal way. This was a puzzle [e.g. Vinayachandron et al, 1999] (Yamgata, Behara, Luo, Masson, Jury, Rao, 2004)

It has turned out that the 1994 anomalous event in the basin is due to the ocean-atmosphere coupled phenomenon. This coupled mode is now widely called the Indian Ocean Dipole (IOD) (Saji et al.1999; Yamagata et al, 2003; Yeshanew and Jury; 2006) It is sometimes referred as the Indian Ocean Zonal (IOZ) mode.

Indian Ocean Dipole (IOD)

Indian Ocean Dipole (IOD) is a natural coupled ocean-atmosphere phenomenon in the Indian Ocean that plays important roles in seasonal and inter-annual climate variations (Yamagata, Behera, Lao, Masson, Jury, Rao, 2004). It is normally characterized by anomalous cooling of SST in the south eastern equatorial Indian Ocean and anomalous warming of SST in the western equatorial Indian Ocean. Associated with these changes the normal convection situated over the east Africa and severe droughts/forest fires over the Indonesian region. The name IOD is coined by Professor Yamagata, Dr.Saji and Other researchers of the climate variations researcher program of frontier Research center for global Change (FRGC) to represent the zonal dipole structure of the

various coupled ocean-atmosphere parameters such as SST, OLR and Sea Surface Height anomalies. Generally, this configuration is also called ***Positive IOD*** (Yamagata et al.2003, 2004). In fact, a negative IOD also evolves preceding/following a positive IOD, with reverse in the configuration of the positive. The IOD is also referred as **IOZM**(Indian Ocean Zonal Mode).It is preferable to use the term IOZM as it matches the out of phase development of the SST extrema in the east and west Indian Ocean, consistent with the Physics suggested by Webster et al.(1999).

The term dipole suggests simultaneous variation in the East and West. The positive IOD is characterized by a reversal of the east-west equatorial gradient in SST across the Indian Ocean, with warmer than normal water along the equatorial east coast of Africa and cool water near Sumatra. The negative IOZM is characterized by reversed anomalies (Saji et al.1999; Webster et al.1999; Reason et al; 2000).

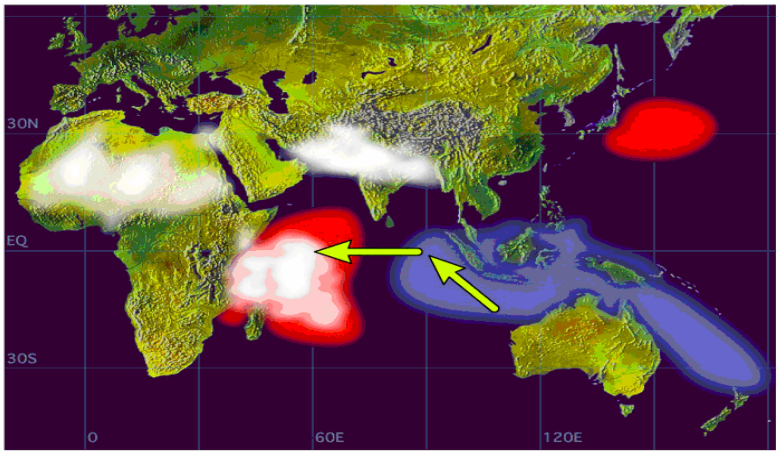

(a) Positive Dipole Mode

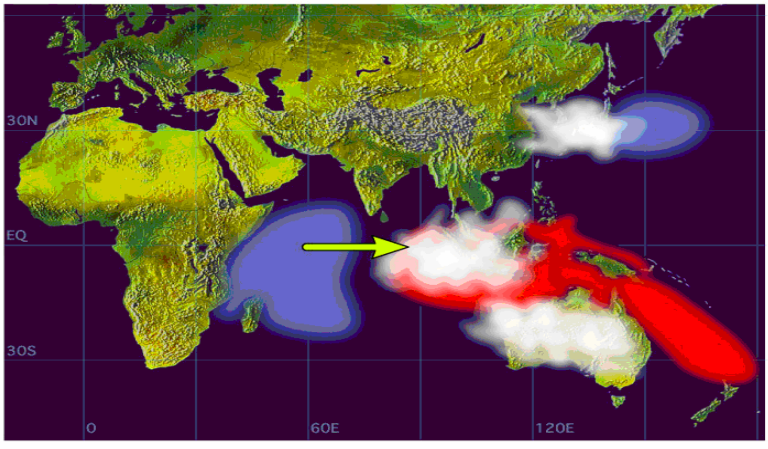

(b) Negative dipole Mode

Fig. 2.6 Schematic diagram of sea surface temperature anomalies (red shading denoting warming; blue cooling) during a positive Indian Ocean dipole (IOD) event (top).White oaths indicate increased convection activity with arrows indicating wind direction. The negative IOD (bottom) which is, in effect, the reversal of the positive IOD-complete with increased convective activity over Australia. Indonesia and Japan. Image courtesy: A.Suryachndra Rao, Institute for Global Change Research, Yokohama City, Japan

During these IOD/IOZ events, an east-west dipole pattern in SST anomalies evolves in tropical Indian Ocean. The changes in SST anomalies are formed to be closely associated with changes in surface winds, equatorial winds reverse direction from westerly to easterlies during the peak phase of the positive IOD events when SST is cool in the east and warm in the west. Changes in surface winds are associated with circulation (Yamagata et al, 2002)

The dipole pattern is not restricted only to SST anomalies. The thermocline rises in the east depends in the central and western parts in response to anomalous equatorial winds during the IOD events, thus giving rise to a subsurface dipole (Rao et al., 2002a).Since the seasonal south easterly winds along the Java coast are also strengthened during the positive IOD events, the anomalous coastal upwelling causes further SST cooling in the east(Behera et al.1999).The dipole pattern related to IOD is thus observed in heat content/sea level anomalies (sea level is anomalously lowered in the east and raised in the central and western Indian ocean during positive IOD events) (Rao et al.2002a;Mc Creary and Anderson 1984;Yeshanew and Jury,2006).The atmospheric component of IOD is seen in OLR anomalies (Behera et al.,1999,2003a;Yamagata et al,2002)and sea level pressure anomalies (Behera et al. and Yamagata et al.,2003).Therefore, IOD indices are derived for various ocean-atmosphere variables (Yamagata et al.,2003).

In the Indian Ocean rim countries, IOD is associated with significant temperatures and rain variability manifesting two large-scale patterns. In one, land temperature and rain are anomalously high over countries west of the Indian Ocean and low to its east .In the second pattern, enhanced rainfall is found over the Asia monsoon trough, extending from Pakistan up to southern china. Also IOD impacts on several regions remote from the Indian Ocean. Strong correlation is found over Europe, north East Asia, North and South America and South Africa concurrent with IOD events. An atmospheric general circulation model suggests that the Indian Ocean sea surface temperature (SST) exerts a greater influence over the East African short rains than the Pacific (Goddard and Graham 1999). Over these regions, positive IOD events are associated with warm land surface anomalies and reduced rainfall. The troposphere above the Indian Ocean exhibits strong variability during IOD events characterized by the following structures.

(1) ***A walker cell anomaly over the equator***

The Indian Ocean cell spans the entire equatorial Indian Ocean, with rising motion off Africa and sinking motion off Indonesia during positive IOD events. The pacific cell likewise spans the equatorial pacific with rising motion over the eastern and sinking motion over the western basin. It is interesting that the ‘walker’ cell associated with IOD appears

to have a weaker cell of opposing sign to its downstream with sinking motion over the Indonesia and the western pacific and rising motion over the central east pacific.

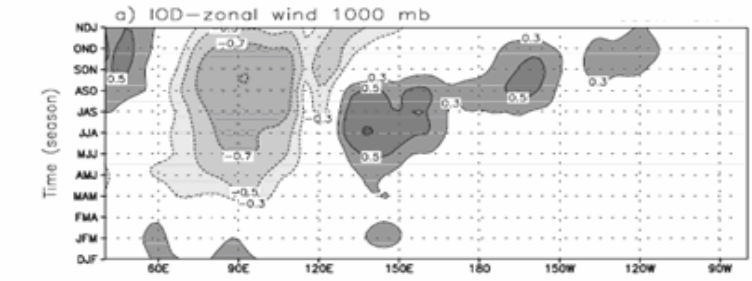

Fig. 2.7 Walker cell in the horizontal plane

At 1000mb, this downstream cell is accompanied by westerly wind anomalies that appear to propagate with time to the east.

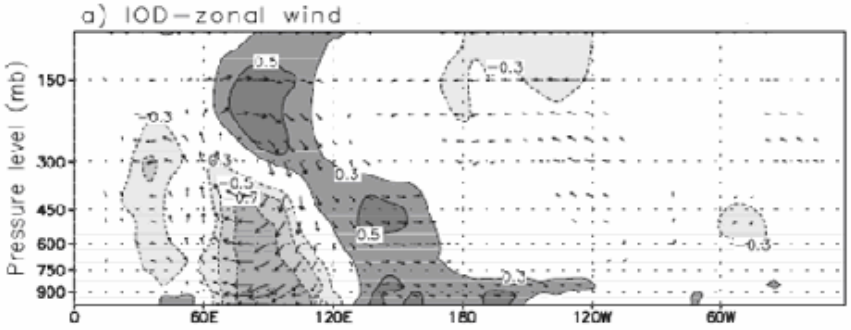

Fig 2.8 Walker cell in the vertical plane

The nature of the above cells in the vertical plane Fig 2.7 and in the horizontal plane Fig 2.6 is suggestive of *Kelvin wave dynamics*. It is possible that structures downstream are forced as a result of the modulated rainfall over the eastern Indian Ocean (Saji et al. 1999).and over the western Indonesia during IOD events.

The convective anomalies over the eastern Indian Ocean and Sumatra may give rise to the observed zonal wind anomalies over the western pacific (Saji and Goswami, 1996)

(2) A deep modulation of monsoon westerlies

The second region where IOD has strong correlation with zonal wind variability is the region of monsoon westerlies over the Arabian Sea and the Bay of Bengal.

During positive IOD events the monsoon westerlies are affected across the entire northern Indian ocean, from the eastern edge of the monsoon westerlies at 40^0 E to its eastern edge at 120^0 E over the east china sea, and over a deep vertical extent from 1000 to 300mb.Considering climatology, during positive IOD events a significant modulation of the vertical shear is seen, since the lower layers (i.e. below 300mb) are accelerated during

this event to levels above it(where climatologically winds are easterlies).Likewise, the horizontal wind shear is greatly affected by this configuration of anomalies. This results in anomalous negative curl, especially over the southern Bay of Bengal and affects Oceanic circulation and upwelling patterns significantly in that region (Han and Webster 2002, Rao et al.2002)

The maximum association of Dipole Mode Index (DMI) with the monsoon westerlies is found over 90^0E, during January through September at 850mb with DMI accounting for about 64%of its variability; and

(3) ***A Hadley cell anomaly over the Bay of Bengal***

The third important change in the atmosphere circulation over the tropical Indian Ocean during IOD events is the development of a meridional circulation (or 'Hadley') cell over the Bay of Bengal.

On the other hand ENSO doesn't appreciably modulate the monsoon Hadley circulation.

At lower levels, DMI is positively correlated with meridional winds between 10^0S and 10^0 N, with the largest correlation at 5^0S and 1000mb explaining about 64% of its variability. At the upper levels the correlation has negative value which implies a return flow occurring between 5^0 s and 20^0N.

In accordance with the theory that predicts a baroclinic oceanic response to wind anomalies in equatorial regions (Mc creary and Anderson, 1984), the anomalies thermocline has a sign opposing that of sea level. Simulation of the ocean state during IOD events in a wide variety of the oceanic models suggests that the dipole SST pattern is brought about primarily by oceanic process such as advection, entertainment and upwelling. In particular, in the eastern Indian ocean the heat budget of the mixed layer is dominated by upwelling and vertical entrainment (Behera et al 1999).However, in the western Indian ocean horizontal advection is an important term, and to some extent so are atmospheric (Mortugudde et al.2000,Li et al 2002)

The origins of IOD are unclear. The zonal SST gradient anomaly is significantly correlated with ENSO during the boreal fall (Saji and Yamagata 2003).However; this seems unlikely for several reasons. Until recent time, it is assumed that the Indian ocean did not have an inter-annual ocean-atmosphere coupling cycle, or it being forced primarily by the annual monsoon cycle and connection with global sale oceanic circulations systems such as ENSO and Tropical Atlantic Ocean (TAO).However this is not the case; recent studies have identified a unique ocean-atmosphere mode characterized by anomalously warm SSTs over in the eastern Indian Ocean (Saji et al.,1999).The evidence indicates Indian Ocean SST anomalies have a significant impact on

regional atmospheric circulation and rainfall anomalies that extended into East and southern Africa. For example, Indian Ocean SST anomalies are thought to have caused the widespread weather problems in 1997 characterized by localized droughts and floods (Reverdin,Cadet and Gutzler,1986;Ogallo,Janiowiak and Halpert,1998;Jury,1996;Goddard and Graham,1999)
In the exratropics, IOD is associated with equivalent bar tropic geo-potential anomalies. These assume annular structure in the northern hemisphere, but Ross by wave-train structure in the southern hemisphere (Saji and Yamagata, 2003)

The coupled mode of IOD locked to boreal summer and fall is distinguished as a dipole in the SST anomalies that are coupled to zonal winds. The equatorial winds reverse their direction from westerlies to easterlies during the peak phase of positive IOD events when SST is cool in the east and warm in the west. In response to changes in the wind, the thermocline rises in the east and subsides in the west. (Yamagata, Behera, Luo, Masson, Jury and Rao 2004)Although the IOD events dominate the ocean-atmosphere variability during its evolution, their less frequent occurrence compared to ENSO events leads the mode to the second seat in the inter-annual variability. (Only one-third of IOD events are associated with ENSO events)
Through changes in atmospheric changes and water vapor transport, a positive IOD event causes drought in Indonesia above normal rainfall in Africa, India, and Bangladesh, and Vietnam, dry as well as hot summer in Europe, Japan, Korea and East china. In southern hemisphere, the positive IOD causes dry winter in Ausralia,and dry as well as warm conditions in brazil. The identification of IOD events in has raised a new possibility to make a real advance in the predictability of seasonal and inter annual climate variations that originate in the tropics (Saji and Yamagata 2003).

2.1.6.2 Tropical Pacific Ocean and climate variability

(Tropical Pacific Ocean: Lon.120E-290E, Lat.20S-20N)

1. Normal Condition

In normal, non-El Niño conditions, the trade winds blow towards the west across the tropical Pacific. These winds across pile up warm surface water in the West Pacific, so that the sea surface is about half meter higher at Indonesia than at Ecuador. The sea surface temperature is about 8 degree C in the West, with cool temperature off South America, due to an upwelling of cold water from deeper levels. This cold water is nutrient-rich, supporting high levels of primary productivity diverse marine ecosystems, and major fisheries. Rainfall is found in rising over the warmest water, and the east Pacific is relatively dry. (NOAA 2004a, b)

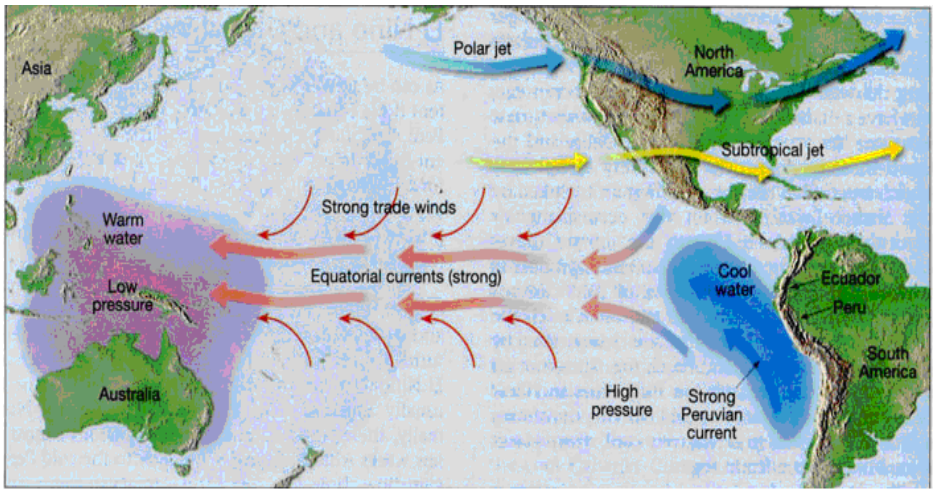

***Fig 2.9 In normal, non-El Nino conditions, the trade winds and strong equatorial currents flow toward the west across the tropical Pacific. At the same time, an intense Peruvian current causes upwelling of cold water along the west coast of South America* (http://www.sbg.ac.at/ipk/avstudio/pierofun/atmo/el-scans/el-nino1.jpg).**

2. El Niño/Southern Oscillation condition (ENSO)

El Nino, an abnormal warming of surface ocean waters in the eastern tropical Pacific, is one part of what's called the **Southern Oscillation**. The Southern Oscillation is the see-saw pattern of reversing surface air pressure between the eastern and western tropical Pacific; when the surface pressure is high in the eastern tropical Pacific it is low in the western tropical Pacific, and vice-versa. Because the ocean warming and pressure reversals are, for the most part, simultaneous, scientists call this phenomenon the El Nino/Southern Oscillation or ENSO for short. South American fishermen have given this phenomenon the name El Nino, which is Spanish for "The Christ Child," because it comes about the time of the celebration of the birth of the Christ Child-Christmas.

The southern Oscillation is a seesaw-like variation, over several-year intervals, of barometric pressure differences between the South Pacific ocean and the western Pacific/eastern Indian ocean.El Nino is a manifestation of the warn phase of the warm phase of the cycle, in which the pool of warm water normally observed in the western Pacific Ocean shifts eastward, diminishing upwelling of cold water along the coast of western South America and along the equator and shifting rainfall patterns away from Australia and Indonesia and eastward into the pacific. The economic impacts of excess rainfall and flooding in South America and droughts in Australia alone are estimated to be in the billions dollars.

ENSO has both a warm and a cold phase. The cold phase is referred to as La Nina, and El Nino is the warm phase.ENSO’s extreme warm (El Nino) and extreme cold (La Nina) events can disrupt

regional and local climates around the globe to varying degrees and in a variety ways, but especially in the tropics and ,most directly, in countries that border the pacific ocean.

3. El Nino Condition

El Nino is an extensive warming of the upper ocean in the tropical eastern Pacific lasting three or more seasons. The southern oscillation is a widespread inter-annual oscillation in sea-level atmospheric pressure between one region near northern Australia and one in the central pacific. These related phenomena, together called ENSO, are the largest short-term climate variations. An El Nino has received world wide attention because of the enormous societal impact (Yamagata, Behera, Luo, Masson, Jury, and Rao, 2004)

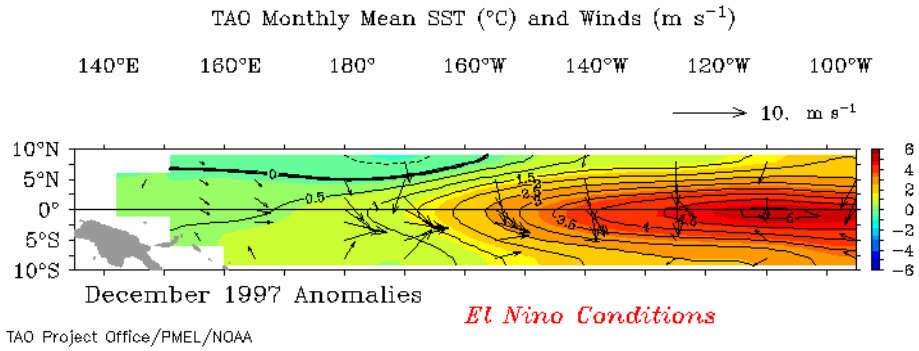

Fig.2.10 The December 1997 Mean/anomaly of SST (^{o}C) and Winds (ms^{-1}).

El Niño is an Oscillation of the ocean-atmosphere system in the tropical Pacific having important consequences for climate around the globe. Among these consequences is increased rainfall across the southern tier of the US and in Peru, which has caused destructive flooding, and drought in the West Pacific, sometimes associated with devastating brush fires in Australia.

Fig. 2.11 Flooded areas in Lakeport, California as a result of 1998 El Nino (*Federal Emergency Management Agency)*

Fig .2.12 Bush fire in Australia as a result of the 1998 El Nino Event (*Photo courtesy of Fred Hoogervirst/Panos Picture/London*)

During El Nino condition, the trade winds relax in the central and Western Pacific leads to a depression of thermocline in the eastern Pacific, and an elevation of the thermocline in the West. This reduced the efficiency of upwelling to cool the surface and cut off the supply of nutrient rich thermocline water to the euphotic zone. The result was a rise in the sea surface temperature and a drastic chain, including commercial fisheries in decline in primary production, the latter of which adversely affected higher trophic levels of the food chain, including commercial fisheries in this region. Rainfall follows the warm water eastward, with associated flooding in Peru and drought in Indonesia and Australia. The eastward displacement of the atmosphere heat source overlying the warmest water results in large changes in the global atmospheric circulation, which in turn force changes in weather in regions for removed from the tropical Pacific.

December 1997 was near the pick of a strong El Nino year. In December 1997, the warm water has spread from the western Pacific Ocean towards the east (in the direction of South America), the "*cold tongue*" has weakened, and the winds in the western Pacific, usually weak, are blowing strongly to wards the east, pushing the warm water eastward. The anomalies show clearly that the water in the center of pacific is much warmer than in a normal December.

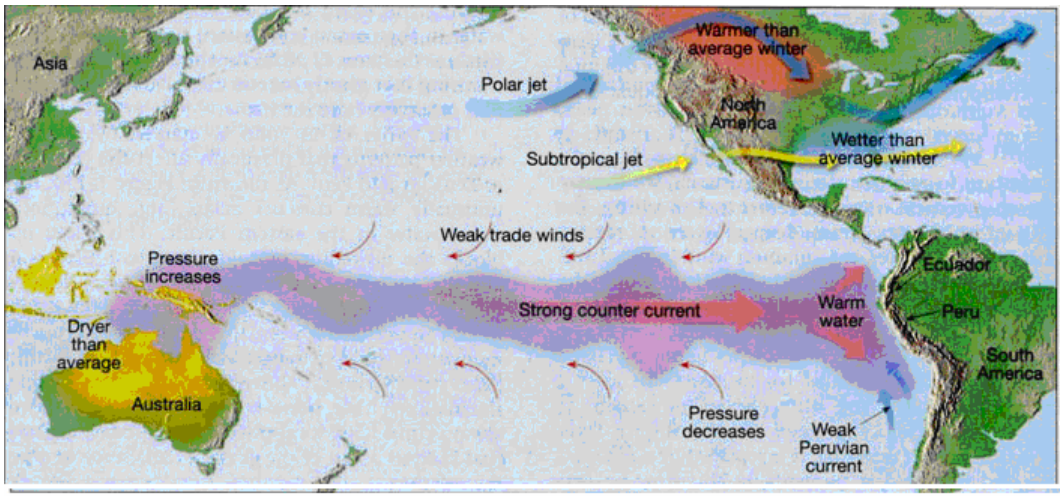

Fig.2.13 El Nino condition: Upon the advent of an ENSO event, the pressure over the eastern and western Pacific flip-flops. This causes the trade winds to diminish, leading to an eastward movement of warm water along the equator. As a result, the surface waters of the central and eastern Pacific warm, with far reaching consequences to weather patterns.
(http://www.sbg.ac.at/ipk/avstudio/pierofun/atmo/el-scans/el-nino2.jpg)

4. La Niña Condition

La Nina (female child) refers to an anomaly of unusually cold sea surface temperature founding the eastern tropical pacific. La Nina occurs roughly half as often as El Nino. La Niña condition is nearly the opposite of El Niño: the trade winds get enhanced associated with unusually cold SST in the eastern equatorial Pacific, thermocline is depressed in western Pacific and elevated in east. It is much wetter than normal across the Pacific Northwest and dryer and dryer and warmer across much of the southern tier. The two phenomena often follow each other resulting in a cycle with a period of 2-7 years.

December 1998 was a strong La Nina (cold) event. The cold tongue (blue) is cooler than usual by about 3^0 Centigrade. The cold La Nina events sometimes (but not always) follow El Niño events.

La Niña is associated with stronger easterly winds at the surface, a stronger thermocline tilt and cold water in the east.

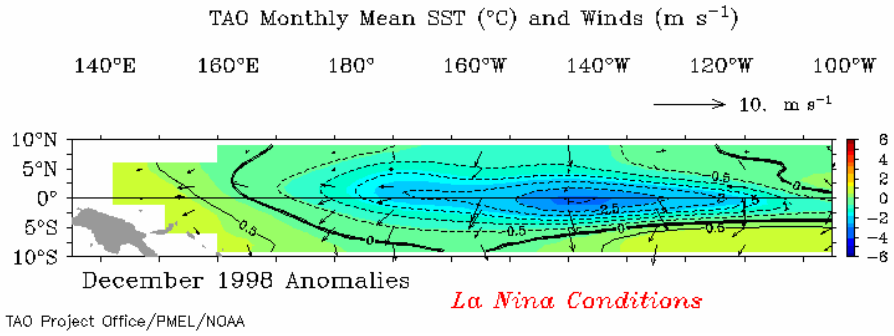

Fig 2.14 The December 1998La Nina Condition :(Monthly mean SST (^{0}c) anomalies and Winds (ms^{-1}): a cold tongue in the east and equatorial Pacific is shown.

Summary of Normal El Niño and La Niña Conditions of the Pacific Ocean

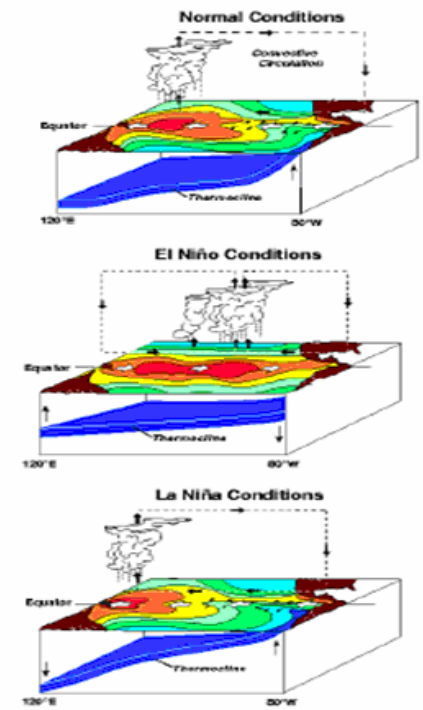

Fig 2.15 Schematic diagram of normal, El Niño, and La Nina conditions in the Pacific Ocean (NOAA 2004c)

In the western tropical Pacific, the sea surface is always warm (around 29^0C), the sea-level pressure is low, and the precipitation is heavy (see fig.2.15).In the eastern Pacific, some ten to fifteen thousand kilometers to the east, the situation is very different. There the water is normally cool (21^0C to 26^0C), the sea-level pressure is high, and the precipitation is low. The cold water in the region of the equatorial eastern pacific (the "cold tongue") persists through out the year but is warmest in April. This normal gradient in sea surface temperature along the equator is associated with westward winds. Although seasonal variations of this pattern occur, conditions are usually warm and wet in the west and cool and dry in the east (fig.2.15a).

Occasionally, however, the worm pool in the western tropical Pacific begins to spread east ward. Accompanying these changes in sea surface temperature, the regions of low sea-level pressure and heavy rainfall move eastward with the warm pool, and the eastern and central Pacific become somewhat cooler and drier. The earliest recognition of these changes was an awareness of unusually warm water appearing from the north, off the coast of Peru, as an enhancement of the normal Christmas warming. This warming of the coastal waters off Ecuador and Peru became known as El Niño. Later, it was recognized that the warming off Peru is part of a far more extensive warming, which extends across the entire tropical Pacific (fig.2.15b).

5. ENSO and Ethiopian Climate Variability

El Niño is associated with reduced easterly (may be even westerly) wind at the surface, a reduced thermocline slope and warm water in the east. It is not fully understood how ENSO affects precipitation patterns in Ethiopia(Orlove and Tosteson,1996).It is thought that ENSO affects precipitation in Ethiopia by displacing and weakening the major rain-bearing systems through its influence on the general circulation of the planetary atmosphere (Haile,1988).Studies of drought events in Ethiopia indicate that the tropical easterly jet and Tibetan high become weakened, and the ITCZ both weakens and shifts to the southeast during times of drought (Krishnamurti and Kanamitsus ,1981).The physical connection between these changes in the atmospheric general circulation and ENSO is complicated and not well undersood.Other factors, such as southern Atlantic and Indian sea-surface temperatures, also influence the rain-bearing systems in Ethiopia (NMSA 1987),and not all ENSO events correlate directly with drought in Ethiopia. The 1982-83 El Niño, for example, did not cause a particularly dry 'kiremt' (Ward and Yeshanew, 1990; Bekele, 1993), although one of the worst droughts in Ethiopian history occurred over 1983-84.

Interest in El Nino in Ethiopia began following the devastating 1983-84 drought.Forcasters at the National metrological Agency were trying to come up with physical interpretations for the occurrence of drought in Ethiopia(Kassahun,2000).ENSO was found to be one of the main factors that lead to drought in Ethiopia. Research at the NMSA began to focus on the links between the distribution of rainfall, Sea Surface temperature (SST) (including the Pacific, Indian and Atlantic Oceans), and Ethiopia (Kassahun, 1999). The NMSA has concluded that increases or decreases in the sea surface temperature (SST) on the Pacific Ocean impacts the amount and distribution of rainfall in Ethiopia (Kassahun, 1999). Normal 'Kiremt' rainfall is disrupted because El Nino weakens the atmospheric system that strengthens rainfall and its distribution during the kiremt season (Kassahun, 1999). The occurrences of El Nino/Southern Oscillation (ENSO) phenomena and SST anomalies have a strong impact on the weather and climate variability of Ethiopian. So the impacts of El Niño events on Ethiopian rainfall are real (Haile 1988).There is also an empirical pattern of association between El Nino and droughts in Ethiopia (Wold-Giorgis 1997, 5)

2.1.6.3 Tropical Atlantic Ocean and Climate variability

(Tropical Atlantic Ocean: Lat.40S-40N, Lon: 60W-15E)

Although the El Nino phenomenon in the pacific has a profound impact on global weather patterns, not all anomalous patterns are linked to El Niño. It has become increasingly clear that other modes of climate variation besides El Niño can have significantly influences on regional

climate. Among them is a variation of sea-surface temperature (SST) seemingly unique to the tropical Atlantic Ocean.

A number of studies have shown a significant response of the atmosphere circulation to tropical Atlantic SSTA's and some studies also point to a significant remote extra-tropical response affecting the North Atlantic Oscillation (Okumuraetal.,2001 ;Rajagolapan et al. ,1998; Watanabe and Kimoto ,1999;Xie and Tanimato,1998;Robertson et al.,2000) few studies have investigated the atmospheric response to South Atlantic SSTA's (Robertson et al,2003)

During some years, the water to the north of the equator in the Atlantic is anomalous, or abnormally, warmer than that to the south. In other years, the opposite condition occurs, and warm water appears in the southern tropical Atlantic. This pattern of sea-surface temperature seems to alternate every 10 years or so, and has a dramatic impact on regional climate in Africa and the Americas. The pattern is often called the *Atlantic sea-surface temperature "dipole"* because the temperature anomaly on one side of the equator tends to be the opposite of the temperature on the other side (although the temperature change is not always simultaneous).

Intense tropical rainfall is confined to the Inter-tropical Convergence Zone (ITCZ), a band of strong air currents rising through the atmosphere (convection). The ITCZ locates over the area of the warmest sea-surface temperature just north of the equator. When sea-surface temperature is warmer than normal in the northern tropical Atlantic (and/or colder than normal in the southern tropical Atlantic), the sea-surface temperature difference between the Northern and Southern Hemispheres (the SST gradient) generates a north-south surface pressure gradient in the atmosphere.

This "pushes" the ITCZ farther north from its normal location. As a result, the band of heavy precipitation migrates northward and creates persistent drought conditions in some South American countries, particularly in northeast Brazil. At the same time, it creates and wetter-than-normal conditions in the Sahel region of Africa. Recent research also suggests that a variation in tropical Atlantic sea-surface temperature has an impact on weather patterns in the southeast United States.

For a long time scientists have tried to understand the physics behind this phenomenon. Recent studies suggest that the SST variability involves interactions between the tropical atmosphere and ocean. Over the tropical Atlantic Ocean, between 30° north and 30° south, the prevailing winds are usually from the northeast in the Northern Hemisphere and from the southeast in the Southern Hemisphere. This wind system, called the trade winds, is sensitive to changes in the tropical SSTs.

An unusually warm sea-surface temperature in the northern tropics, for example, will produce a southerly wind anomaly near the equator because of the greater difference in surface air pressure between regions to the north and south.

Owing to the effects of Earth's rotation, counterclockwise circulation of winds will be set up in each hemisphere, which weakens the northeast trade winds in the Northern Hemisphere and strengthens the southeasterly trade winds in the Southern Hemisphere.

As a result, less heat is transported through evaporation from the ocean surface to the atmosphere in the northern tropics. (Evaporation and heat removal are largely controlled by the wind speed in the region; weaker winds can remove less heat from the ocean's surface.) Therefore, the already warm surface water in the northern tropics will warm even more, which will allow an even weaker northeasterly trade wind, and so on. This process is called a ***positive air-sea feedback*** because it enhances the unusual climate conditions.

As the warm surface temperature builds up in the northern tropics due to the positive feedback, ocean circulation gyres carry relatively cold waters from the south Atlantic and from the northern multitudes into the northern tropical Atlantic to counteract the warming effect. This process is called a negative feedback.

The negative feedback eventually cancels out the warm anomaly and leads to a reversal of the sea-surface temperature in northern tropical Atlantic, bringing colder-than-normal surface temperatures. The positive feedback then acts to enhance this reversed SST pattern. The interplay between the positive and negative feedbacks can produce a decadal oscillation in the coupled ocean-atmosphere system, which could provide an explanation for the Atlantic SST "dipole" oscillation.

If the tropical Atlantic variability can indeed be described as a self-sustaining oscillation, then there is a good possibility that this variability can be predicted using a computer model that captures the essential physics of the oscillation. The predictability follows simply from the fact that a cycle is sequential, and therefore one part of the cycle must follow another. The possibility of predicting low-frequency SST variability in the tropical Atlantic region has long been a central concern because of its significant influence on rainfall over northeast Brazil and the Sahel region of Africa. Rainfall changes in both areas have an extraordinary economic and societal impact (Chang, 1998; Marshal et al.2001).

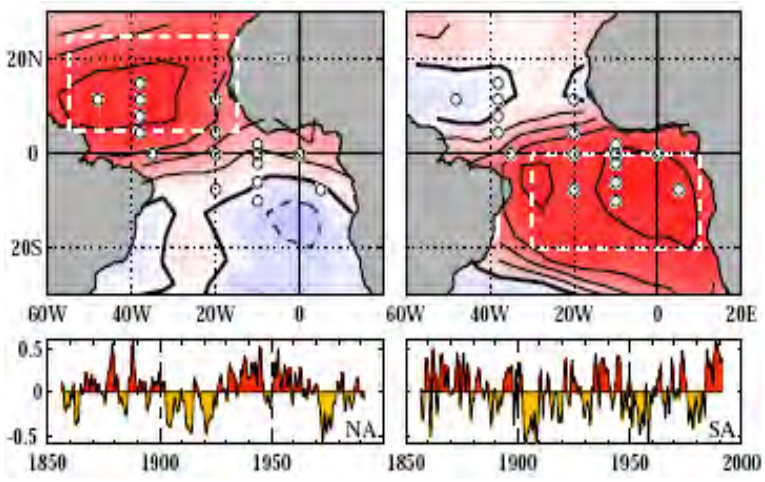

2.16. Tropical Atlantic Ocean Dipole (From Enfield et.al, 1998)

2.2Atmospheric Circulation

Atmospheric circulation is the large-scale movement of air, and the means (together with ocean circulation) by which heat is distributed on the surface of the Earth. The major driving force of atmospheric circulation is solar heating, which on average is larger near the equator and smallest at the poles. The atmospheric circulation transported energy pole wards, thus reducing the resulting equator-to-pole temperature contrast. The mechanisms by which this is accomplished differ in tropical and extra tropical latitudes.

2.2.1 Hadley Cell

The Hadley cell is a circulation pattern that dominates the tropical, atmosphere, with rising motion near the equator, pole ward flow 10-15kilometers above the surface, descending motion in the subtropics, and equator ward flow near the surface. This circulation is intimately related to the trade winds, tropical rain belts, subtropical deserts and the jet streams. The Hadley cell causes air to rise near the equator, and the walker cell results in air rising over the western Pacific Ocean. In general, rainfall amounts increase near the equator, and as you travel westward across the Pacific.

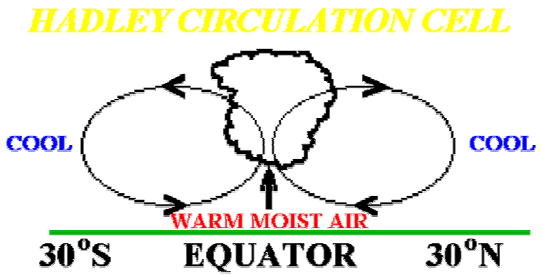

Fig.2.17 Hadley Circulation Cell
(http://www.atmos.umd.edu/~owen/CHPI/IMAGES/circs02.html)

Continuity Equation

$$\frac{\partial u}{\partial x}+\frac{\partial v}{\partial y}+\frac{\partial w}{\partial r}=0 \qquad (2.12)$$

Where u and v are the horizontal wind vectors and • is the wind vector along the vertical direction.

$$\frac{\partial u}{\partial x}+\frac{\partial v}{\partial y}=-\frac{\partial w}{\partial r} \qquad (2.13)$$

The expression on the left can be recognized as the horizontal wind vector V, as abbreviated by the symbol $\nabla \cdot V$.

The continuity equation states that horizontal divergence ($\nabla.V$ >0) is accompanied by a squeezing together in the vertical ($\frac{\partial w}{\partial r}$ <0) and horizontal convergence ($\nabla.V$ <0) is accompanied by vertical stretching ($\frac{\partial w}{\partial r}$ >0) (Wallace and Hobbs, 1977)

2.2.2 Walker Circulation

The walker circulation is an atmospheric circulation of air at the equatorial Pacific Ocean, responsible for creating ocean upwelling off the coasts of Peru and Ecuador. This brings nutrient-rich cold water to the surface; increasing fishing stocks. It was discovered by Jacob Bjerknes in 1969 and was named after the English physicist sir Gilbert Walker who discovered the southern oscillation.

The walker circulation is caused by the pressure gradient force that results from a high pressure system over the eastern Pacific Ocean, and a low pressure system over Indonesia. When the walker circulation weakens or reverses, an El Niño results, causing the ocean surface to be warmer than average, as upwelling of cold water occurs less or not at all. An especially strong walker circulation causes a La Niña, resulting in cooler ocean temperatures due to increased upwelling.

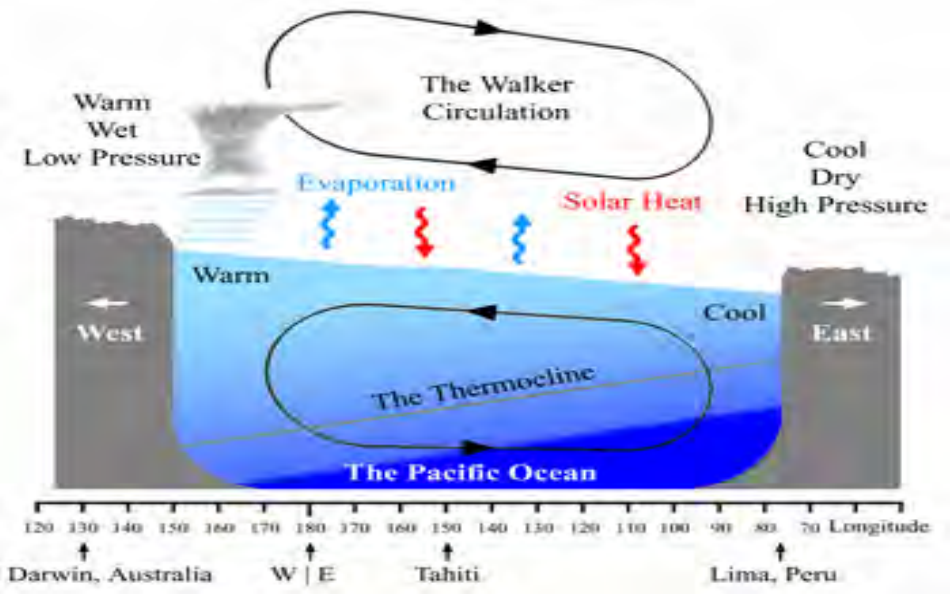

Fig 2.18 Walker Circulation (http://en.wikepedia.org/wiki/Image:la Nina.png)

Several studies have investigated the relationship between the short rains and the El Nino Southern Oscillation (ENSO).(Nicholson and Kim, 1997), for example, find a strong connection between ENSO and rainfall over much of the African continent and suggest a linkage through ENSO-induced SST anomalies in the Indian Ocean, which in turn modulate inter-annual variability of rainfall over Africa

2.3 Description of Ethiopia and its Rivers

2.3.1River Basins of Ethiopia

Ethiopia is called the water tower of Africa. It is home to many rivers such as the Blue Nile and Wabi Shebelle, making it potentially suitable for irrigated agriculture (Wolde-Georgis, 1997).

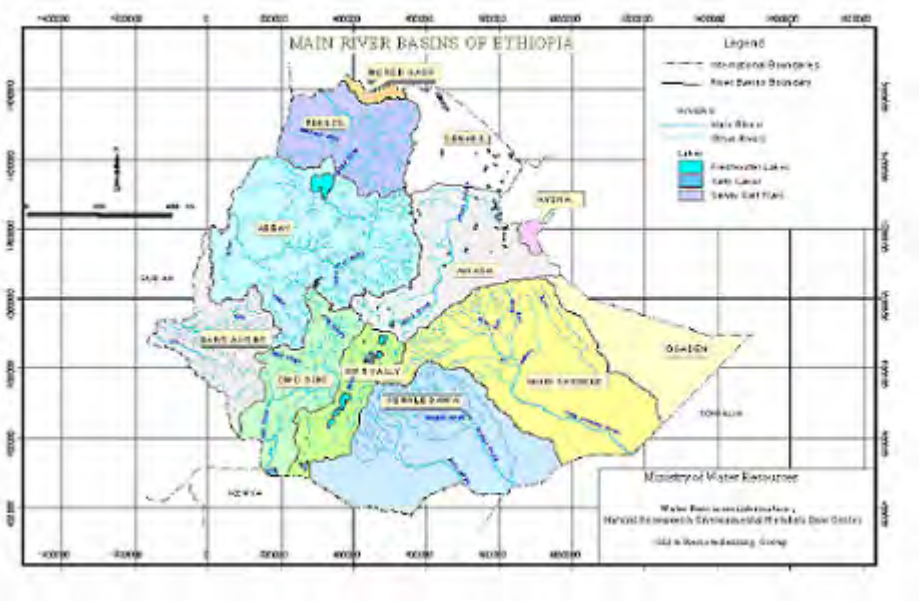

Fig. 2.19. River Basins of Ethiopia (Ethiopia Ministry of Water Resource)

The area of Ethiopia is 1,235,000km^2. The country is located in the northeastern section of Africa, commonly known as the Horn of Africa. The central topographic feature of the country is high central plateau, with elevations between 1500-3000 meters (with some peaks over 3500 meters) that is divided by the East African Rift Valley that runs from northeast to southwest through the country. Surrounding the plateau and mountains are the lowlands, with elevation below 1500 meters. This topographical diversity sets the stage for great heterogeneity in climate and other important elements of the biophysical environment (Orlove and Tosteston, 1996)

2.3.2. Rainfall Regimes of Ethiopia

Rainfall varies enormously across the country. While precipitation in the lowlands in the south/southeast,east,and north averages below 500mm/year,some areas of the highlands average over 2000mm/year (Mc Cann,1994).In addition to this spatial variability, rainfall is highly variable

over seasonal and inter-annual time scales. In most of the country, there are two rainy seasons-the short spring rains (February-May) known as 'Belg' and the main rainy season (June-September) *known* as 'Kiremet'.In the western part of the country, however, there is only one rainfall peak during the year. High interannual variability in precipitation is characteristic of both the belg and the kiremt, though the spring rains tend to be less reliable.

Fig.2.20 The Rainfall Regimes of Ethiopia (NMA)

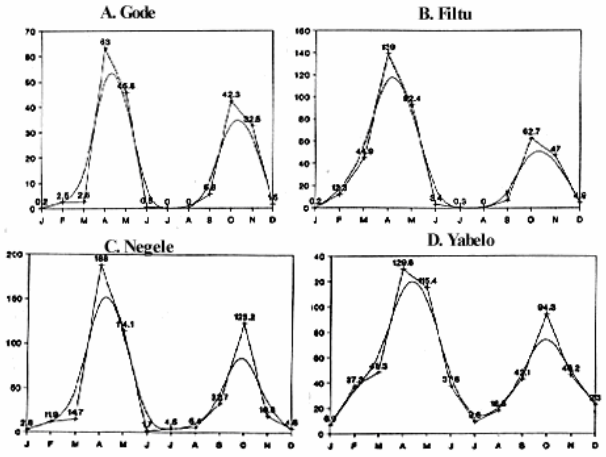

Fig.2.21 Monthly Distribution of Rainfall (in mm) in Rainfall Regime C (National Meteorological Agency)

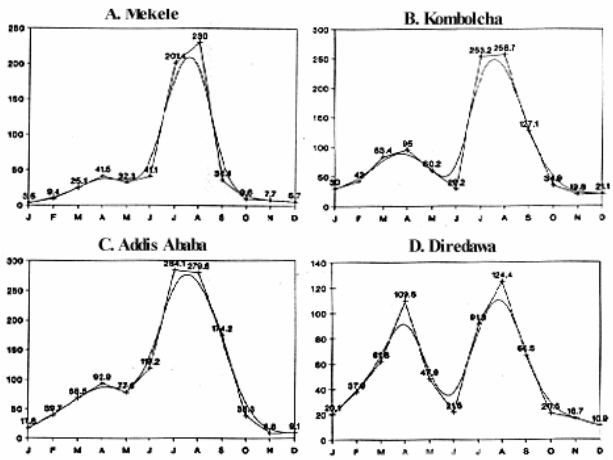

Fig.2.22 Monthly Distribution of Rainfall (in mm) in Rainfall Regime A (National Meteorological Agency)

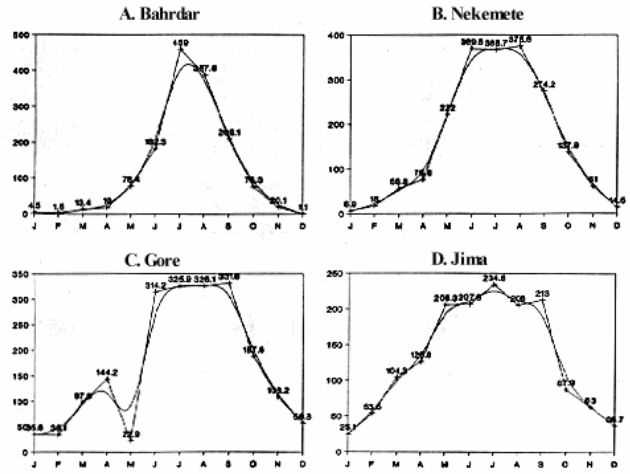

Fig.2.23 monthly Distribution of rainfall (in mm) in Rainfall regime B (National meteorological Agency)

The central and most of the eastern half of the country have two rainy periods 'Kiremt' (June to September) and 'Belg' (Feb to May) and one dry period 'Bega'(Oct to Jan) Fig.2.22.The southern and the south eastern parts of Ethiopia Fig.2.21 have two distinct rainfall and dry periods **MAM** and **SON**, and DJF and JJA, respectively.

The western part of Ethiopia has one rainfall peak during the year Fig.2.23. The length of the rainy period decreases, and the length of the dry period increases as one goes toward the north with in this region, as a result of the meridional migration of the ITCZ (Inter-Tropical Convergence Zone).

2.3.3 Atmospheric Dynamics over Ethiopia

The large scale atmospheric dynamics that affect the Ethiopian climate are quite complex. During 'Belg', the Arabian ridge or anticyclone (when it is displaced to the North Arabian Sea),the penetration of deep, large-amplitude troughs in mid-latitude westerlies, and southward movement of the subtropical jet. During Kiremt, the ITCZ, the southwest Indian Ocean anticyclone, the south Atlantic anticyclone, and other atmospheric features control precipitation (Bekele 1997).During periods of drought, the states of and relationships among these atmospheric systems change. The major droughts in Ethiopia are in 1957, 1965, 1973, 1983-84, 1987, and 1993-94 occurred following El Nino events (Wold-Georgis, 1997).

Chapter Three

Data and Methods

This section dwells on the data used and the methods employed to establish the connection of the tropical oceans and the southern Ethiopian climate, vegetation and hydrological variability. Multiform data and vigorous techniques are used.

3.1 Data

The datasets consist of climate, ocean, vegetation and hydrological data. The temporal and spatial characteristics of the data used are described here.

3.1.1 Ocean Data

To understand the Tropical oceans thermodynamic and atmospheric modulation on Southern Ethiopian climate variability, sea surface temperature (SST) and heat content data over Pacific, Atlantic and Indian Oceans are used. The Ocean Sea Surface Temperature (SST) and heat content Singular Value Decomposition (SVD) data are obtained from buoys and both geostationary and polar orbiting Satellite systems. The National Ocean and Atmosphere Administration (NOAA) uses its satellites to generate such data. These data are provided freely by the International Research Institute for climate Prediction (IRI).

3.1.1.1 Sea Surface Temperature (SSTs) Data

The SST SVD data of tropical Oceans used in this paper are enhanced by both buoy and satellite information in the NOAA-NCDC extracted from version 2 of ERSST reanalysis. Available records are extracted with in the domain of Indian Ocean latitude (30N-30S) longitude (40E-120E), Atlantic Ocean latitude (40S-40N) longitude (60W-15E) and Pacific Ocean latitude (20S-20N) longitude (120E-290E), which has SST data set in the time series that ranges from January, 1951-December, 2000 for a period of 50 years.

3.1.1.2 Heat Content

The tropical Oceans heat content SVD data used in this paper are enhanced by both buoy and satellite information in the UMD Carton goa extracted from beta 7 of hc125. Available records are extracted with in the domain of Indian Ocean latitude (30N-30S) longitude (40E-120E), Atlantic Ocean latitude (40S-40N) longitude (60W-15E) and Pacific Ocean latitude (20S-20N) longitude

(120E-290E), which has heat content data set in the time series that ranges from January, 1951-December, 2000 for a period of 50years.

3.1.2 Climate Data

The generated climate Singular Value Decomposition (SVD) data such as precipitation were obtained from International Research Institute for climate prediction (IRI) data library.

3.1.2.1 Precipitation

Continues monthly Rainfall departures interpolated to 0p5x0p5 prcp resolution were obtained from DEKLIM VASClim0 PrcpClim that has recorded data more than 50years.But we only use a 50 years of the recorded data from Jan 1951 to Dec 2000 over Ethiopia which covers 3N to 18N latitude and 32E to 48E longitude area.

3.1.3 Normalized Difference Vegetation Index (NDVI) Data

Normalized Difference Vegetation Indices (NDVI) is a measure or estimate of the amount of radiation being absorbed by plants. The amount of radiation absorbed is directly related to evapotranspiration, since the plant must cool primarily by evaporation water. The evapotranspiration is constrained by the amount of water in the soil. And for relatively low rainfall amounts, the amount of water in the soil is constrained by rainfall. Hence NDVI correlates with rainfall (Rowland et al. 1996).

Satellite data processed into normalized Difference Vegetation Indices (NDVI) can be used to indicate deficiencies in rainfall and portray meteorological and/or agricultural patterns both timely and spatially, thus serving as an indicator of regional drought patterns.

The Normalized Difference Vegetation Index Singular value Decomposition (SVD) data were obtained from the IRI dataset using the URL 'home mbell users mesfin ndvig EAF EAfrNDVlglarge Max anomalies' over the whole Ethiopian region (3N-18N, latitude and 32E-48E, longitude) for a period of about 20years ranging from July 1981 to Dec.2000.

Table 3.1 Summary of the ocean and climate data

No.	Variable	Area	Time Period	Used for
1	SST	All Oceans	1951-2000	Ocean
2	Heat Content	All Oceans	1951-2000	Ocean
3	Precipitation	Ethiopia	1951-2000	climate
4	NDVI(Vegetation)	Ethiopia	1981-2000	climate

3.1.4 Hydrological Data

Continuous monthly southern Ethiopia Rivers discharge flow and lakes level data of rivers such as Ghibe and lakes such as Awassa and Lake Zeway (Rift valley lakes) were obtained from Ethiopian Ministry of Water Resource. These dataset have actually got some problems in recording. The gap that is missed in recording filled after observing the pattern of flow and some basic statistical methods. Together with rainfall, the discharge flow and lakes level index of the rivers and lakes describe the temporal variability of southern Ethiopia climate.

Table 3.2 Hydrological station of southern Ethiopia

MAIN CATCHM.	SUB CATCHM.	RIVER/LAKE	SITE	INSTA. DATE	REG.STATE
RIFT V.(08)	NORTHERN 1	LAKE ZIWAY	@ ZIWAY	17-5-74	OROMYA
RIFT V.(08)	CENTRAL (2)	L. AWASSA	@ AWASSA	7-9-69	SOUTHERN
G.-OMO.(09)	UPPER GHIBE	GHIBE	@ SEKA	30-1-1979	SOUTHERN

G.-OMO:-Ghibe-OMO; RIFT V.:-RIFT VALLEY; WABI

NB1:-The reason that these rivers are selected among many others is the data availability.

NB2:-In this research we are limited to the Awassa and Zeway lakes to show the association between Tropical oceans thermodynamic and atmospheric circulation and hydrological variability over Southern Ethiopia.

3.2 Methods

To establish the spatial-temporal modes of variability of tropical oceans in terms of thermodynamics and heat content standard methods such as singular value decomposition (SVD), regression and correlation, and composite reanalysis techniques are used. These are documented below.

3.2.1 Singular Value Decomposition (SVD)

Singular value decomposition (SVD) is quite possibly the most widely-used multivariate statistical technique used in the atmospheric sciences. The technique was first introduced to meteorology in a 1956 paper by Edward Lorenz, in which he referred to the process as empirical orthogonal function (EOF) analysis. Today, it is also commonly known as principal-component analysis (PCA).

The purpose of singular value decomposition is to reduce a dataset containing a large number of values to a dataset containing significantly fewer values, but which still contains a large fraction of the variability present in the original data. Often in the atmospheric and geophysical sciences, data

will exhibit large spatial correlations. SVD analysis results in a more compact representation of these correlations, especially with multivariate dataset and can provide insight into spatial and temporal variations exhibited in the fields of data being analyzed (IRI Statistical Analysis Tutorial).

The SVD provides as outputs spatial and temporal modes and eigenvalues (variances).The first structure is the single pattern that represents the most variance in the data. The structures are the elements of the eigenvectors of the variance-covariance matrix of the data. The eigenvectors are also known as Ego's. The first eigenvector (EOF) points to the direction in which the data vectors jointly exhibit the most variability. Essentially, a new coordinate system is created, with each axis aligned along the direction of maximum joint variability.

The second structure is the pattern that describes the second largest amount of variance, calculated the same way as the first structure. A very important property of the second structure is that it is completely uncorrelated with the first structure, as well as all other following structures. The second eigenvector is perpendicular to the first eigenvector, which is perpendicular to the third eigenvector and so on. This property is what led Lorenz to call the technique empirical *orthogonal* function analysis. All structures are mutually uncorrelated.

The variance of the nth principal component is the nth eigenvalue. Therefore, the total variation exhibited by the data is equal to the sum of all eigenvalues.Eigenvalues are normalized such that the sum of all eigenvalues equals 1. A normalized eigenvalue will indicate the percentage of total variance explained by its corresponding structure. Structures have also been normalized so that the root mean square equals 1. This way, the structures can be expressed in terms of standard deviation.

As output of SVD, there are time series associated with each structure. These time series are also known as principal components. The first time series is calculated by projecting the data matrix onto the first eigenvector of the variance-covariance matrix of the data, the second time series by projecting onto the second eigenvector, and so on.

SVD Theorem

Let A be an m x n matrix, where $m \geq n$. Then A can be decomposed as follows:

$$A=UWV^T \qquad (3.1)$$

Where U is an m x n orthonormal matrix: $UU^T = I_m$, W is an n x n diagonal matrix.

$$\Lambda = \begin{bmatrix} w_1 & 0 & \dots & 0 \\ 0 & w_2 & \dots & 0 \\ 0 & 0 & 0 & w_n \end{bmatrix} \qquad (3.2)$$

V is an n x n orthonormal matrix; $VV^T = I_n$ .The diagonal elements of W are called the singular values. I will refer to the singular value w_i as the singular value of the i^{th} columns of U and V.The singular value decomposition exists always and is unique up to 1)Same permutations in columns of U,V and V.2)Linear combinations of columns of U and V with equal singular values.

If X is a matrix $X_{i,j}$ will represent the element in the i^{th} row,j^{th} column, and X_i will represent the i^{th} column vector. Note $A_{i,j} = \sum_{k=1}^{n} w_{k,k} U_{i,k} V_{i,k}$ .Thus we can approximate A well by deleting columns of U and V with small singular values.

3.2.2 Correlation

The correlation is one of the most common and most useful statistics. A correlation is a single number that describes the degree of relationship between two variables. It is defined as the measure of linear association between two variables. A single value, commonly referred to as the correlation coefficient, is often needed to describe this association. The value has two special properties. First, it is bounded by -1 and 1. If the correlation is exactly -1, there is a perfect, negative linear association between the two variables; the scatter plot of the two variables falls along one line with negative slope. Conversely, if the correlation is exactly 1, there is a perfect, positive linear correlation. Secondly, the square of the correlation describes the amount of variability in one variable that is described by the other variable. This variable is called ***variance***.

The degree of the association is assured by the significance. The significance of the correlation is used to determine minimum threshold for the correlation coefficient at a given significance level. The 90%.95%, 98% and 99% two-tailed significance levels of the correlation coefficient are listed in the table below (assuming normally distributed datasets).

Note that the degrees of freedom (df) =n-2 for sample of size n.

df	90%	95%	98%	99%	df	90%	95%	98%	99%
4	.729	.811	.882	.917	40	.257	.304	.358	.393
6	.622	.707	.789	.834	45	.243	.288	.338	.372
8	.549	.632	.716	.765	50	.231	.273	.322	.354
10	.497	.576	.658	.708	60	.211	.250	.295	.325
12	.458	.532	.612	.661	70	.195	.232	.274	.302
14	.426	.497	.574	.623	80	.183	.217	.256	.283
16	.400	.468	.542	.590	90	.173	.205	.242	.267
18	.378	.444	.516	.561	100	.164	.195	.230	.254
20	.360	.423	.492	.537	200	.116	.138	.164	.181
25	.323	.381	.445	.487	300	.095	.113	.134	.148
30	.295	.349	.409	.449	400	.082	.098	.116	.128
35	.275	.325	.381	.418	500	.073	.088	.104	.115

For instance, for a sample of n=32 with a correlation coefficient of 0.449 is significance at 99%.For samples between the given degree of freedom is determined by interpolation.

3.2.3 Regression

Regression is a prediction of levels of one variable when another is held constant at several levels based on average variation remaining constant over time due to the tendency in nature for extreme scores to move toward the mean. It is used for individuals on the basis of information gained from a previous sample of similar individuals.

Regression equation: • = a + bx (3.3)

• = estimated y and is the value on the y-axis across from the point on the regression line for the predictor x value. This is the estimated value of the criterion variable given a value of the predictor variable.

a = the intercept point of regression line and the y-axis. It is calculated through the equation a= $\bar{y} + b\bar{x}$; therefore the means of both variables in the sample and the value of b must be known before a can be calculated.

b = the slope of the regression line and is calculated by this formula: $b = \frac{\sum(x-\bar{x})(y-\bar{y})}{\sum(x-\bar{x})^2}$

x = an arbitrary chosen value of the predictor variable for which the corresponding value of the criterion variable is desired.

3.2.4 Atmospheric Analysis

Atmospheric composite structures are formed for any two dichotomies: wet and dry; high and low flow and the likes. The main thrust of atmospheric composite identification is to find out the atmospheric causes or signals under extreme events (Yeshanew and Jury, 2006).In this study, atmospheric composite are used to identify the mechanisms for wet and dry events precipitation during the SON and MAM seasons of Southern Ethiopia.

In this analysis variables such as vector wind, specific humidity, precipitable water and precipitation rate, Outgoing Long wave Radiation (OLR) are used for different seasons in Ethiopia.

A) Wind Vector

Wind vectors indicate direction and speed. In fig (3.1) the black arrows are wind vectors. These vectors indicate direction and intensity of the wind. The vectors point in the direction to which the wind is blowing and in the figure, winds are primarily blowing from west to east. Intensity of the wind is conveyed through the size of the vector. The longer the arrows is the stronger the winds.

Fig.3.1 Wind Vectors (From WW20 University of Illinois)

For example, wind vectors in the vicinity of the blue arrow are longer than those near the green arrow. This means that by the blue arrow, the winds are stronger, than by the green arrow. Wind vectors are also useful in finding regions of upper level convergence and divergence, which indicate regions of upward and downward motions. Upward motion is typically associated with clouds and precipitation.

B) Outgoing Long-wave Radiation (OLR)

Outgoing Long wave Radiation (OLR) is an indicator of both how warm the earth's surface is and how clear the atmosphere is overhead. OLR is determined from the Earth Radiation Budget Experiment (ERBE) and Advanced Very High Resolution Radiometer (AVHRR) sensors which appear on a series of NOAA satellite. Warm surfaces radiate more in the long wave range. Low values of OLR are typically due to clouds in the atmosphere. The radiation from below the clouds gets trapped by them and it is the temperature of the cloud top heights which determine the amount of long wave radiation measured at the Top of the Atmosphere (TOA).

C) Specific Humidity

The specific humidity (q) of moist air is the ratio of the mass of water vapour (Mw) to the mass of moist air (Ma+Mw) in which the mass of water vapour is contained.

$$q = \frac{Mw}{Ma + Mw} \qquad (3.4)$$

Where q is measured in g/kg

D) Precipitable Water

A convenient measure of the water vapour of a column of air is the ***precipitable water*** (*W*).This is defined as the total amount of water vapour in a layer of air expressed as a depth of liquid water in millimeters or inches. That is, precipitable water is the depth of water which would result from the condensation of all the water vapour in the column of air. It is of course, impractical for this to our in nature and all air masses contain some precipitable water.

Chapter Four

Results and Discussion

The results obtained from the study are documented here for understanding climate, water level, and river flow as well as vegetation variability over the southern part of Ethiopia. The leading spatial and temporal structures of the three tropical oceans SST and Heat content are discussed in section 4.1.The leading spatial and temporal structures of rainfall modes of Ethiopia are given in section 4.2 and that of vegetation modes over Ethiopia are given in section 4.3.

4.1 Space-time modes of physical variability

4.1.1 Tropical Oceans Sea Surface Temperature modes

The spatial mode of Pacific Ocean SST exhibits a warm tongue anomaly of $>2^0$C in the east equatorial pacific shown in fig. 4.1a.This is related to the El Niño condition and how it affects the southern part of Ethiopia climate variability will be discussed in sections 5.A dipole structure is seen in the second mode which shows the emerging of cold tongue in the east pacific while the warm anomaly is getting lost from the east (around Ecuador) fig. 4.1b.The third mode of spatial structure exhibits a warm anomaly at the center of Pacific Ocean occurred between the two cold anomalies at the east and west end of the ocean as it is shown in part three of fig.4.1.The equatorial N-S contrast of the Atlantic Ocean is shown in the second mode fig.4.3 ,$>2^0$C warm anomaly above the equator in the northern hemisphere between 0^0 and 30^0N and a negative anomaly between 0^0 and 30^0S.A negative cold SST anomaly is seen around the Gulf of Guinea in the third mode of Atlantic SST pattern fig.4.3c.

A negative dipole of the Indian Ocean SST pattern is illustrated by the second mode of Spatial structure which has a cold anomaly of $>1^0$C in the west and of $>1^0$c in the east of the Indian Ocean as is shown in fig. 4.5b and a negative SST pattern is exhibited around Australia in the third mode of the Indian Ocean SST spatial structure. These together are the main causes for the zonal and meridional atmospheric circulation that controls the variability of climate over the southern part of Ethiopia.

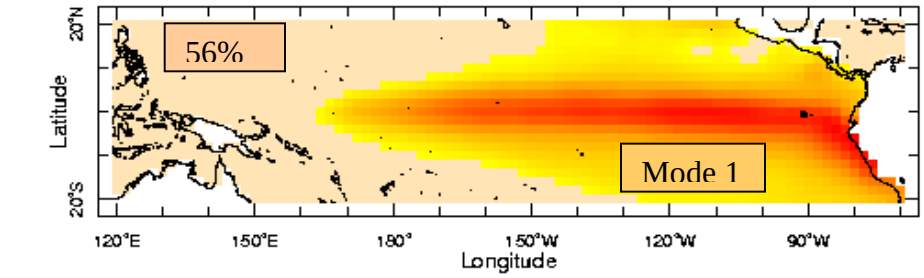

1.

a) The ENSO mode of equatorial east pacific ocean

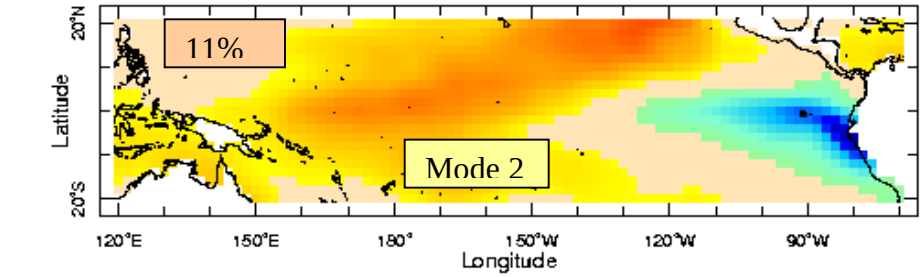

2.

b) The dipole mode of Pacific Ocean

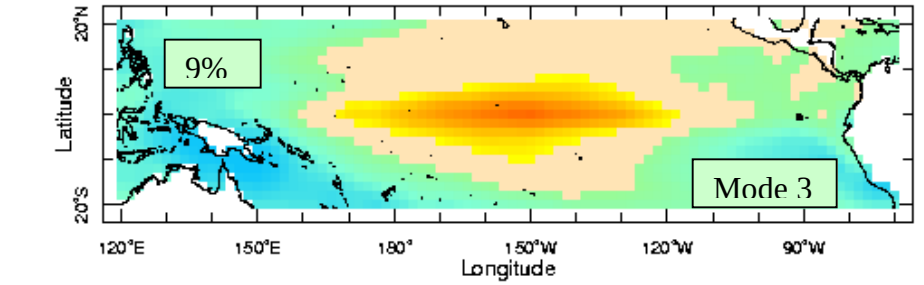

3.

C) The equatorial warm Pacific mode

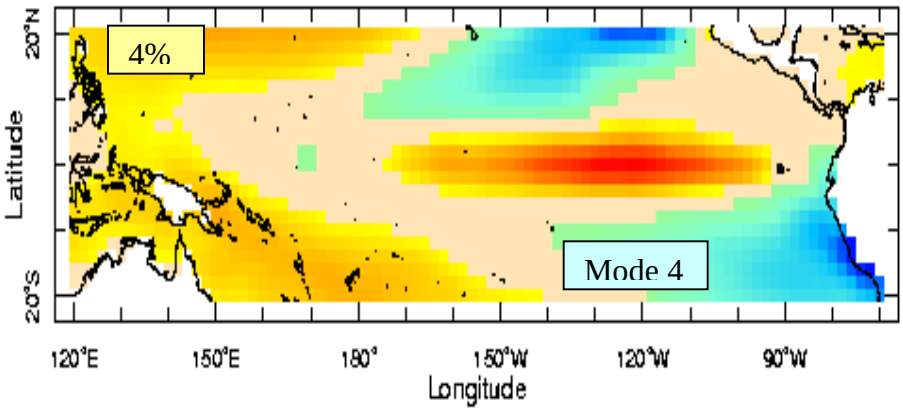

4.

d) Equatorial warm pool

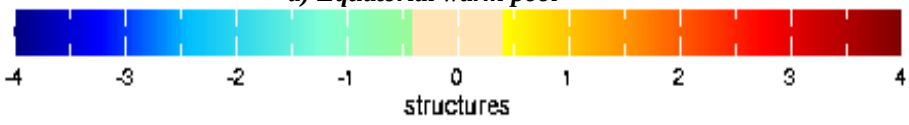

Fig. 4.1 The leading spatial structures of SST over Pacific Ocean

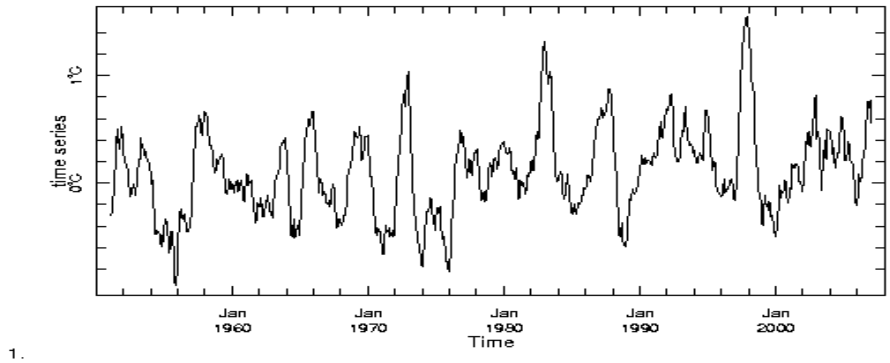

a) Strong inter-annual signal

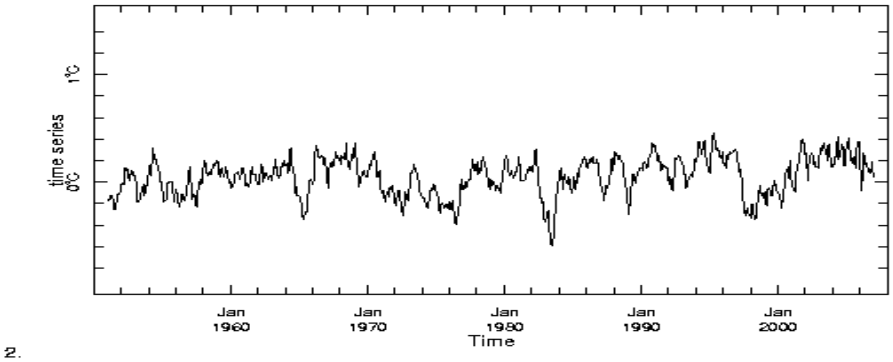

b) Inter-annual mode

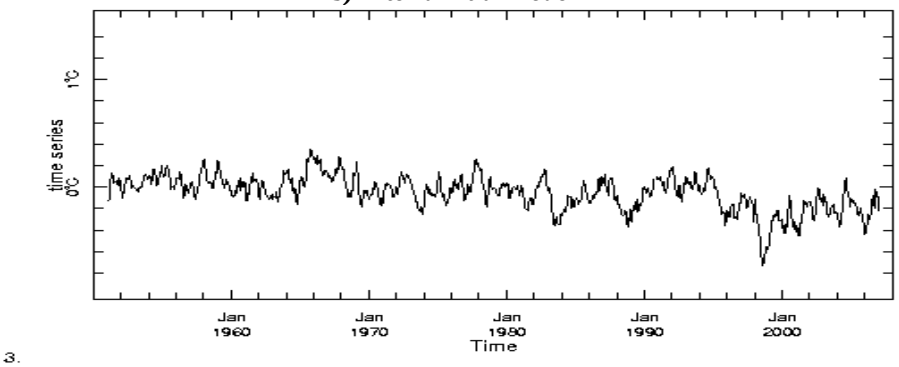

c) Inter-annual mode

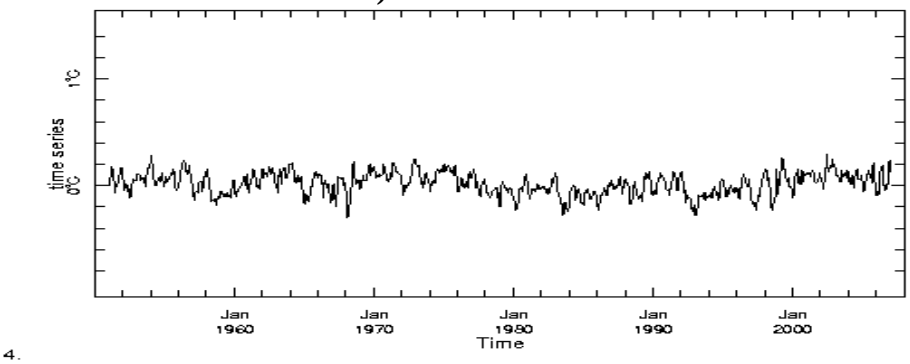

d) Inter-annual mode

Fig. 4.2 The leading temporal structures of SST over Pacific Ocean

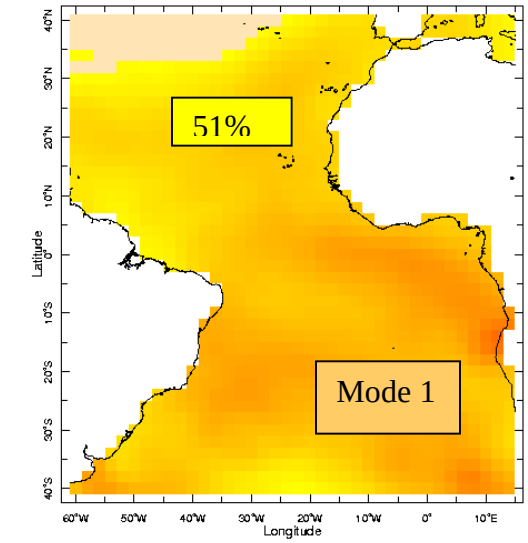

1.

a) A trend structure (Warm Atlantic)

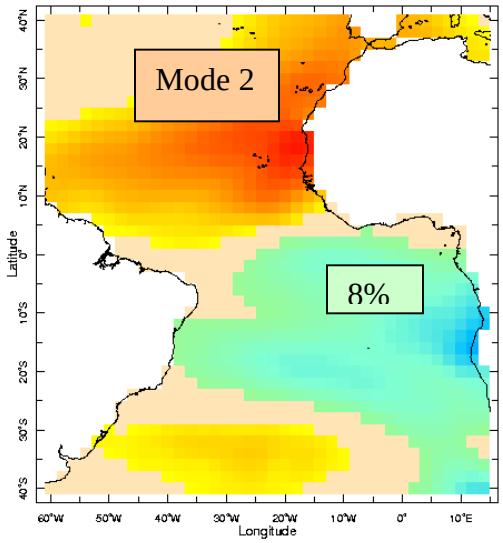

2.

b) N-S equatorial Atlantic dipole

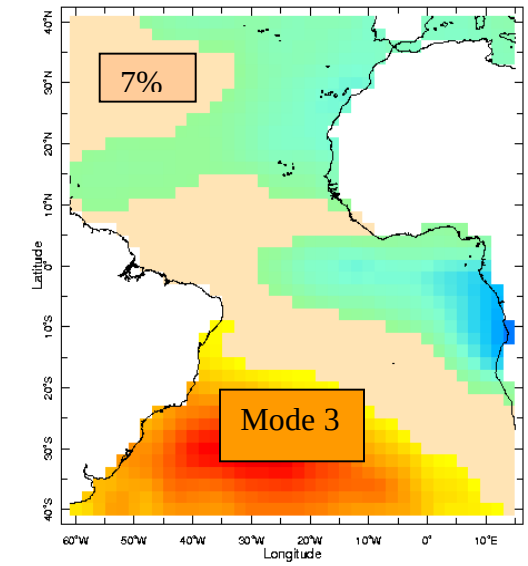

3.

c) Equatorial Atlantic SST mode establishing dipole structure in southern Atlantic Ocean.

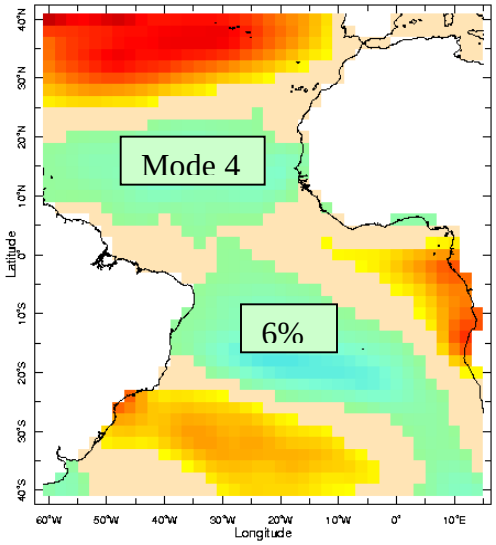

4.

d) A pair of dipole structure in North and southern Atlantic

Fig 4.3 the leading spatial structures of SSTs over Atlantic

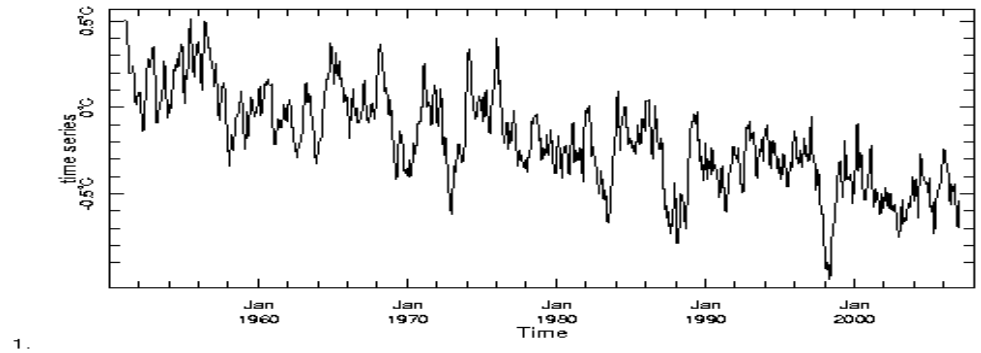

1.

a) Trend structure embedded with

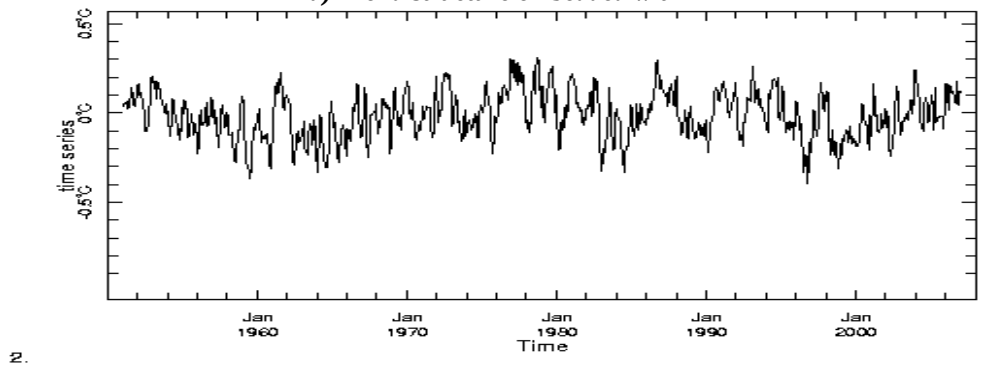

2.

b) Decadal signal

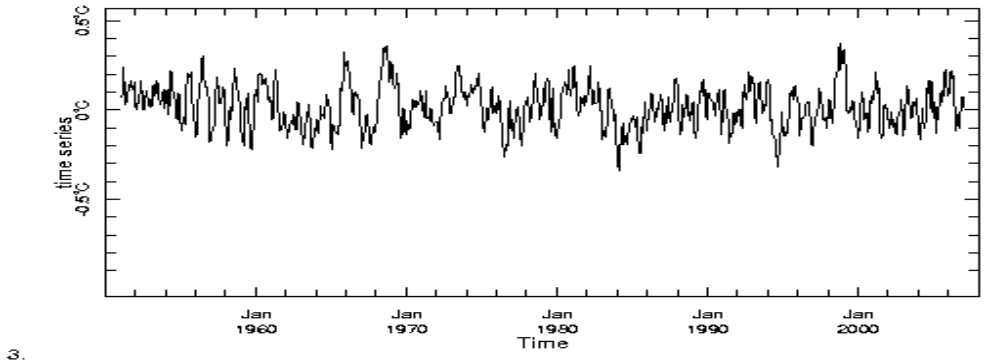

3.

c) Inter-annual mode

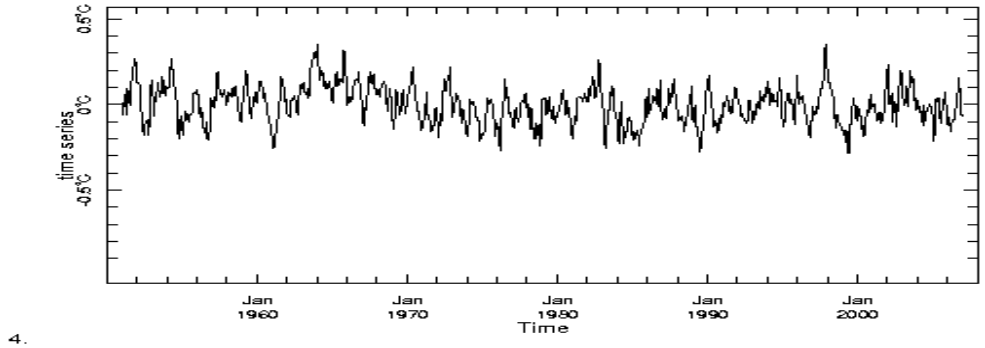

4.

d) Inter-annual mode

Fig.4.4 The leading temporal structures of SST over Atlantic

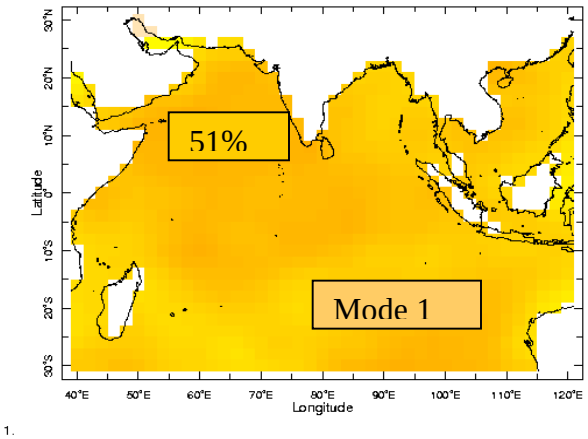

1.

a) A trend mode of Indian Ocean

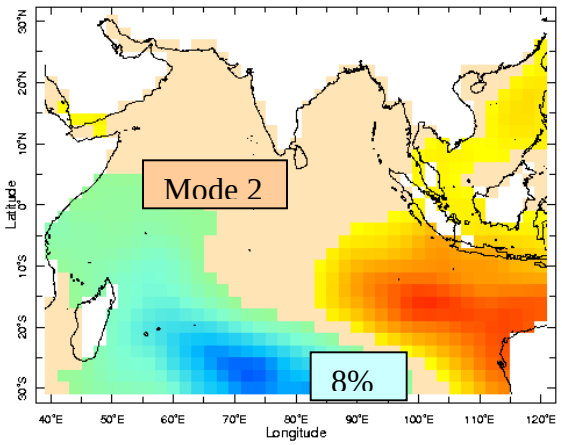

2.

b) IOD dipole (Negative)

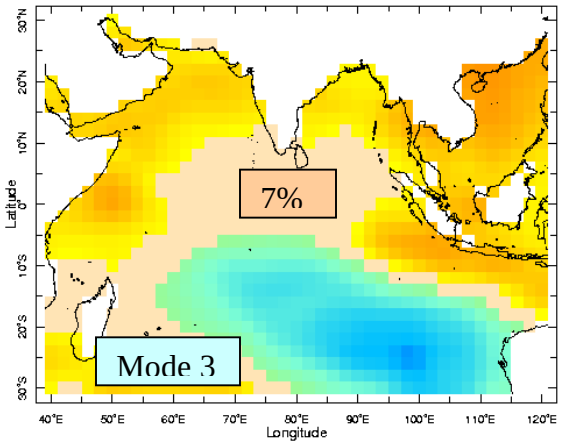

3.

c) Wave like structure of Indian Ocean

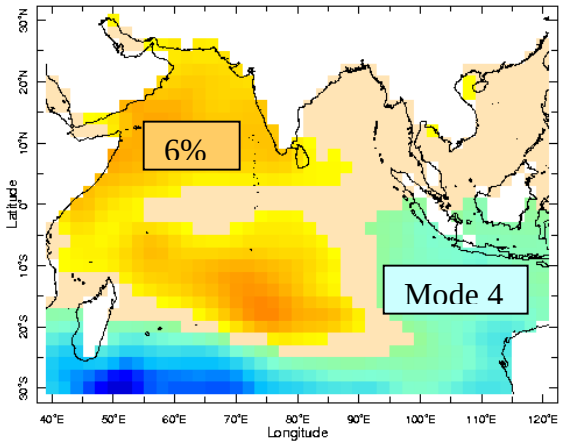

4.

d) Equatorial and eastern dipole mode

Fig. 4.5 The leading spatial structures of SSTs over Indian Ocean

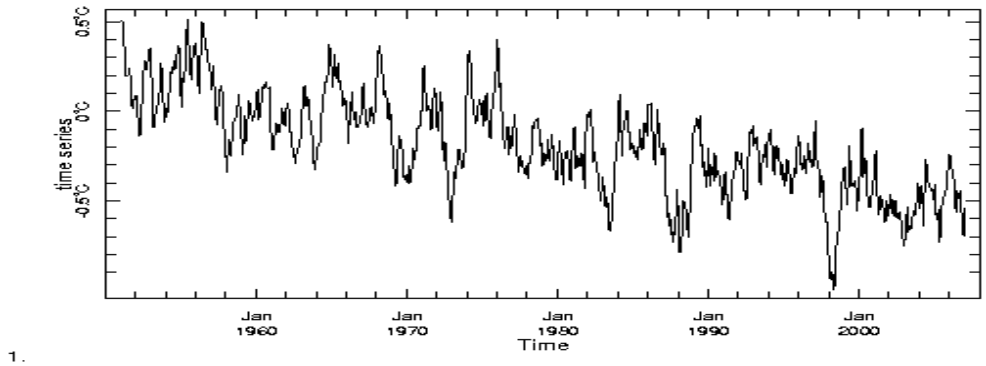

1.

a) Trend structure

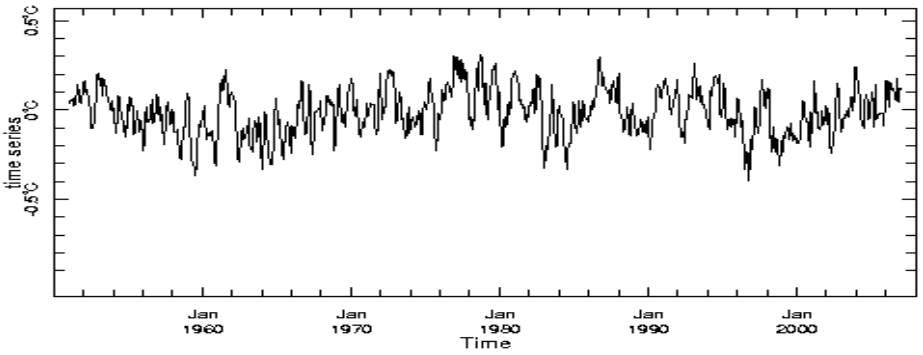

2.

b) Lower frequency in the 60 and 70s

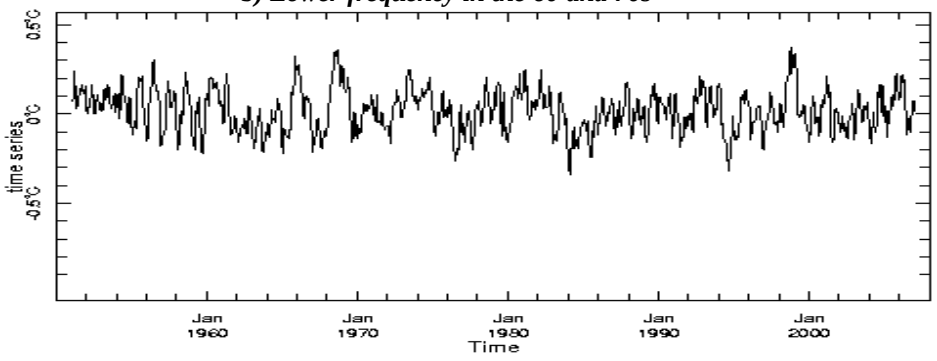

3.

c) Inter-annual mode

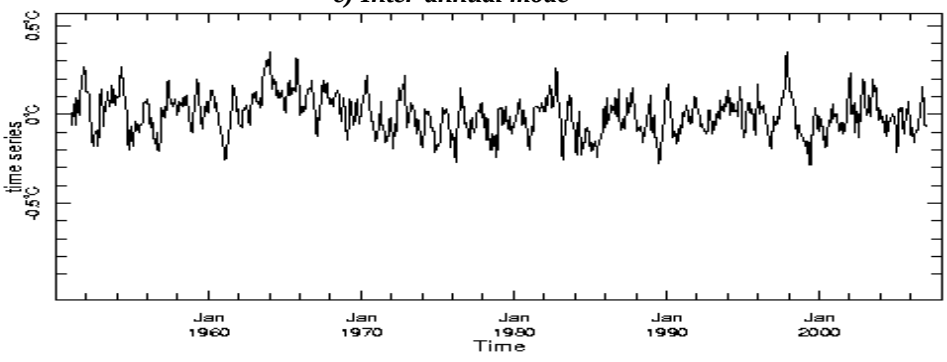

4.

d) Inter-annual mode

Fig. 4.6 The leading temporal structures of SST over Indian Ocean

4.1.2 Tropical Oceans heat content modes

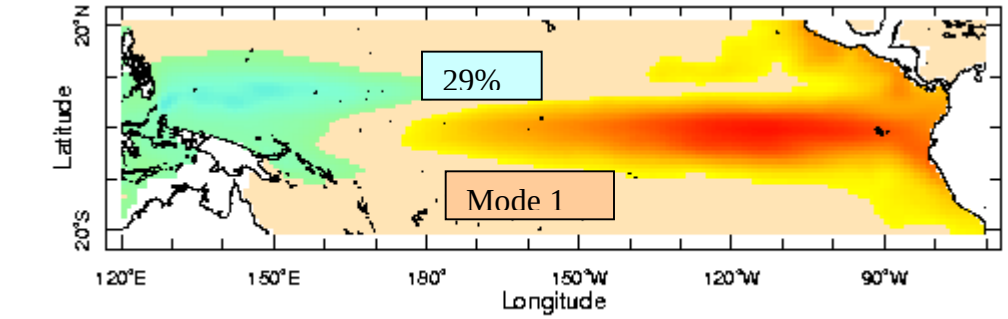

1.

a) ENSO mode (Warm tongue at central and east equatorial Pacific)

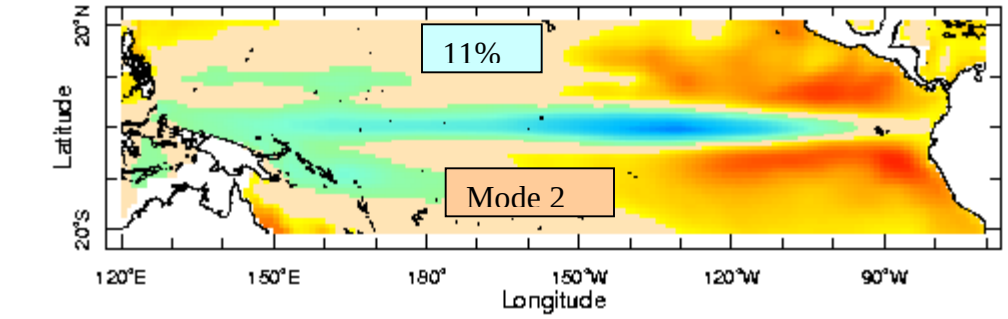

2.

b) The emergence of La Nina condition

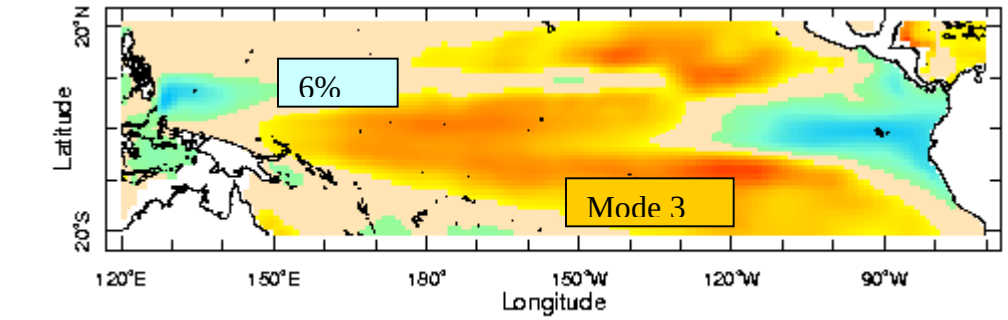

3.

c) La Nina mode

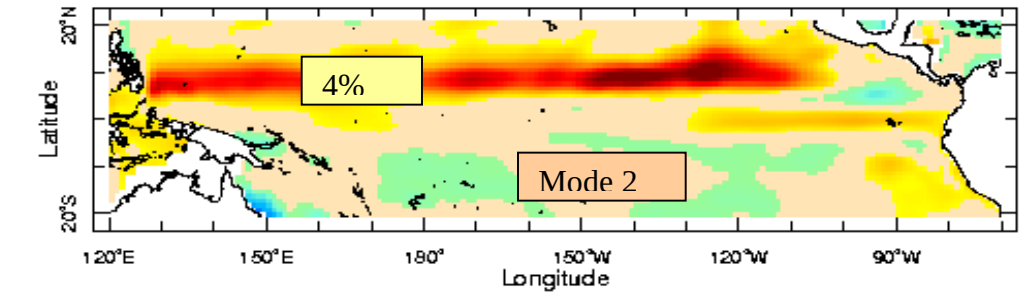

4.

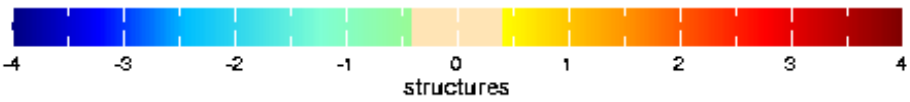

Fig. 4.7 The leading spatial structures of heat content over Pacific Ocean

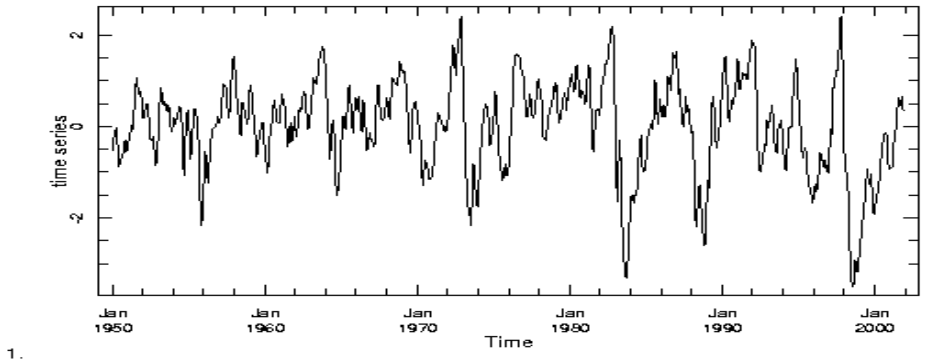

1.

a) Inter-annual mode

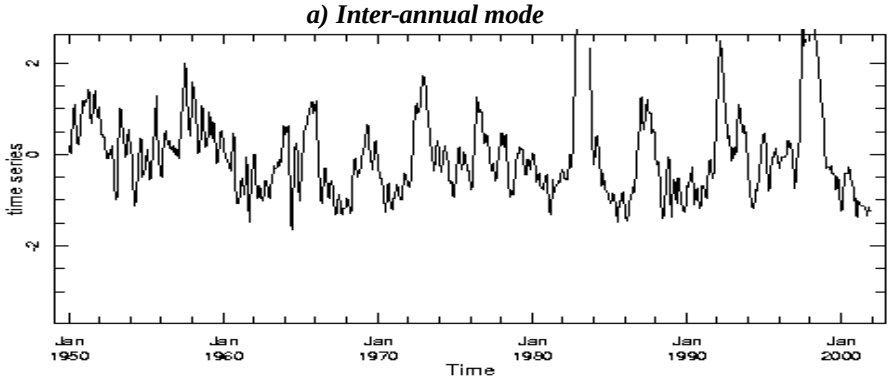

2.

b) Inter-annual mode

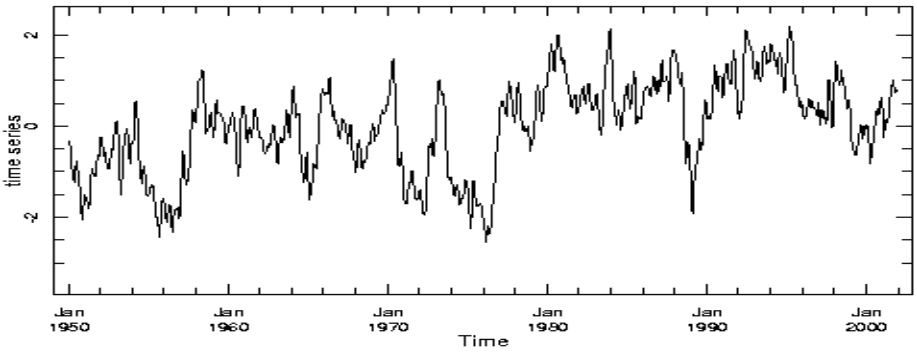

3.

c) Inter-annual Mode

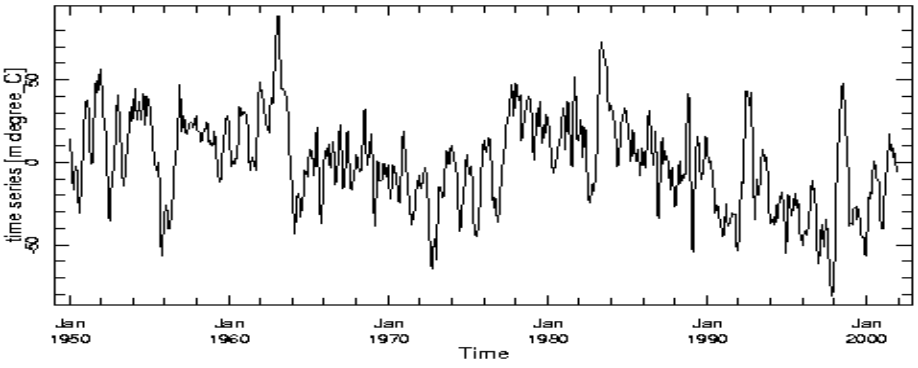

4.

d) Inter-annual M ode

Fig. 4.8 The leading temporal structures of heat content over Pacific Ocean (a, b, c, d, and e)

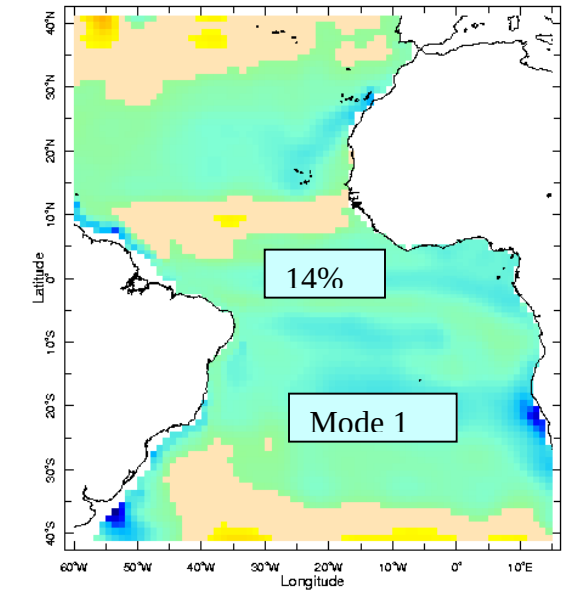

1.

a) Trend mode

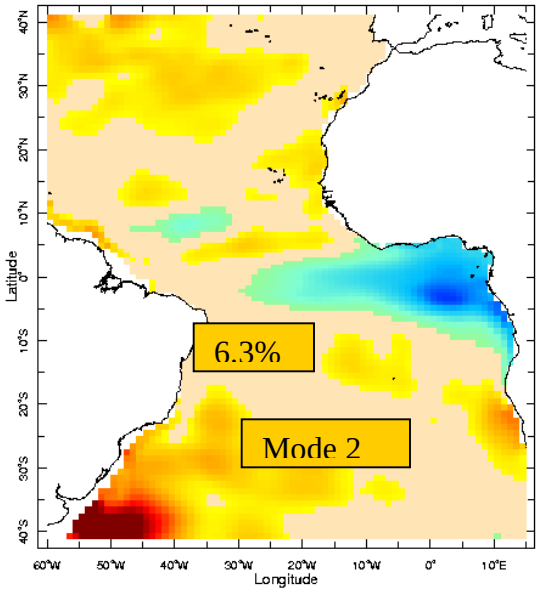

2.

b) East Atlantic cold tongue mode

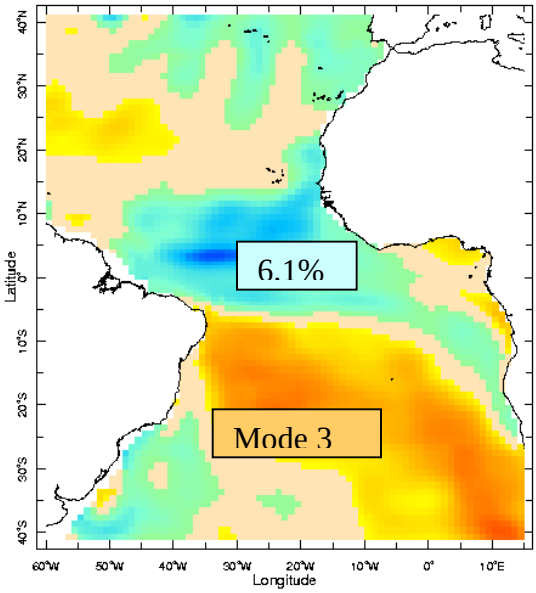

3.

c) Equatorial N-S dipole mode

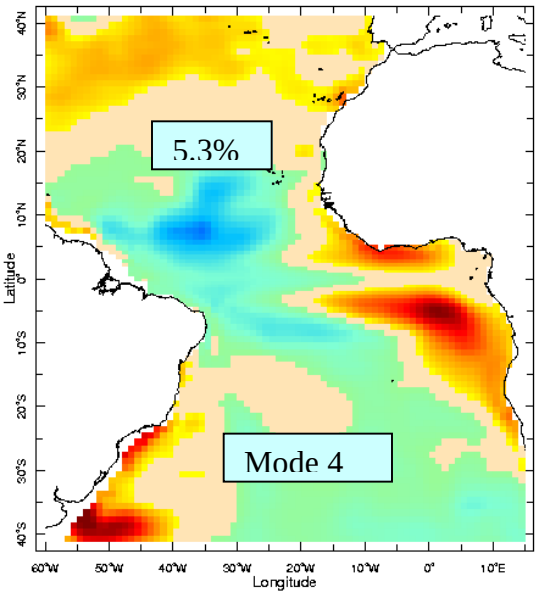

4.

d) Equatorial W-E contrast mode

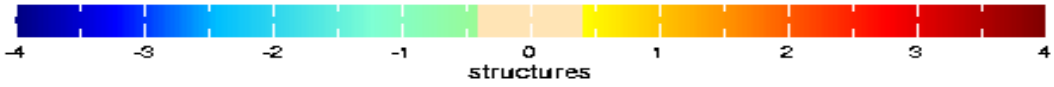

Fig. 4.9 The leading spatial structures of heat content over Atlantic

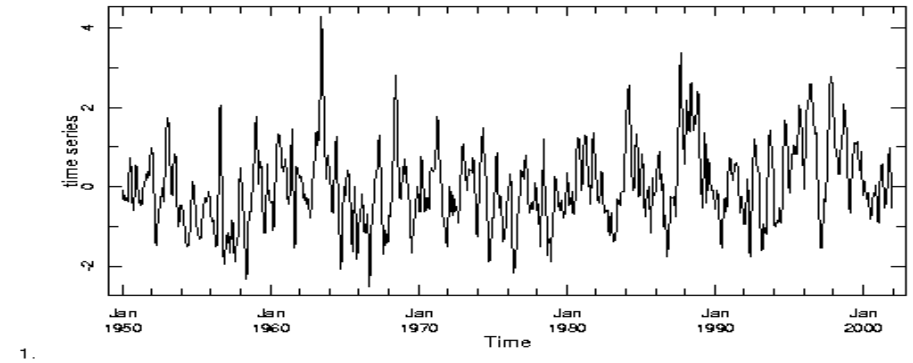

1.

a)Inter-annual

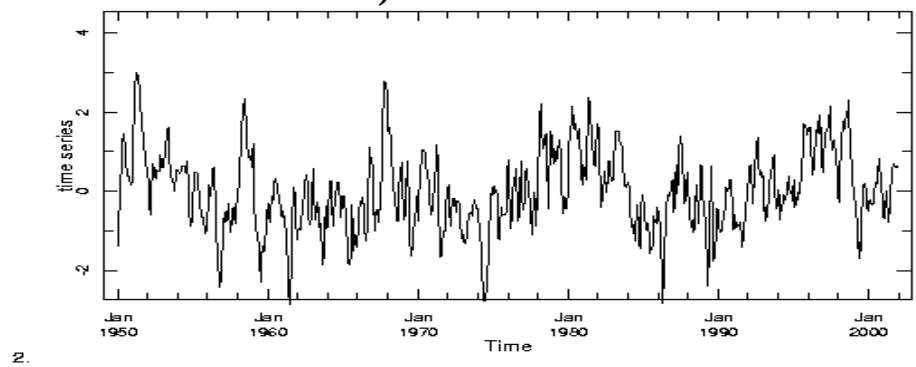

2.

b) Inter-annual Mode

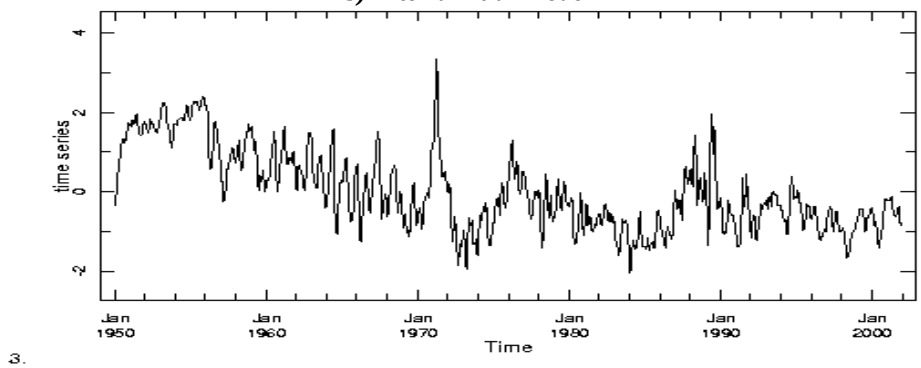

3.

C) Inter-decadal Mode

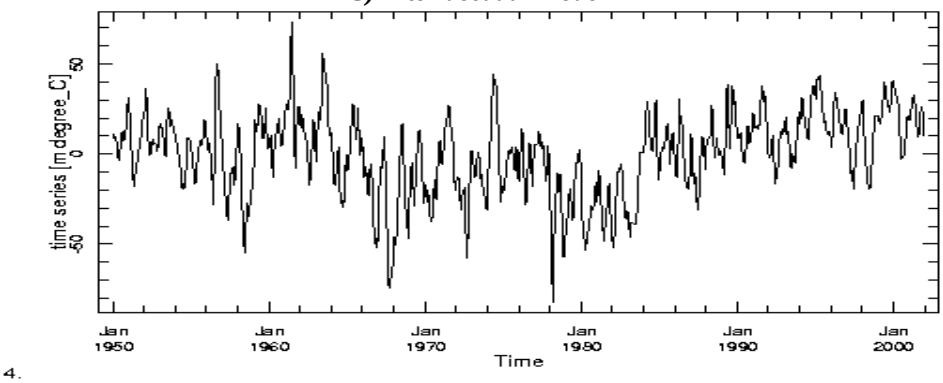

4.

d)) Inter-annual Mode

Fig. 4.10 The leading temporal structures of heat content over Atlantic Ocean (a, b, c and d)

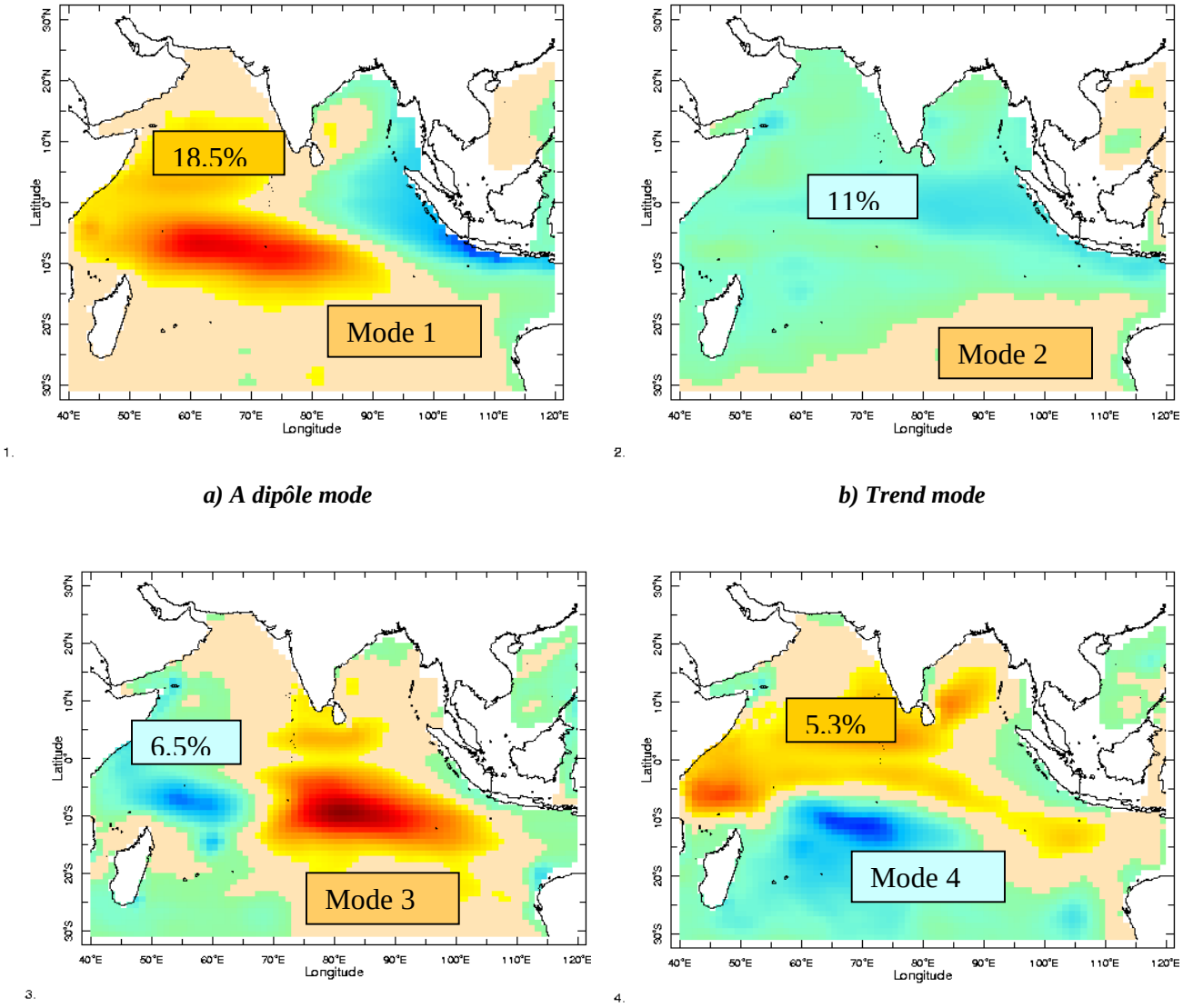

a) A dipôle mode

b) Trend mode

c) IOD-2 type mode

d) équatorial dipôle mode

Fig. 4.11 The leading spatial structures of heat content over Indian Ocean

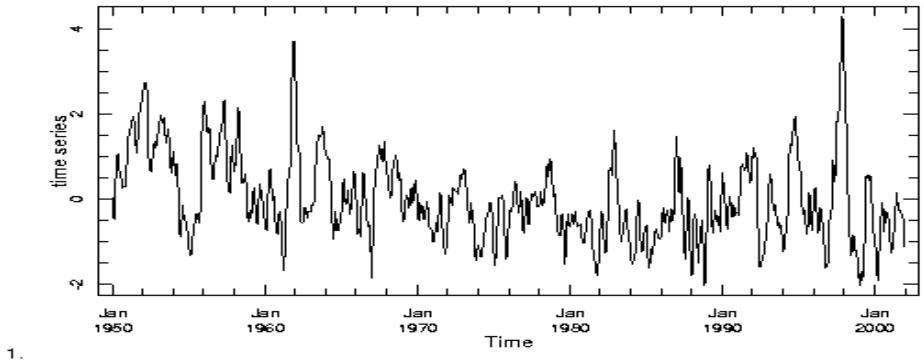

a) Inter-annual Mode

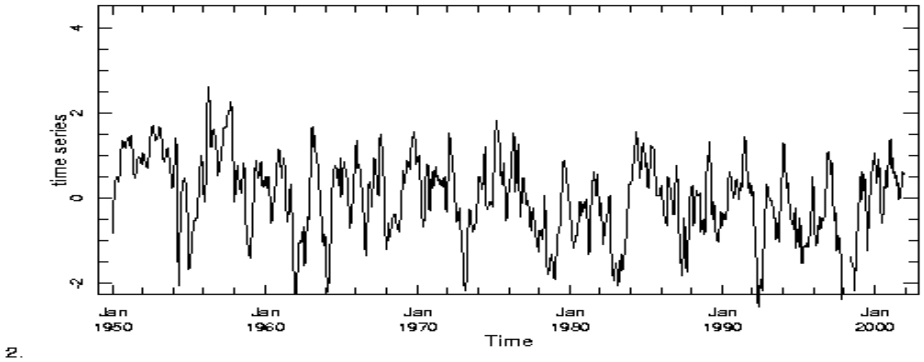

b) Inter-annual Mode

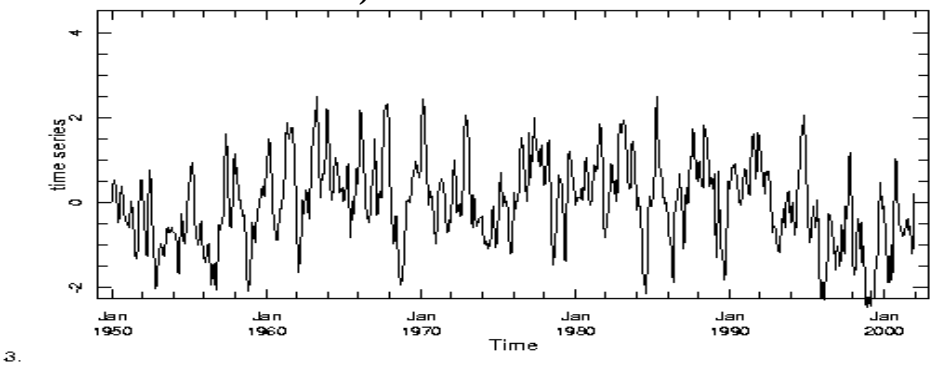

c) Inter-annual Mode

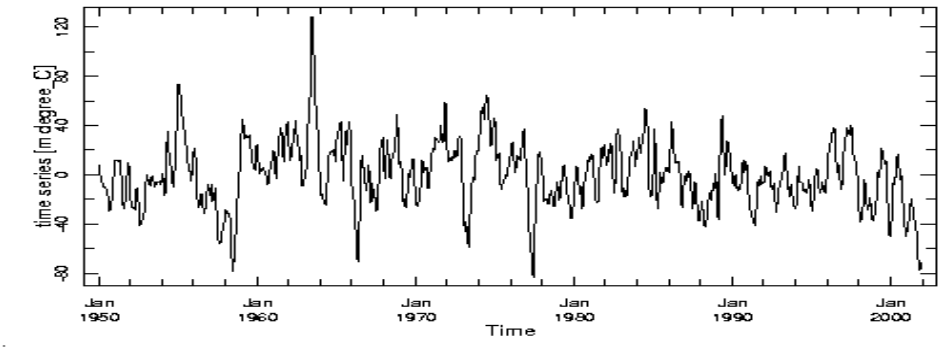

d) Inter-annual Mode

Fig. 4.12 The leading temporal structures of heat content over Indian Ocean

4.2 Ethiopian Rainfall modes

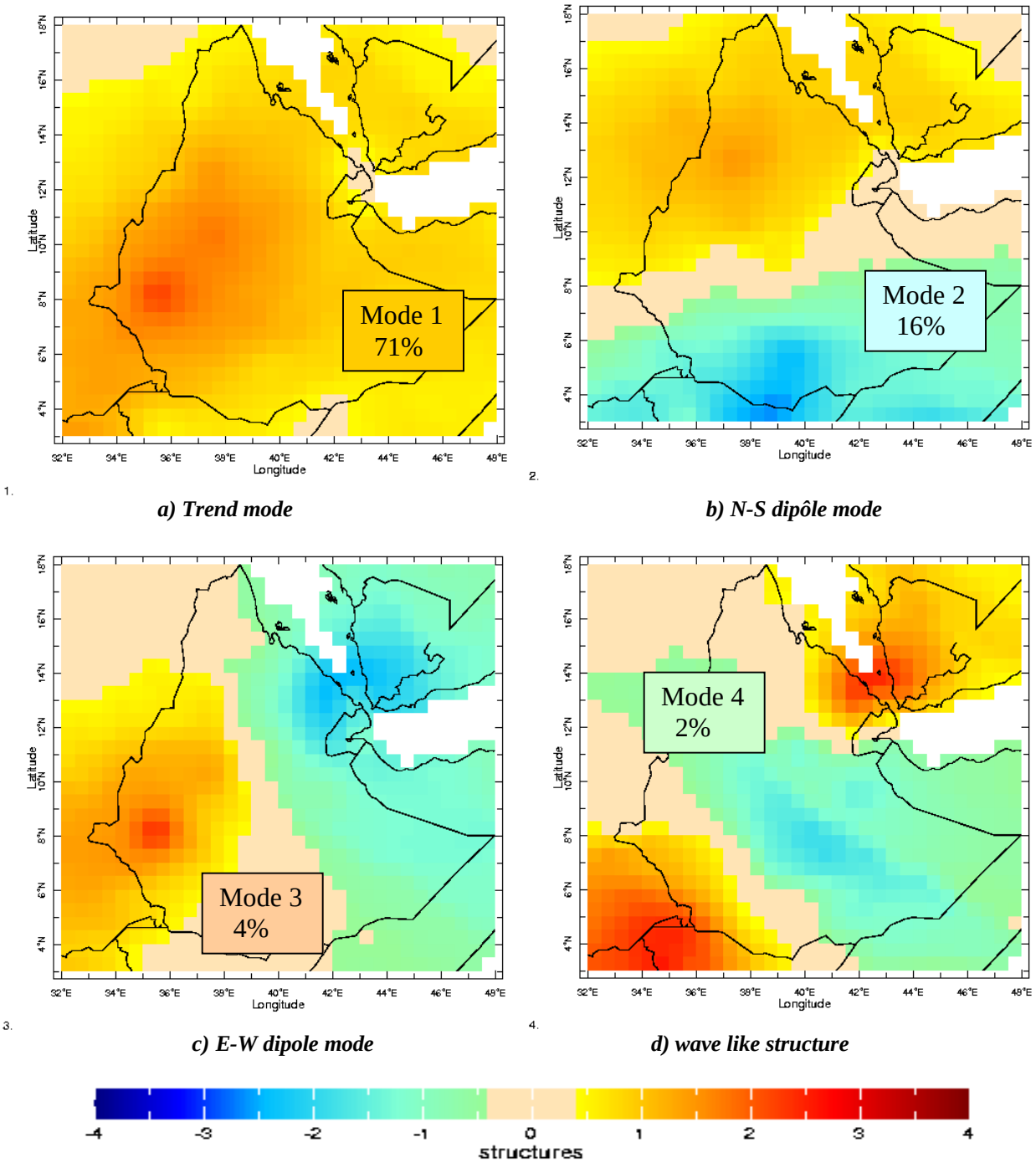

a) Trend mode

b) N-S dipôle mode

c) E-W dipole mode

d) wave like structure

Fig.4.13 The leading Spatial structures of precipitation over Ethiopia

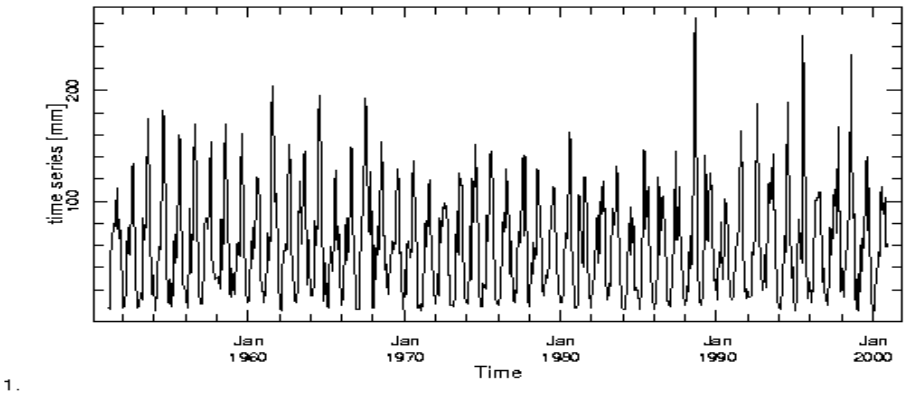

1.

a) Strong Inter-seasonal Mode

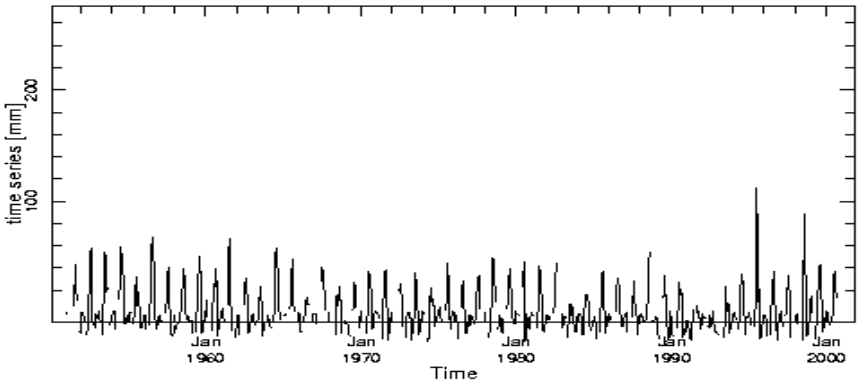

2.

b) Weak Inter-seasonal Mode

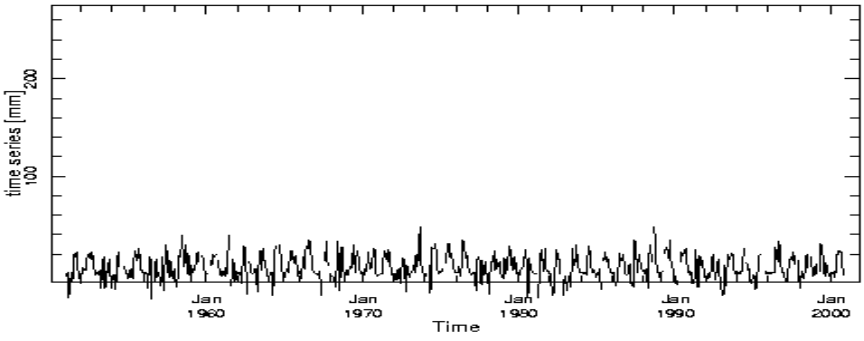

3.

C) Weak inter-seasonal Mode

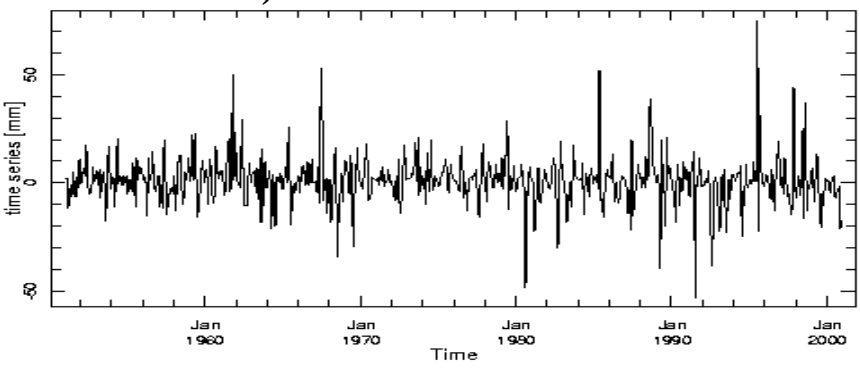

4.

d) Inter-seasonal

Fig.4.13 The leading temporal structure of precipitation over Ethiopia

4.3 Ethiopian vegetation modes

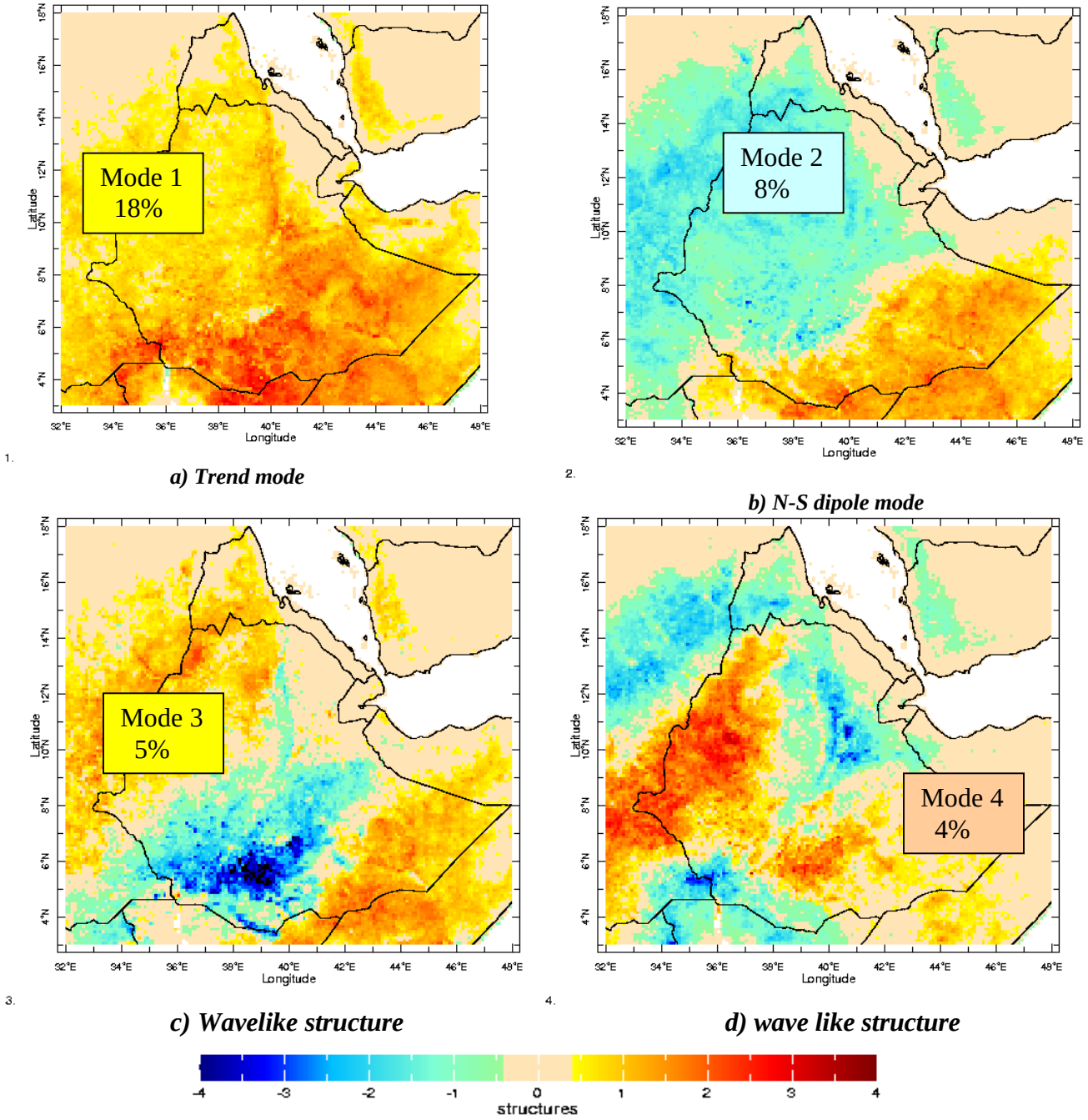

1.

a) Trend mode

2.

b) N-S dipole mode

3.

c) Wavelike structure

4.

d) wave like structure

Fig.4.14 the leading spatial structures of vegetation over Ethiopia

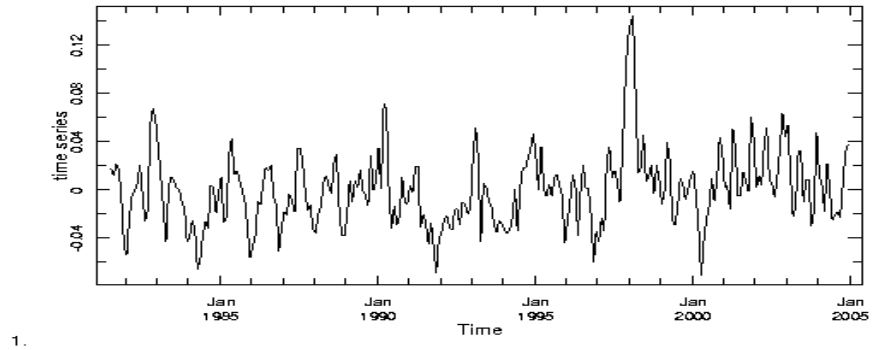

1.

a) Inter-annual mode

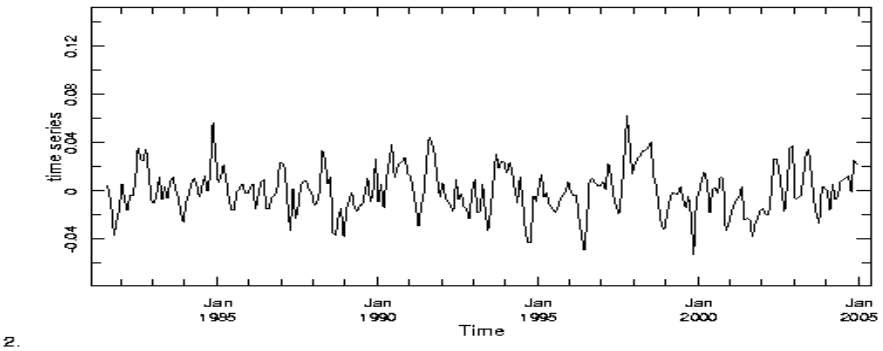

2.

b) Weak Inter-annual mode

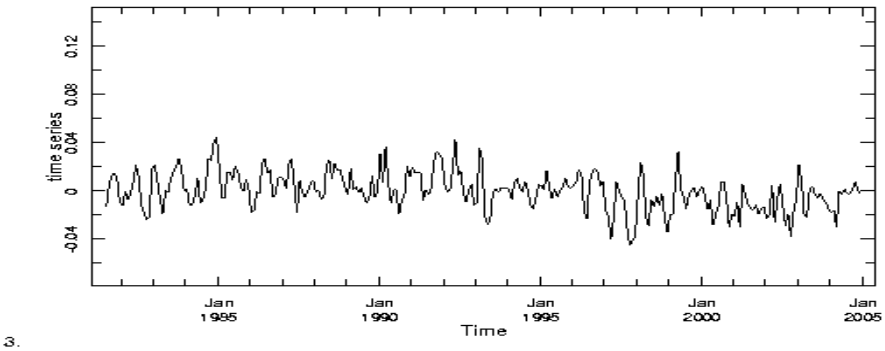

3.

c) Inter-seasonal Mode

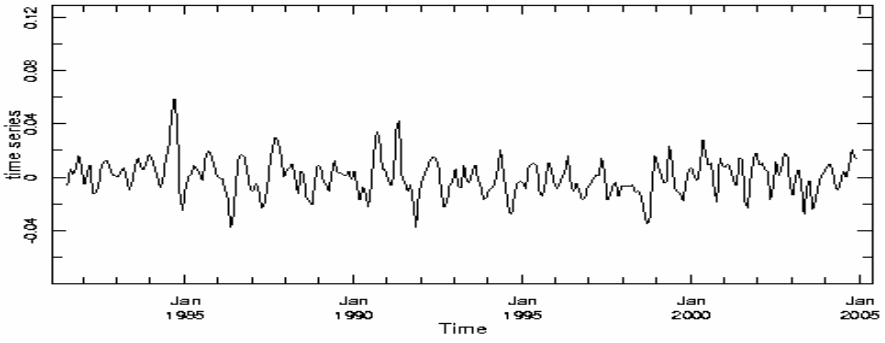

4.

d) Inter-seasonal mode

Fig.4.14 the leading temporal structures of vegetation over Ethiopia (a, b, c, and d)

4.4 Associations between Tropical oceans and Ethiopian climate, hydrology and climate

In this sub-section the associations between different climate variables of the southern part of Ethiopia and tropical oceans SSTs and heat content using correlation are documented. Only values above 90% confidence using a t-test of significant correlation table are marked with red and bold in the correlation tables. The following correlation tables can clearly show the seasonal relationship between SSTs and heat content and different climate variables over Ethiopia.

4.4.1 Association between Indian Ocean SST and Ethiopian Rainfall

The table 4.1 shows the linear correlation between tropical Indian Ocean SST and precipitation over Ethiopia. Values only 90% and above are marked in bold in the table. The tropical Indian Ocean is exhibited correlated strongly with the short rain season of the southern part of Ethiopia. A 99% confidence level is found from the correlation analysis (r=-0.64).The MAM season of the precipitation is also correlated strongly with the simultaneous season of the tropical Indian ocean. Among the different seasons of the tropical Indian Ocean SST December through February is the most significant one in making correlation with the different seasons of precipitation except March through May.

Table 4.1 Correlation between the main mean seasonal precipitation of South Ethiopia and tropical Indian Ocean

		SON			DJF			MAM			JAS		
		I Ind Pc1	*Ind pc2*	*Ind pc3*	*Ind pc1*	*Ind pc2*	*Ind pc3*	*Ind pc1*	*Ind pc2*	*Ind pc3*	*Ind pc1*	*Ind pc2*	*Ind pc3*
	Prcpt pc1	0.140	0.073	**0.406**	0.141	0.152	0.181	0.050	0.055	-0.083	-0.035	0.211	0.118
SON	Prcpt pc2	-0.219	0.052	**-0.640**	-0.188	-0.070	-0.221	-0.009	0.043	0.011	-0.001	-0.174	-0.063
	Prcpt pc3	-0.126	-0.006	**-0.367**	-0.097	0.066	-0.139	-0.025	0.220	0.093	0.037	-0.200	-0.061
	Prcpt pc1	-0.054	0.048	**0.271**	0.106	0.118	**0.451**	0.075	0.165	-0.001	-0.137	**0.299**	0.099
DJF	Prcpt pc2	-0.088	0.127	**-0.376**	-0.197	0.101	**-0.486**	-0.097	0.056	-0.022	0.061	**-0.231**	-0.104
	Prcpt pc3	-0.001	0.115	-0.181	-0.123	0.013	-0.186	-0.148	0.131	0.105	-0.007	-0.195	**-0.364**
	Prcpt pc1	0.114	-0.185	-0.040	0.007	-0.097	-0.099	0.107	**-0.231**	0.000	0.111	-0.063	0.012
MAM	Prcpt pc2	-0.038	0.053	-0.058	0.085	0.042	-0.094	0.010	0.016	-0.219	-0.024	-0.112	-0.147
	Prcpt pc3	-0.161	**0.260**	0.106	-0.057	0.149	0.207	-0.170	**0.351**	0.096	**-0.286**	0.222	-0.032
	Prcpt pc1	**-0.253**	0.151	0.194	**-0.247**	0.099	**0.241**	**-0.482**	0.106	0.136	**-0.372**	**0.350**	-0.086
JAS	Prcpt pc2	**-0.407**	0.098	0.002	**-0.289**	0.215	0.157	**-0.295**	**0.405**	0.100	**-0.243**	**0.263**	**-0.359**
	Prcpt pc3	0.100	0.103	-0.105	0.001	0.002	-0.128	0.127	-0.022	-0.137	0.096	-0.187	0.116

Precp represents for precipitation (rainfall), PCs stand for temporal modes of Atlantic, Indian and Pacific oceans.

4.4.2 Association between Atlantic Ocean SST and Ethiopian Rainfall

The table 4.2 shows the linear correlation between the tropical Atlantic ocean SST and precipitation. The values of this correlation coefficient are marked in bold in the table having 90% and above confidence level (r=-0.241 to r=0.404).

The Table 4.2 also shows the correlation between September through November (SON) precipitation and the subsequent (DJF), the simultaneous (SON), the prior (JAS) and March through May, The values >90% confidence level are marked with red. These show the tropical ocean is strongly correlated with the SON season precipitation with a 99% confidence level(r=0.404)at most and 90% confidence level (r=0.241) but no simultaneous correlation is seen between MAM precipitation and MAM tropical ocean SST only 90%confedence level value correlation is investigated in the SON and DJF seasons of the Ocean SST.

Table 4.2 Correlation between the mean seasonal precipitation of South Ethiopia and tropical Atlantic Ocean

			SON			DJF			MAM			JAS	
		Atl Pc1	*Atl pc2*	*Atl pc3*	*Atl pc1*	*Atl pc2*	*Atl pc3*	*Atl pc1*	*Atl pc2*	*Atl pc3*	*Atl pc1*	*Atl pc2*	*Atl pc3*
	Prcpt pc1	**-0.248**	0.037	-0.187	-0.180	**-0.241**	0.000	-0.108	-0.108	0.021	-0.130	-0.135	**0.251**
SON	Prcpt pc2	**0.371**	**-0.323**	0.217	**0.404**	0.024	-0.022	**0.345**	-0.180	0.043	**0.275**	0.133	**-0.272**
	Prcpt pc3	0.097	-0.102	0.074	**0.316**	0.179	0.063	**0.269**	0.036	-0.011	0.218	0.069	-0.093
	Prcpt pc1	0.166	0.084	0.194	-0.170	0.051	0.173	-0.115	0.078	0.144	0.050	-0.041	**0.293**
DJF	Prcpt pc2	0.061	**-0.273**	0.133	**0.289**	-0.171	0.103	**0.243**	**-0.255**	0.159	0.114	0.051	**-0.251**
	Prcpt pc3	0.079	-0.128	0.151	0.120	0.065	0.017	0.035	-0.041	-0.055	0.061	-0.125	**-0.441**
	Prcpt pc1	-0.027	0.016	0.048	0.175	0.142	0.065	0.038	0.086	-0.082	-0.084	0.076	-0.118
MAM	Prcpt pc2	-0.028	-0.106	-0.026	-0.217	**-0.233**	-0.076	-0.111	-0.190	-0.032	0.006	-0.097	-0.030
	Prcpt pc3	**0.274**	0.085	0.148	-0.046	0.024	0.030	0.019	0.064	0.109	0.181	-0.088	0.003
	Prcpt pc1	-0.003	0.137	-0.082	-0.195	-0.008	0.033	-0.069	0.077	-0.018	0.096	**-0.272**	0.132
JAS	Prcpt pc2	**0.279**	-0.053	-0.156	0.135	-0.099	-0.030	0.202	-0.085	0.114	**0.410**	-0.219	0.075
	Prcpt pc3	-0.017	-0.177	**0.403**	0.181	-0.015	0.137	0.132	-0.114	0.062	-0.019	0.124	-0.034

4.4.3 Association between Pacific Ocean SST and Ethiopian Rainfall

The table 4.3 shows the tropical Pacific Ocean has a strong relationship with the precipitation over Ethiopia. Only values of the correlation coefficient above 95% confidence level are marked in bold in the correlation table and this implies the Pacific Ocean is correlated more strongly than the other two tropical oceans with Ethiopian climate variability. The DJF season particularly has a 99% confidence level correlation coefficient on the season September through November rather than the other seasons. It should be noted that this does not to mean it has no impact on the other three seasons this is clearly put in the table. And we can also understand that most of the correlation coefficients are negative this means the tropical Pacific Ocean has an almost negative correlation with Ethiopian climate variability. The El Niño condition is occurred during this season.

Table 4.3 the correlation between Tropical pacific ocean SST and precipitation over South Ethiopia

			SON			DJF			MAM			JAS	
		Pac Pc1	*Pac pc2*	*Pac pc3*	*Pac pc1*	*Pac pc2*	*Pac pc3*	*Pac Pc1*	*Pac pc2*	*Pac pc3*	*Pac Pc1*	*Pac pc2*	*Pac pc3*
	Prcpt pc1	0.121	-0.267	-0.020	0.123	**-0.375**	-0.215	0.034	-0.180	**-0.309**	-0.038	-0.074	**-0.479**
SON	Prcpt pc2	**-0.454**	0.203	-0.167	**-0.436**	0.223	0.026	-0.174	-0.023	0.182	0.035	-0.009	**0.544**
	Prcpt pc3	**-0.353**	0.120	-0.170	**-0.412**	0.098	0.054	**-0.298**	0.062	**0.284**	-0.097	-0.020	**0.376**
	Prcpt pc1	0.204	0.134	0.211	**0.336**	0.167	**0.390**	**0.345**	0.009	0.238	0.163	-0.020	0.016
DJF	Prcpt pc2	**-0.310**	-0.076	-0.224	**-0.426**	-0.107	-0.293	**-0.438**	-0.006	-0.118	-0.253	-0.071	0.100
	Prcpt pc3	-0.191	-0.064	-0.196	**-0.271**	-0.021	-0.223	**-0.323**	0.024	-0.102	-0.269	0.081	0.137
	Prcpt pc1	-0.197	0.241	-0.148	-0.195	0.017	-0.091	0.005	0.008	-0.053	0.153	0.036	0.061
MAM	Prcpt pc2	0.134	-0.257	-0.012	0.164	-0.097	-0.053	0.076	-0.157	-0.143	-0.042	-0.045	-0.151
	Prcpt pc3	0.166	-0.067	**0.314**	0.203	0.192	**0.332**	0.107	0.118	**0.318**	-0.018	0.065	0.171
	Prcpt pc1	0.262	0.059	**0.315**	0.201	0.099	0.212	-0.121	0.208	0.091	**-0.440**	0.245	-0.196
JAS	Prcpt pc2	-0.082	-0.187	-0.006	-0.131	-0.137	-0.054	**-0.326**	-0.020	0.024	**-0.406**	0.039	-0.079
	Prcpt pc3	-0.259	-0.095	-0.227	-0.246	-0.146	-0.106	-0.034	**-0.272**	-0.028	0.138	-0.213	0.200

4.4.4 Association between Tropical Indian Ocean temporal modes and Awassa lake level

The table 4.4 shows the linear correlation between the tropical Atlantic ocean SST and Lake Awassa water level. The values of this correlation coefficient are listed in the table. Only 99% confidence levels are marked in bold. It is seen from the table that Lake Awassa water level is positively strongly correlated with the tropical Indian Ocean with 99% confidence level.

The table 4.4 also shows the strong correlations between the different modes and seasons of lake's level (SON, DJF, MAM and JAS) and the subsequent, the simultaneous, the prior and the season next to the prior seasons and modes of Indian Ocean SSTs. The values with 99% confidence level only are marked with red and bold. These show that tropical Indian ocean SST is strongly correlated with the Awassa lake level.

Table 4.4 Correlation between the mean seasonal water level of Awassa and Tropical Indian Ocean

		SON			DJF			MAM			JAS		
		Indpc1	**Indpc2**	**Indpc3**	**Indpc1**	**Indpc2**	**Indpc3**	**Indpc1**	**Indpc2**	**Indpc3**	**Indpc1**	**Indpc2**	**Indpc3**
SON	**Awassa**	**0.566**	0.334	-0.092	**0.626**	0.452	-0.061	**0.475**	0.404	-0.204	**0.526**	0.258	-0.273
DJF	**Awassa**	**0.584**	0.324	0.007	**0.695**	0.476	0.043	**0.491**	0.345	-0.238	**0.489**	0.285	-0.214
MAM	**Awassa**	**0.607**	0.266	0.045	**0.734**	0.464	0.139	**0.516**	0.304	-0.241	**0.485**	0.291	-0.185
JAS	**Awassa**	**0.614**	0.268	0.084	**0.738**	0.462	0.202	**0.531**	0.214	-0.273	**0.516**	0.341	-0.217

4.4.5 Association between Tropical Atlantic Ocean SST and Awassa lake level

Table 4.5 shows the linear correlation between the Awassa lake level and tropical Atlantic Ocean SST.Only 99% confidence level values are listed in bold in the table. The Awassa lake level is seen negatively strongly correlated with the Atlantic ocean sea surface temperature (SST) confidence level of the correlation is 99% and the coefficient of correlation ranges from r=-0.451 to r=-580.The different seasons and modes of the lake level have also negative correlation with the different seasons and modes of the tropical Atlantic ocean.

Table 4.5 Correlation between the mean seasonal water level of Awassa and Tropical Atlantic Ocean

		SON			DJF			MAM			JAS		
		Atlpc1	Atlpc2	Atlpc3	Atlpc1	Atlpc2	Atlpc3	Atlpc1	Atlpc2	Atlpc3	Atlpc1	Atlpc2	Atlpc3
SON	**Awassa**	**-0.569**	-0.286	0.092	**-0.508**	-0.352	0.137	**-0.471**	-0.360	0.119	**-0.457**	-0.350	0.094
DJF	**Awassa**	**-0.579**	-0.215	0.081	**-0.549**	-0.329	0.160	**-0.519**	-0.304	0.085	**-0.451**	-0.279	0.144
MAM	**Awassa**	**-0.568**	-0.167	0.063	**-0.580**	-0.278	0.174	**-0.561**	-0.247	0.084	**-0.491**	-0.236	0.190
JAS	**Awassa**	**-0.538**	-0.175	0.076	**-0.548**	-0.299	0.172	**-0.572**	-0.263	0.033	**-0.530**	-0.259	0.186

4.4.6 Association between Tropical pacific ocean SST and Awassa lake level

Table 4.6 shows the linear correlation between Awassa lake level and tropical Pacific Ocean SST.The Awassa lake level is seen negatively strongly correlated with the tropical Pacific Ocean SST.The confidence level of the correlation is 99% and these values are marked in the table in bold. Not only between the simultaneous seasons are the strong correlation but between the subsequent, the prior and the season next to the prior season also found strong correlation. In the table, these values of 99% confidence level are also marked with red and bold.

Table 4.6 Correlation between the mean seasonal water level of Awassa and Tropical Pacific Ocean

		SON			DJF			MAM			JAS		
		Pacpc1	Pacpc2	Pacpc3	Pacpc1	Pacpc2	Pacpc3	Pacpc1	Pacpc2	Pacpc3	Pacpc1	Pacpc2	Pacpc3
SON	Awassa	0.115	0.106	**-0.532**	0.034	0.100	**-0.571**	0.117	0.117	**-0.623**	0.068	0.197	-0.433
DJF	Awassa	0.199	0.043	**-0.491**	0.136	0.037	**-0.552**	0.219	0.063	**-0.605**	0.123	0.151	**-0.461**
MAM	Awassa	0.225	0.064	-0.446	0.186	0.023	**-0.505**	0.297	0.039	**-0.574**	0.176	0.161	**-0.467**
JAS	Awassa	0.217	0.139	-0.449	0.186	0.002	**-0.546**	0.319	-0.002	**-0.610**	0.211	0.167	**-0.508**

4.4.7 Association between Tropical Indian ocean SST and Ethiopian vegetation

Table 4.7 shows the linear correlation among the different seasons and modes of vegetation over Ethiopia and the tropical Indian Ocean SST. Values with 90% and above are marked in bold in the table. Generally, the vegetation is positively strongly correlated with the tropical Indian Ocean SST.The September through November season (SON) of the tropical Indian ocean SST is positively strongly correlated with the simultaneous (SON) season, the subsequent (DJF) and the prior (JAS) and the season before the prior (JAS) (r=0.380 to r=0.564 range).The December through February season of the tropical Indian ocean SST has also a general positive strong correlation except the JAS season that has a negative correlation with r=-0.384. The MAM Indian ocean SST season has a positive strong correlation with the simultaneous MAM, subsequent JAS and prior DJF seasons of the vegetation but it has weak correlation with the SON season of the vegetation over Ethiopia. Finally, the JAS season of the Indian ocean SST has a generally positive correlation with all seasons of the vegetation except the MAM season.

Table 4.7 Correlation between the mean seasonal Ethiopian vegetation and Tropical Indian Ocean SST

		Indpc1	Indpc2	Indpc3	Indpc1	Indpc2	Indpc3	Indpc1	Indpc2	Indpc3	Indpc1	Indpc2	Indpc3
		SON	SON	SON	DJF	DJF	DJF	MAM	MAM	MAM	JAS	JAS	JAS
ndvipc1	SON	**0.435**	0.240	**0.424**	0.285	0.158	0.134	0.042	0.273	0.068	-0.010	**0.392**	-0.058
ndvipc2	SON	-0.134	-0.077	0.215	-0.103	-0.054	0.050	-0.305	-0.285	0.124	-0.337	-0.049	-0.004

ndvipc3	SON	**0.534**	0.288	**0.564**	**0.477**	0.283	0.203	0.163	0.142	-0.047	0.167	**0.636**	0.122
ndvipc1	DJF	**0.400**	0.210	**0.544**	**0.424**	0.124	0.230	-0.003	0.198	-0.194	-0.118	**0.638**	0.003
ndvipc2	DJF	0.112	-0.203	**0.396**	0.159	-0.080	0.180	-0.039	-0.128	0.282	-0.064	0.245	0.156
ndvipc3	DJF	**0.465**	0.225	-0.119	**0.499**	0.309	-0.170	**0.521**	**0.630**	-0.090	**0.698**	0.236	**-0.365**
ndvipc1	MAM	0.271	-0.094	0.033	0.319	0.319	0.234	0.216	0.145	0.047	0.228	0.069	-0.094
ndvipc2	MAM	0.266	**0.426**	0.112	0.279	0.243	-0.059	-0.030	0.155	-0.011	-0.034	0.097	0.150
ndvipc3	MAM	**0.380**	**0.460**	-0.179	**0.431**	0.130	-0.012	0.255	**0.462**	-0.204	0.082	0.223	-0.036
ndvipc1	JAS	0.221	0.109	0.162	0.012	0.234	-0.048	-0.085	-0.016	-0.161	0.146	0.103	-0.185
ndvipc2	JAS	-0.079	-0.111	0.151	-0.102	**-0.384**	0.157	0.031	-0.272	0.365	-0.119	0.027	0.280
ndvipc3	JAS	**0.552**	0.017	-0.229	**0.726**	**0.452**	0.021	**0.629**	**0.496**	-0.031	**0.535**	0.118	0.208

ndvi represents vegetation (normalized difference vegetation index)

4.4.8 Association between Tropical Atlantic Ocean and the Ethiopian vegetation

Table 4.8 shows correlation between Ethiopian vegetation and tropical Atlantic ocean SST.Negative correlation coefficients are found from the table that explain the vegetation and the tropical Atlantic ocean SST are negatively strongly correlated. Values with 90% and above confidence levels are marked in bold. The SON of Atlantic ocean SST is negatively strongly correlated with simultaneous season and with DJF and MAM of the vegetation but correlated weakly with the JAS, the DJF of Atlantic with the DJF and with the SON and MAM but correlated weakly with JAS, the MAM of the Atlantic is correlated strongly with all except JAS having weak positive correlation and the JAS with the JAS and DJF of the vegetation strongly.

Table 4.8 Correlation between the mean seasonal Ethiopian vegetation and Tropical Atlantic Ocean SST

		Atlpc1	*Atlpc2*	*Atlpc3*	*Atlpc1*	*Atlpc2*	*Atlpc3*	*Atlpc1*	*Atlpc2*	*Atlpc3*	*Atlpc1*	*Atlpc2*	*Atlpc3*
		SON	**SON**	**SON**	**DJF**	**DJF**	**DJF**	**MAM**	**MAM**	**MAM**	**JAS**	**JAS**	**JAS**
ndvipc1	SON	**-0.503**	-0.031	-0.010	**-0.437**	-0.290	-0.018	-0.283	-0.174	0.113	**-0.366**	-0.294	0.231
ndvipc2	SON	-0.065	0.091	-0.086	-0.314	-0.115	-0.045	**-0.462**	-0.009	-0.189	-0.124	-0.082	-0.070
ndvipc3	SON	**-0.489**	0.348	0.202	**-0.660**	-0.092	0.167	**-0.641**	0.154	0.196	**-0.629**	-0.094	**0.429**
ndvipc1	DJF	**-0.606**	0.178	-0.036	**-0.761**	-0.010	0.024	**-0.702**	0.099	0.024	**-0.522**	**-0.393**	**0.524**
ndvipc2	DJF	-0.012	**0.399**	-0.326	**-0.486**	0.123	-0.105	**-0.595**	0.299	-0.100	-0.331	0.042	0.220
ndvipc3	DJF	-0.256	-0.189	-0.067	-0.035	-0.034	0.040	-0.101	-0.129	0.351	-0.178	-0.120	0.014
ndvipc1	MAM	-0.070	0.020	0.136	-0.199	0.135	**0.398**	-0.249	0.084	0.212	-0.213	0.137	0.287
ndvipc2	MAM	**-0.366**	-0.166	0.014	**-0.451**	-0.299	0.046	**-0.404**	-0.258	-0.147	-0.229	0.008	0.067
ndvipc3	MAM	**-0.542**	**-0.426**	-0.044	-0.339	**-0.368**	-0.221	-0.190	**-0.447**	-0.011	-0.183	-0.224	-0.014
ndvipc1	JAS	0.034	0.051	-0.152	-0.016	-0.188	0.102	-0.116	-0.071	-0.128	-0.213	-0.050	-0.178
ndvipc2	JAS	0.133	0.125	0.156	0.061	0.182	-0.201	0.029	0.171	0.005	0.041	-0.023	0.187
ndvipc3	JAS	-0.200	-0.066	-0.044	-0.224	-0.130	0.236	-0.222	-0.109	**0.365**	**-0.363**	0.297	0.264

4.4.9 Association between Tropical Pacific Ocean SST and Ethiopian vegetation

Table 4.9 shows the correlation between the vegetation over Ethiopia and the tropical Pacific Ocean SST.The values of correlation coefficient with 90% and above confidence level are marked in bold in the table. The SON of the pacific ocean SST is positively strongly correlated with the SON of the vegetation and a 99% confidence level (r=0.741) correlation with the DJF of the NDVI but is seen weakly correlated with the JAS season of the vegetation. The DJF season of the Pacific Ocean SST has also a similar pattern with the SON season of the tropical pacific above. The MAM season has almost a negative strong correlation with all seasons except the JAS to which there is a weak correlation. The JAS season of the tropical Pacific Ocean SST is negatively strongly correlated with all its simultaneous and other seasons of vegetation over the area in point.

Table 4.9 Correlation between the mean seasonal Ethiopian vegetation and Tropical Pacific Ocean

		Pacpc1	Pcapc2	Pacpc3	Pacpc1	Pacpc2	Pacpc3	Pacpc1	Pacpc2	Pacpc3	Pacpc1	Pacpc2	Pacpc3
		SON	**SON**	**SON**	**DJF**	**DJF**	**DJF**	**MAM**	**MAM**	**MAM**	**JAS**	**JAS**	**JAS**
Ndvipc1	SON	0.105	-0.191	-0.235	0.078	-0.207	**-0.389**	-0.096	-0.016	**-0.494**	-0.205	-0.081	**-0.461**
Ndvipc2	SON	**0.527**	-0.355	0.279	**0.439**	-0.101	0.185	0.310	-0.199	-0.018	0.041	-0.118	-0.355
Ndvipc3	SON	**0.528**	-0.150	0.066	**0.552**	-0.263	-0.136	**0.477**	-0.235	**-0.381**	0.159	-0.213	**-0.522**
Ndvipc1	DJF	**0.550**	**-0.396**	-0.110	**0.512**	**-0.464**	-0.278	**0.393**	**-0.368**	**-0.576**	-0.069	-0.150	**-0.722**
Ndvipc2	DJF	**0.741**	-0.264	**0.423**	**0.669**	-0.083	0.251	**0.426**	-0.042	0.005	0.150	-0.049	-0.423
Ndvipc3	DJF	-0.167	0.180	**-0.418**	-0.209	0.069	**-0.514**	-0.119	0.113	**-0.516**	-0.005	0.183	-0.136
Ndvipc1	MAM	-0.054	**0.383**	-0.057	-0.023	0.155	0.016	0.016	0.228	0.041	0.089	0.156	-0.026
Ndvipc2	MAM	**0.396**	**-0.370**	-0.148	0.201	-0.131	-0.271	-0.083	0.024	**-0.370**	-0.189	-0.162	**-0.375**
Ndvipc3	MAM	-0.029	-0.206	**-0.405**	-0.149	-0.156	**-0.532**	-0.107	-0.174	**-0.644**	-0.014	-0.197	**-0.384**
Ndvipc1	JAS	0.118	-0.130	0.003	-0.011	-0.166	-0.190	-0.126	-0.078	-0.303	-0.213	0.080	-0.200
Ndvipc2	JAS	0.034	-0.114	0.093	0.145	-0.095	0.186	0.210	-0.224	0.303	0.285	**-0.429**	0.004
Ndvipc3	JAS	-0.037	0.323	-0.085	-0.006	0.099	0.019	0.221	0.151	-0.017	**0.434**	0.026	-0.021

4.4.10 Association between vegetation and Rainfall over Ethiopia

Table 4.10 shows the linear correlation between vegetation and Precipitation. Positive and negative strong correlations are found from the correlation table. The SON season of precipitation has a strong correlation with all seasons of the vegetation except JAS season. The DJF season of precipitation is also correlated with all seasons of the vegetation except the JAS.The MAM season is only strongly correlated with the MAM season of the vegetation. The JAS season of the precipitation is strongly correlated with all seasons.

Table 4.10 Correlation between the mean seasonal vegetation and Precipitation

		Prsppc1	Prcppc2	Prcppc3	Prcppc1	Prcppc2	Prcppc3	Prcppc1	Prcppc2	Prcppc3	Prcppc1	Prcppc2	Prcppc3
		SON	SON	SON	DJF	DJF	DJF	MAM	MAM	MAM	JAS	JAS	JAS
ndvipc1	SON	**0.590**	**-0.514**	**-0.407**	0.126	-0.065	-0.129	0.125	-0.239	-0.135	0.110	**0.501**	-0.312
ndvipc2	SON	0.172	**-0.422**	-0.312	0.113	-0.193	-0.021	-0.284	0.276	0.075	0.175	-0.170	0.002
ndvipc3	SON	**0.650**	**-0.631**	**-0.515**	0.356	-0.321	-0.245	-0.179	0.003	0.205	0.327	0.272	-0.372
ndvipc1	DJF	**0.853**	**-0.891**	**-0.481**	**0.423**	**-0.541**	**-0.441**	-0.144	0.028	0.137	**0.365**	**0.417**	**-0.415**
ndvipc2	DJF	0.226	**-0.531**	**-0.416**	0.129	-0.240	0.013	-0.213	0.127	0.150	0.341	0.279	**-0.447**
ndvipc3	DJF	0.058	-0.011	0.134	-0.354	0.391	**0.444**	-0.159	0.072	0.027	-0.023	**0.561**	-0.297
Ndvipc1	MAM	0.051	-0.179	-0.009	**0.524**	-0.230	-0.131	**0.443**	**-0.632**	-0.262	0.108	0.254	-0.203
ndvipc2	MAM	0.276	**-0.400**	-0.105	-0.145	0.174	0.253	-0.334	0.041	-0.032	0.296	**0.443**	-0.252
ndvipc3	MAM	**0.520**	**-0.370**	-0.095	-0.162	-0.063	-0.175	-0.304	0.296	0.214	0.057	0.158	0.111
Ndvipc1	JAS	0.039	0.000	-0.270	**-0.417**	0.360	**0.453**	0.140	-0.040	-0.146	0.241	**0.450**	-0.203
ndvipc2	JAS	0.178	-0.199	-0.096	**0.374**	-0.353	-0.307	0.175	-0.106	0.014	**-0.451**	**-0.386**	0.337
ndvipc3	JAS	0.156	-0.166	0.281	0.191	-0.068	-0.150	-0.018	-0.263	0.083	0.105	0.305	-0.269

4.4.11 Association between Tropical Indian Ocean heat content and Ethiopian Rainfall

Table 4.11 shows the linear correlation between precipitation over Ethiopia and tropical Indian Ocean heat content (hc125).The precipitation is correlated strongly with the indicated ocean heat content. Only values with 95% and above are marked in bold in the table. In general the precipitation has a negative strong correlation with the ocean heat content (r_{max}=-0.748 correlation coefficient which is in 99% confidence level) except the MAM season to which the Indian Ocean heat content is correlated weakly. The SON of the ocean to the SON of the precipitation, the DJF of the ocean to the SON and the DJF exhibit stronger correlation showing 99% confidence level(r=0.6,-0.748,-0.662 and-0.522 among others).As a conclusion the Indian ocean is strongly correlated to the precipitation over Ethiopia.

Table 4.11 the correlation between Tropical Pacific Ocean heat content and precipitation over Ethiopia

		Indpc1	Indpc2	Indpc3	Indpc1	Indpc2	Indpc3	Indpc1	Indpc2	Indpc3	Indpc1	Indpc2	Indpc3
		SON	SON	SON	DJF	DJF	DJF	MAM	MAM	MAM	JAS	JAS	JAS
Precpc1	SON	**0.600**	-0.035	0.044	**0.480**	-0.074	-0.265	0.154	-0.158	-0.233	0.154	-0.007	**-0.447**
Precpc2	SON	**-0.748**	-0.009	-0.182	**-0.662**	0.125	0.262	**-0.372**	**0.304**	**0.338**	-0.113	0.198	**0.411**
Precpc3	SON	**-0.391**	-0.131	-0.032	**-0.384**	0.084	0.104	-0.232	**0.321**	0.128	-0.150	0.194	0.053
Precpc1	DJF	0.131	0.240	-0.203	**0.317**	-0.010	-0.139	**0.274**	-0.054	-0.005	-0.051	-0.030	-0.078
Precpc2	DJF	**-0.332**	-0.094	-0.106	**-0.522**	0.023	0.114	**-0.453**	0.129	0.094	0.006	0.142	0.198
Precpc3	DJF	-0.162	0.005	-0.207	**-0.324**	-0.002	0.025	**-0.331**	0.136	0.136	-0.085	0.095	**0.399**
Precpc1	MAM	-0.244	-0.195	-0.144	-0.188	0.105	0.007	-0.008	0.011	0.157	-0.054	-0.050	0.245
Precpc2	MAM	0.054	0.125	-0.076	0.014	-0.096	-0.018	-0.163	0.014	-0.146	-0.004	0.056	-0.254

Precpc3	**MAM**	0.137	**0.385**	-0.042	0.144	0.085	0.030	0.130	0.176	0.013	0.128	0.162	-0.047
Precpc1	**JAS**	**0.370**	0.158	0.076	**0.277**	-0.025	-0.048	0.241	0.004	-0.097	0.103	-0.070	0.038
Precpc2	**JAS**	0.200	**0.376**	-0.126	0.195	0.271	**-0.393**	-0.014	0.218	-0.271	**-0.299**	0.235	-0.129
Precpc3	**JAS**	**-0.489**	-0.183	-0.148	**-0.381**	-0.140	0.256	-0.273	0.032	0.267	-0.072	0.096	0.070

4.4.12 Association between Tropical Atlantic Ocean heat content and Ethiopian Rainfall

Table 5.12 shows the linear correlation between the precipitation over Ethiopia and the Atlantic Ocean heat content. The values with 90% and above are marked in bold in the table. The precipitation is seen correlated linearly with the Atlantic Ocean heat content but the confidence level is lower than the heat content of the Pacific Ocean. The SON and JAS of the heat content are correlated weakly with the DJF of the precipitation.

Table 4.12 the correlation between Tropical Atlantic ocean hc125 and precipitation over Ethiopia

		Atlpc1	Atlpc2	Atlpc3	Atlpc1	Atlpc2	Atlpc3	Atlpc1	Atlpc2	Atlpc3	Atlpc1	Atlpc2	Atlpc3
		SON	SON	SON	DJF	DJF	DJF	MAM	MAM	MAM	JAS	JAS	JAS
Precpc1	**SON**	-0.185	-0.150	-0.163	-0.151	0.093	0.060	-0.203	0.103	0.004	-0.157	-0.066	-0.057
Precpc2	**SON**	**0.261**	0.139	0.051	**0.325**	0.058	-0.175	**0.362**	-0.079	-0.035	**0.250**	0.100	0.076
Precpc3	**SON**	0.129	-0.028	0.202	0.163	-0.190	0.111	**0.238**	**-0.241**	0.204	**0.263**	0.023	0.227
Precpc1	**DJF**	0.134	0.033	-0.020	0.076	-0.009	-0.090	0.077	0.203	-0.065	0.109	0.108	-0.066
Precpc2	**DJF**	-0.014	0.042	0.036	0.098	0.025	-0.002	0.144	**-0.240**	0.033	0.126	0.027	0.132
Precpc3	**DJF**	0.078	0.024	0.161	0.050	**-0.261**	0.080	0.065	**-0.363**	0.065	0.138	-0.031	0.203
Precpc1	**MAM**	-0.121	-0.155	0.128	-0.050	-0.076	0.222	-0.086	-0.224	0.248	-0.059	-0.183	0.104
Precpc2	**MAM**	0.009	0.113	-0.065	-0.110	0.190	-0.155	-0.061	**0.410**	-0.138	-0.061	**0.258**	-0.073
Precpc3	**MAM**	**0.290**	0.210	-0.146	**0.244**	0.053	**-0.309**	0.186	0.219	**-0.390**	0.200	0.146	-0.157
Precpc1	**JAS**	0.060	**-0.252**	-0.126	0.162	-0.132	-0.129	0.226	-0.105	-0.170	0.077	-0.223	-0.179
Precpc2	**JAS**	0.138	-0.194	-0.228	**0.290**	-0.107	**-0.325**	**0.270**	0.009	**-0.292**	0.121	0.058	-0.200
Precpc3	**JAS**	0.020	0.129	**0.311**	-0.034	-0.042	**0.276**	-0.019	-0.085	**0.252**	0.172	0.123	**0.299**

4.4.13 Association between Tropical Pacific Ocean heat content and Ethiopian Rainfall

Table 4.13 shows the linear correlation between the tropical Pacific Ocean heat content and the precipitation over Ethiopia. A generally negative strong correlation is exhibited between the precipitation and the pacific heat content with the simultaneous, the subsequent, the prior and the season before the prior with some exceptions. The MAM season of the precipitation is only correlated strongly with the simultaneous season of the tropical Pacific Ocean heat content but has weak correlation with the other seasons of the ocean heat content and also weak correlation is seen between the DJF of the ocean heat content and the JAS and MAM of the precipitation.

Table 4.13 Correlation between Tropical Pacific Ocean hc125 and precipitation over Ethiopia

		Pacpc1	Pacpc2	Pacpc3	Pacpc1	Pacpc2	Pacpc3	Pacpc1	Pacpc2	Pacpc3	Pacpc1	Pacpc2	Pacpc3
		SON	SON	SON	DJF	DJF	DJF	MAM	MAM	MAM	JAS	JAS	JAS
Precpc1	**SON**	0.196	0.033	-0.195	0.058	**0.295**	**-0.402**	-0.056	0.150	**-0.278**	-0.221	0.197	-0.163
Precpc2	**SON**	**-0.468**	-0.004	-0.026	**-0.383**	**-0.407**	0.230	-0.081	**-0.365**	0.078	**0.291**	**-0.337**	0.060
Precpc3	**SON**	**-0.447**	0.112	-0.136	**-0.339**	**-0.358**	0.136	-0.191	**-0.377**	0.067	0.067	**-0.508**	0.093
Precpc1	**DJF**	0.247	-0.197	0.035	**0.416**	-0.099	-0.077	**0.423**	0.125	-0.046	0.084	0.217	-0.069
Precpc2	**DJF**	**-0.361**	0.057	-0.157	**-0.448**	-0.118	-0.002	**-0.401**	**-0.284**	-0.055	-0.083	**-0.352**	-0.082
Precpc3	**DJF**	-0.232	0.028	-0.127	-0.269	-0.128	0.086	**-0.383**	-0.174	0.007	-0.168	**-0.370**	0.063
Precpc1	**MAM**	-0.176	-0.021	0.144	-0.169	-0.067	0.095	0.086	-0.193	0.186	0.131	-0.079	0.131
Precpc2	**MAM**	0.123	0.134	-0.194	0.083	0.183	-0.174	-0.058	**0.306**	**-0.282**	-0.030	0.180	-0.125
Precpc3	**MAM**	0.185	-0.057	-0.142	0.225	-0.060	-0.086	0.062	0.123	-0.060	0.065	0.025	-0.107
Precpc1	**JAS**	**0.295**	-0.085	0.051	0.190	0.128	-0.001	-0.209	0.211	0.069	**-0.448**	0.115	-0.164
Precpc2	**JAS**	-0.022	-0.004	**-0.325**	-0.132	0.075	-0.193	**-0.340**	0.043	-0.098	**-0.311**	-0.130	**-0.294**
Precpc3	**JAS**	**-0.296**	0.045	-0.129	-0.220	-0.213	-0.105	0.088	-0.266	-0.188	0.204	-0.179	0.015

4.4.14 Association between Tropical Pacific Ocean and Ethiopian vegetation

Table 4.14 shows the linear correlation between the vegetation and tropical Pacific Ocean heat content. Values 90% and above are marked with in bold in the table. The SON season of the heat content has positive strong correlation with the SON and DJF seasons of the NDVI over Ethiopia and a negative correlation with the MAM season of the NDVI over Ethiopia. But this same season of the ocean heat content has weak correlation with the JAS season of the NDVI over the Ethiopia. The JAS season of the vegetation is also weakly correlated with the simultaneous season of the heat content. The rest of the positive and negative strong correlations between vegetation and heat content are listed in the table below.

Table 4.14 the correlation between Tropical Pacific Ocean hc125 and vegetation over Ethiopia

		Pacpc1	**Pacpc2**	**Pacpc3**	**Pacpc1**	**Pacpc2**	**Pacpc3**	**Pacpc1**	**Pacpc2**	**Pacpc3**	**Pacpc1**	**Pacpc2**	**Pacpc3**
		SON	**SON**	**SON**	**DJF**	**DJF**	**DJF**	**MAM**	**MAM**	**MAM**	**JAS**	**JAS**	**JAS**
ndvipc1	**SON**	0.047	-0.014	-0.302	-0.112	**0.386**	-0.350	-0.259	0.147	-0.237	**-0.400**	0.141	**-0.381**
ndvipc2	**SON**	**0.500**	-0.022	-0.120	**0.423**	0.345	-0.232	0.260	**0.429**	-0.239	-0.088	**0.394**	-0.182
ndvipc3	**SON**	**0.567**	-0.145	-0.161	**0.418**	**0.509**	**-0.526**	0.185	**0.532**	**-0.370**	-0.212	**0.641**	**-0.514**
ndvipc1	**DJF**	**0.526**	0.007	**-0.384**	0.346	**0.609**	**-0.663**	0.119	**0.573**	**-0.515**	**-0.429**	**0.614**	**-0.519**
ndvipc2	**DJF**	**0.739**	-0.242	-0.034	**0.647**	**0.382**	-0.209	0.324	**0.575**	-0.048	-0.011	**0.490**	-0.284
ndvipc3	**DJF**	-0.137	0.007	-0.055	-0.274	0.036	-0.012	**-0.386**	-0.071	0.069	-0.023	-0.215	0.068
ndvipc1	MAM	-0.031	**-0.414**	0.166	0.043	-0.274	0.036	0.089	-0.260	0.298	0.081	-0.088	0.139
ndvipc2	MAM	0.245	0.181	**-0.384**	0.031	**0.467**	-0.156	-0.255	0.309	-0.160	-0.290	0.124	-0.351
ndvipc3	MAM	-0.079	0.280	**-0.489**	**-0.368**	**0.392**	-0.322	-0.330	0.097	**-0.399**	-0.100	0.092	**-0.375**
ndvipc1	JAS	0.131	0.037	-0.111	-0.108	0.327	-0.082	**-0.388**	0.255	-0.022	-0.267	0.057	-0.191
ndvipc2	JAS	0.107	-0.049	-0.100	0.233	-0.021	-0.158	**0.416**	-0.032	-0.149	0.273	0.123	-0.183
ndvipc3	JAS	0.007	0.052	0.217	**0.396**	-0.312	-0.260	-0.222	-0.001	0.065	-0.120	0.107	0.038

4.4.15 Association between Tropical Indian Ocean heat content and Ethiopian vegetation

Table 4.15 shows the liner correlation between the vegetation over Ethiopia and the tropical Indian Ocean heat content. Only values 98 and 99% confident are marked in bold in the table. The vegetation is strongly correlated with the tropical Indian Ocean heat content with positive and negative correlation depending on the seasons. The SON of the ocean heat content has a positive strong correlation with the simultaneous (SON) and the subsequent (DJF) seasons of the vegetation with 99% confidence level (r=0.593and r=0.589 to 0.668, respectively).The DJF of the ocean heat content both ± strong correlation (r=0.528 to r=-0.592 and r=0.638 to r=-0.600) with the SON and DJF of the vegetation over Ethiopia. The MAM season of the vegetation is negatively strongly correlated to the SON and DJF of the ocean heat content. The JAS season of the ocean heat content has negative and positive strong correlation with the DJF and JAS seasons of the vegetation only. As a conclusion, there is strong correlation on the SON and DJF seasons by the different seasons of the Indian Ocean except the JAS which has a weak correlation with the SON season of the vegetation.

Table 4.15 The correlation between Tropical Indian ocean heat content and vegetation over Ethiopia

		Indpc1	Indpc2	Indpc3	Indpc1	Indpc2	Indpc3	Indpc1	Indpc2	Indpc3	Indpc1	Indpc2	Indpc3
		SON	SON	SON	DJF	DJF	DJF	MAM	MAM	MAM	JAS	JAS	JAS
ndvipc1	SON	0.304	0.012	-0.197	0.203	-0.292	**-0.412**	-0.183	-0.292	-0.229	-0.285	0.131	-0.356
ndvipc2	SON	0.306	0.296	0.034	0.393	-0.260	0.027	**0.410**	**-0.414**	0.232	0.110	-0.185	0.230
ndvipc3	SON	**0.593**	0.197	-0.405	**0.528**	-0.161	**-0.592**	0.319	-0.315	**-0.630**	0.174	-0.271	-0.293
ndvipc1	DJF	**0.668**	0.357	-0.255	**0.638**	-0.221	**-0.600**	0.268	**-0.461**	**-0.434**	-0.173	-0.227	**-0.542**
ndvipc2	DJF	**0.589**	**0.468**	0.071	**0.652**	-0.048	-0.359	**0.620**	**-0.623**	-0.183	0.209	**-0.424**	0.091
ndvipc3	DJF	-0.006	0.092	-0.047	-0.231	0.290	-0.383	-0.322	0.246	**-0.582**	-0.081	0.171	-0.401
ndvipc1	MAM	-0.091	0.166	**-0.438**	0.154	0.174	-0.360	0.235	-0.123	-0.041	0.174	0.028	0.093
ndvipc2	MAM	0.200	-0.016	-0.276	0.082	**-0.446**	-0.256	-0.055	-0.335	0.002	0.138	0.087	-0.006
ndvipc3	MAM	-0.007	0.042	-0.178	-0.154	-0.244	-0.170	-0.360	0.143	-0.117	0.034	0.387	-0.408
ndvipc1	JAS	0.131	-0.039	-0.031	-0.138	0.213	-0.161	-0.101	-0.060	-0.245	0.078	-0.309	-0.064
ndvipc2	JAS	0.029	0.071	0.022	0.301	-0.062	-0.110	0.223	-0.194	0.101	-0.082	0.085	0.114
ndvipc3	JAS	-0.068	0.179	-0.300	0.086	**0.410**	-0.312	0.251	0.089	-0.312	**0.535**	0.018	-0.331

4.4.16 Association between Tropical Atlantic Ocean heat content and Ethiopian vegetation

Table 4.16 shows the linear correlation between vegetation over Ethiopia and tropical Atlantic Ocean heat content. Values 90% and above are marked in bold in the table. The tropical Atlantic Ocean heat content is seen correlated negatively strongly with the vegetation over Ethiopia. The confidence level is comparably less than both the tropical Indian and pacific oceans heat content confidence level. The MAM season here also is correlated weakly with the DJF, the MAM and the JAS seasons of the Atlantic Ocean heat content. Next to the MAM season of the vegetation the JAS season is correlated positively with the DJF and

negatively correlated with the simultaneous (JAS) season of the tropical Atlantic but has a weak correlation with the SON and the MAM seasons of the tropical Atlantic Ocean heat content.

Table 4.16 the correlation between Tropical Atlantic Ocean heat content and vegetation over Ethiopia

		Atlpc1	Atlpc2	Atlpc3	Atlpc1	Atlpc2	Atlpc3	Atlpc1	Atlpc2	Atlpc3	Atlpc1	Atlpc2	Atlpc3
		SON	SON	SON	DJF	DJF	DJF	MAM	MAM	MAM	JAS	JAS	JAS
ndvipc1	SON	**-0.414**	-0.130	-0.234	-0.278	-0.081	-0.069	**-0.375**	-0.116	-0.147	-0.193	0.068	-0.216
ndvipc2	SON	0.156	-0.184	0.123	-0.210	-0.244	0.134	-0.313	0.032	-0.184	-0.113	0.057	0.010
ndvipc3	SON	**-0.375**	0.094	-0.347	-0.170	0.237	-0.111	**-0.478**	0.220	-0.311	**-0.457**	0.000	**-0.519**
ndvipc1	DJF	**-0.431**	-0.108	-0.326	**-0.397**	0.044	-0.076	**-0.579**	0.212	-0.329	**-0.479**	0.138	**-0.415**
ndvipc2	DJF	-0.013	-0.289	0.015	-0.204	-0.286	-0.109	**-0.451**	-0.026	**-0.402**	**-0.476**	-0.088	-0.306
ndvipc3	DJF	**-0.429**	0.273	-0.355	-0.203	0.261	-0.281	-0.301	-0.124	-0.152	**-0.422**	0.153	-0.304
ndvipc1	MAM	-0.209	-0.089	-0.135	0.194	0.000	0.006	0.011	0.000	0.014	-0.080	0.109	-0.277
ndvipc2	MAM	-0.299	**-0.460**	0.022	-0.191	-0.355	0.077	-0.091	-0.257	-0.092	-0.145	-0.070	0.118
ndvipc3	MAM	**-0.547**	-0.230	**-0.405**	-0.328	0.061	-0.279	-0.194	0.102	-0.324	-0.074	0.174	-0.092
ndvipc1	JAS	-0.238	-0.180	-0.005	0.116	-0.002	-0.126	-0.002	-0.210	-0.251	**-0.382**	-0.307	-0.110
ndvipc2	JAS	0.111	-0.018	-0.003	-0.282	-0.274	0.020	-0.171	0.002	0.084	0.216	-0.098	0.074
ndvipc3	JAS	-0.304	-0.030	-0.337	0.339	**0.376**	-0.321	0.115	0.323	-0.313	-0.261	0.172	**-0.543**

4.5 Contributions of tropical oceans to Climate, hydrology and NDVI variability

4.5.1 Contribution of tropical oceans to the water level variability of Lake Awassa

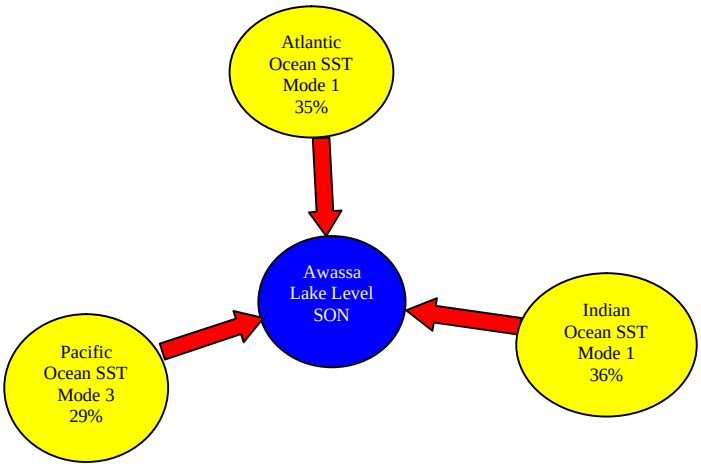

Fig. 4.15 conceptualization graph indicating contributions of Tropical Oceans for Awassa Lake level

The regression equation is

$$Awassa_{SON} = -0.440 - (0.451 * Atlpc1_{SON}) + (0.459 * Indpc1_{SON}) - (0.367 * Pacpc3_{SON})$$

Where

$Atlpc1_{SON}$ is the first mode of Atlantic Ocean for SON season,

$Indpc1_{SON}$ is the first mode of Indian Ocean for SON season, and

$Pacpc3_{SON}$ is the third mode of Pacific Ocean for SON season, -0.440 is the constant and -0.451, 0.459, and-0.367 are coefficients of regression.

$$r^2_{adjusted} = 0.535 \qquad (4.2)$$

$r^2_{adjusted}$ is r square adjusted which explains the total contribution in the regression method.

The equation explains in the first place the association between the tropical ocean SSTs and the Awassa lake level variability. The Pacific Ocean mode3 SON season and Atlantic Ocean mode 1 SON season have negative relationship with the Awassa SON season water level. They have inverse relationships. With the Indian Ocean, Awassa SON season lake level has a positive relationship. Secondly the coefficients together are used to explain their contributions to the variability of the lake level.

The square R adjusted shows the total contribution of the tropical oceans over the Awassa lake level in SON season which is about 54%.

4.5.2 Contribution of tropical oceans to precipitation SON over south Ethiopia

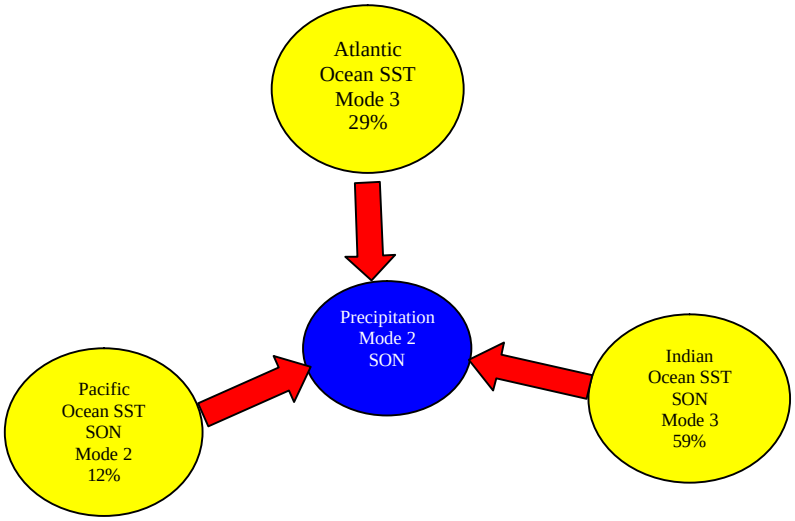

Fig. 4.16 Diagram illustrating the contributions of tropical oceans to precipitation over south Ethiopia

The regression equation is

$$\Pr cppc2_{SON} = 0.041 - (0.644 * Indpc3_{SON}) + (0.318 * Atlpc3_{SON}) + (0.134 * Pacpc2_{SON})$$

Where

$\Pr ecpc2_{SON}$ is the second mode precipitation in SON season

$$r^2_{Adjusted} = 0.499 \qquad (4.4)$$

This r square adjusted explains the tropical oceans contribute about 50% to precipitation over South Ethiopia.

4.5.3 The contribution of tropical oceans to MAM precipitation over south Ethiopia

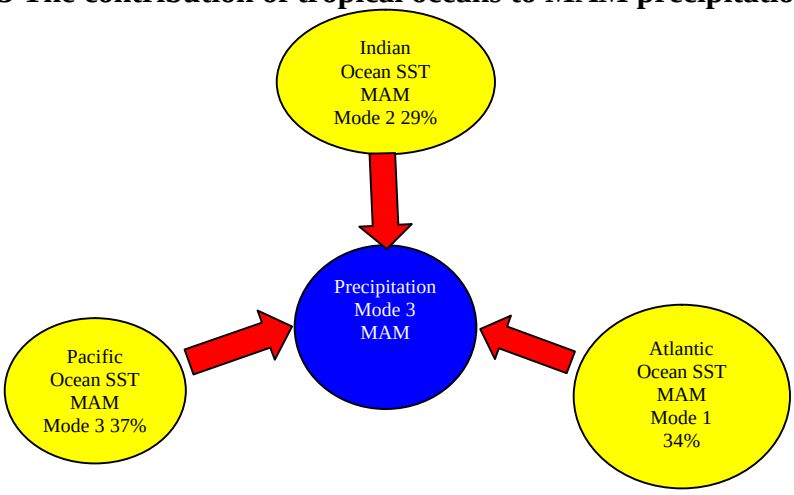

Fig. 4.17 Diagram illustrating contribution of Tropical Oceans to precipitation over south Ethiopia MAM season.

The regression equation is

$$\Pr ecpc3_{MAM} = -0.019 + 0.416 * Indpc2_{MAM} - 0.484 * Atlpc1_{MAM} + 0.531 * Pacpc3_{MAM}$$

$$r^2_{adjusted} = 0.242 \qquad (4.6)$$

The square r adjusted value explains that the tropical oceans' contribution to MAM season precipitation over south Ethiopia is very small.

4.5.4 Contribution of tropical oceans to SON NDVI over south Ethiopia

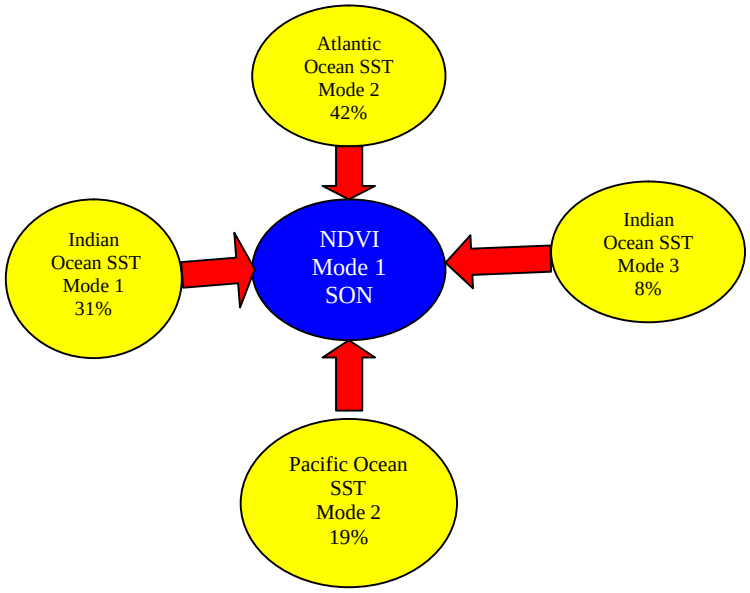

Fig. 4.18 Conceptual diagram illustrating the contributions of Tropical Ocean to NDVI over SON season of Ethiopia.

The regression equation is

$$NDVIpc1_{SON} = -0.540 - 0.826 * Atlpc2_{SON} + 0.614 * Indpc1_{SON} + 1.146 * Indpc3_{SON} + 0.369 * Pacpc2_{SON}$$

$$r^2_{adjusted} = 0.516 \qquad (4.8)$$

The tropical oceans contribute 51.6% of the NDVI variability. This is shown by the R square adjusted from the equation 6.9.

The above equation gives the Atlantic Ocean has a negative relationship with the NDVI and contributes 42% of the total contribution of the tropical oceans to the NDVI variability. The Indian and Pacific Ocean have positive relationship with the NDVI variability and contribute 39% and 19%, respectively. The individual contribution of the Tropical oceans is explained in the conceptual diagram.

4.5.5 Contribution of tropical oceans to SON NDVI over south Ethiopia

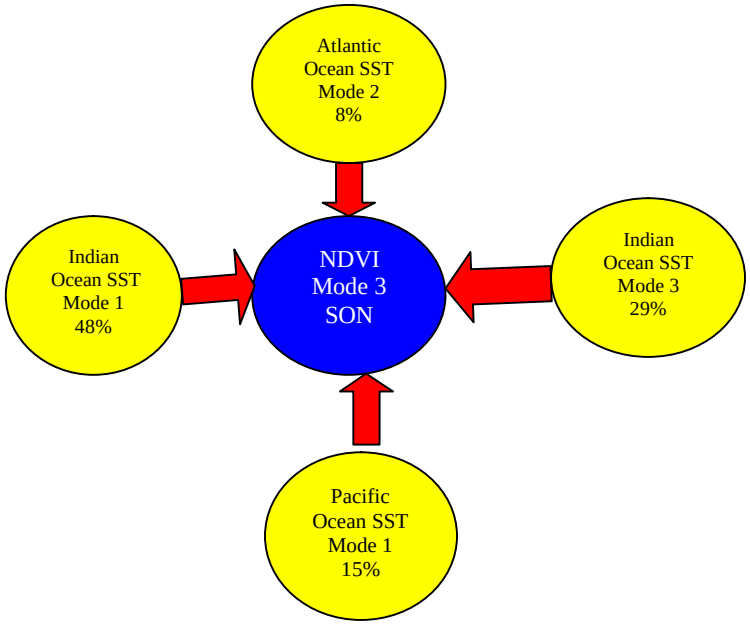

Fig. 4.19. Conceptual diagram illustrating the contribution of Tropical Oceans to Mode (3) NDVI during SON season of Ethiopia.

The regression equation

$$NDVIpc3_{SON} = -0.534 - 0.829 * Atlpc2_{SON} + 0.403 * Atlpc3_{SON} - 0.857 * Indpc2_{SON} + 10133 * Pacpc1_{SON}$$

$$r^2_{adjusted} = 0.419 \qquad (4.10)$$

The total contributions of the tropical oceans SST to the Mode (3) SON season of the NDVI over Ethiopia is 42% with the individual contributions of Atlantic, Indian and pacific oceans 8%,77% and 15%,respectively.

4.5.6 Contribution of tropical oceans to Mode 2 NDVI over south Ethiopia during MAM season

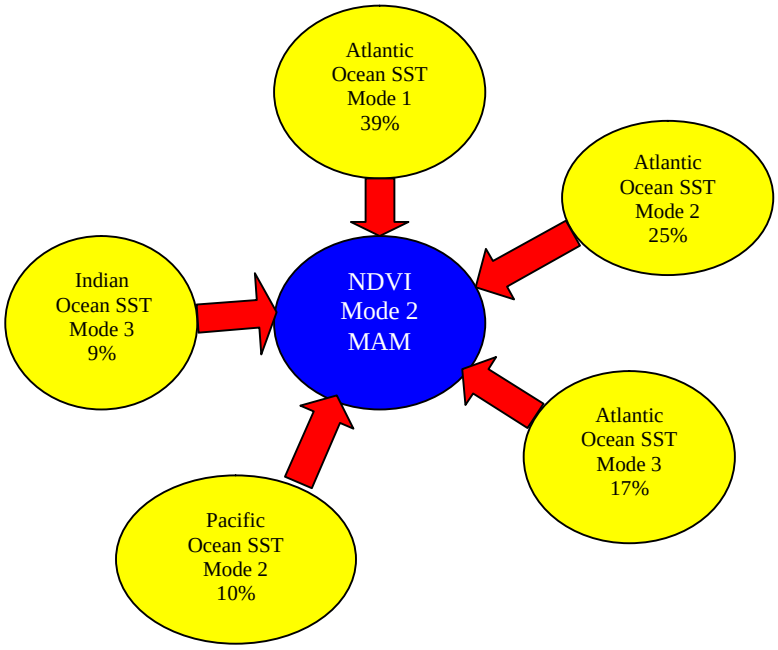

Fig 4.20 Conceptual diagram illustrating the contributions of tropical oceans to the MAM season of Mode (2) NDVI

The regression equation

$$NDVIpc2_{MAM} = -0.750 - 0.948 * Atlpc1_{MAM} - 0.606 * Atlpc2_{MAM} - 0.418\, Atlpc3_{MAM} + 0.209\, Indpc3_{MAM} + 0.252\, Pacpc2_{MAM}$$

$$r^2_{adjusted} = 0.404 \qquad (4.12)$$

The total contribution of the tropical oceans is about 40%.The Atlantic Ocean has a negative association (81%) and the Indian and Pacific (9% and 10%, respectively) have positive association with the MAM season NDVI Mode2 of Ethiopia.

4.5.7 Contribution of tropical oceans to MAM NDVI Mode 3 over south Ethiopia

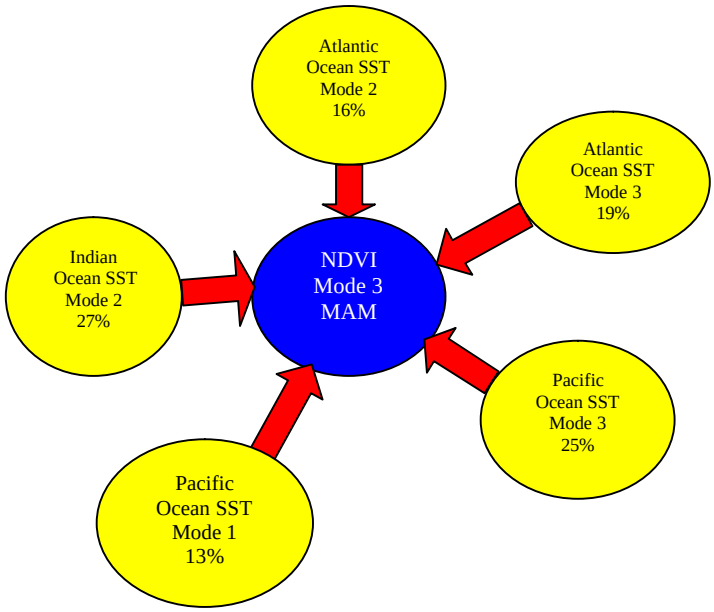

Fig 4.21 Conceptual diagram representing the contributions of tropical oceans to the MAM season of NDVI mode (3) over Ethiopia.

The regression equation is

$$NDVIpc3_{MAM} = -0.289 - 0.274 * Atlpc2_{MAM} - 0.325 * Atlpc3_{MAM} + 0.463\, Indpc2_{MAM} + 0.223\, Pacpc1_{MAM} - 0.437\, Pacpc3_{MAM}$$

$$r^2_{adjusted} = 0.448 \qquad (4.14)$$

The total contribution of the different modes of the tropical oceans to the MAM season of Mode (3) NDVI over south Ethiopia is 44.8% with the individual contributions of Atlantic Ocean (25%), Indian Ocean (27%) and Pacific Ocean (38%).

4.5.8 Contribution of the SON Mode (1) Precipitation to the SON Mode (1) NDVI

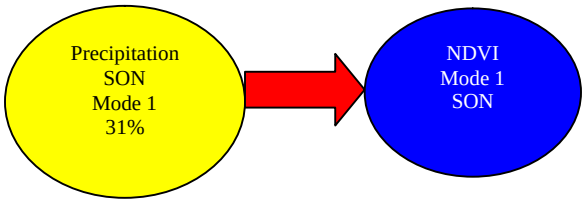

Fig 4.22. Conceptual diagram illustrating the association between Mode (1) Precipitation and Mode (1) NDVI during SON season.

The regression equation is

$$NDVIpc1_{SON} = -0.142 + 0.493 * \Pr ecpc1_{SON} \qquad (4.15)$$

$$r^2_{adjusted} = 0.310 \qquad (4.16)$$

The association between Mode (1) Precipitation and Mode (3) NDVI during this SON season is 31%.

4.5.9 Contribution of the SON Mode (1) Precipitation to the SON Mode (3) NDVI

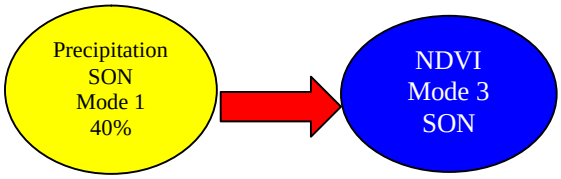

Fig. 4.23. Conceptual diagram illustrating the association between Mode (3) Precipitation and Mode (1) NDVI during SON season.

The regression equation is

$$NDVIpc3_{SON} = -0.074 + 0.589 * \Pr ecpc1_{SON} \qquad (4.17)$$

$$r^2_{adjusted} = 0.389 \qquad (4.18)$$

The association between Mode (1) Precipitation and Mode (3) NDVI during this SON season is 40%.

4.5.10 Contribution of the tropical oceans heat content to the SON Mode (1) precipitation

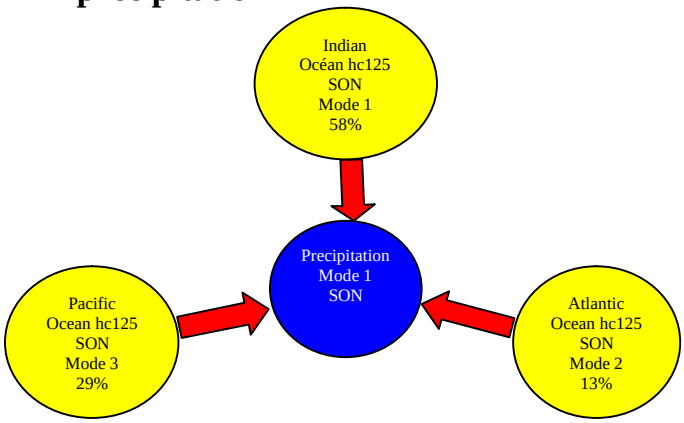

Fig 4.24 Conceptual diagram illustrating the contribution of tropical ocean heat content to the SON season Mode (1) precipitation over south Ethiopia

The regression equation

$$\Pr ecpc1_{SON} = -0.064 + 0.648\, Indhcpc1_{SON} - 0.14\, Atlhcpc2_{SON} - 0.326\, Pachcpc3_{SON}$$

$$r^2_{adjusted} = 0.491 \qquad (4.20)$$

The total contribution of the tropical ocean heat content to the SON season Mode (1) precipitation is 49%.The contribution of the individual is listed in the diagram.

4.5.11 Contribution of the tropical oceans heat content to the SON Mode (2) precipitation

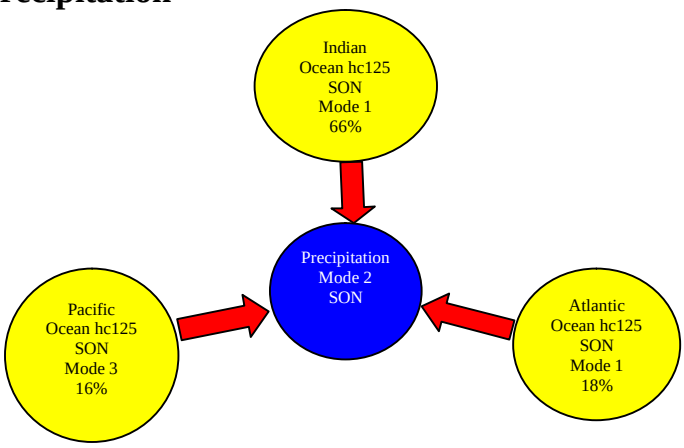

Fig 4.25 Conceptual diagram illustrating the contribution of tropical ocean heat content to the SON season Mode (2) precipitation over south Ethiopia

The regression equation is

$$\Pr ecpc2_{SON} = 0.028 - 0.742\, Indhcpc1_{SON} + 0.204\, Atlhcpc1_{SON} + 0.176\, Pachcpc3_{SON}$$

$$r^2_{adjusted} = 0.588 \qquad (4.22)$$

The total contribution of the tropical oceans to the Mode (2) SON season of the precipitation over south Ethiopia is 58.8%.The Indian Ocean is explained the 66% of the total contribution of the tropical oceans heat content. The Atlantic and Pacific consist of 18% and 16% individually, respectively.

Generally, the contribution of tropical ocean heat content to the MAM season precipitation is very small.

4.5.12 Contributions of the tropical oceans heat content over the SON season of the NDVI over Ethiopia

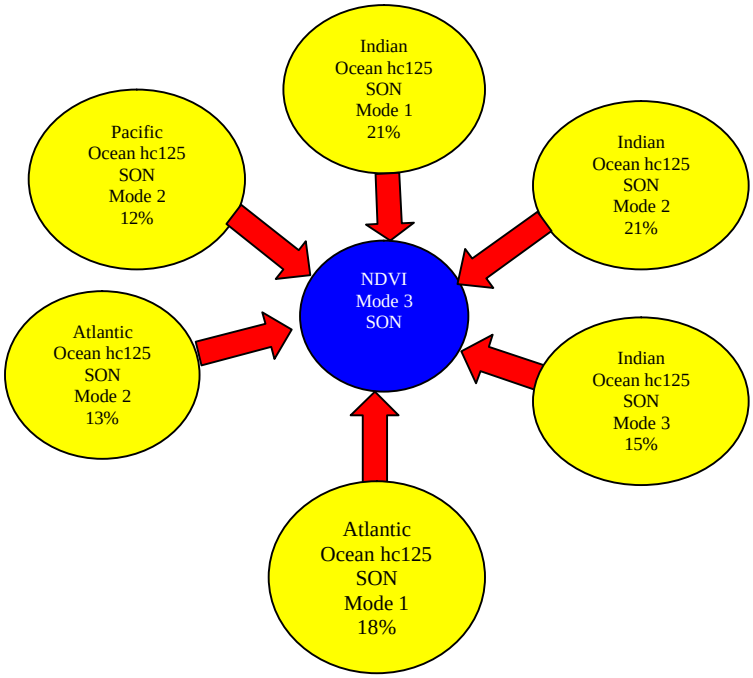

Fig 4.26 Conceptualized diagram illustrating the contributions of tropical oceans heat content to the Mode (3) SON season of NDVI over Ethiopia.

$$r^2_{adjusted} = 0.856 \qquad (4.23)$$

The total contribution of the tropical heat content over the SON mode (1) season of the NDVI IS 86%.The Atlantic, Indian and pacific oceans contribute individually31%, 57% and 12% respectively.

The tropical oceans heat content does not have significant contribution to the MAM season of the NDVI.

4.6 Atmospheric dynamics and Tropical oceans modulation to Ethiopian climate, hydrology and vegetation

The composite atmospheric circulation and SST structures are plotted using the wet minus dry MAM and SON seasons of climate and hydrology over the southern region of Ethiopia to understand the atmospheric and oceanic cause for climate, hydrology extremes. These seasons are selected because they are the main rainfall seasons of the region. The atmosphere and Ocean composites are formed as wet minus dry events.

4.6.1Atmospheric and oceanic causes for SON precipitation Mode (2)

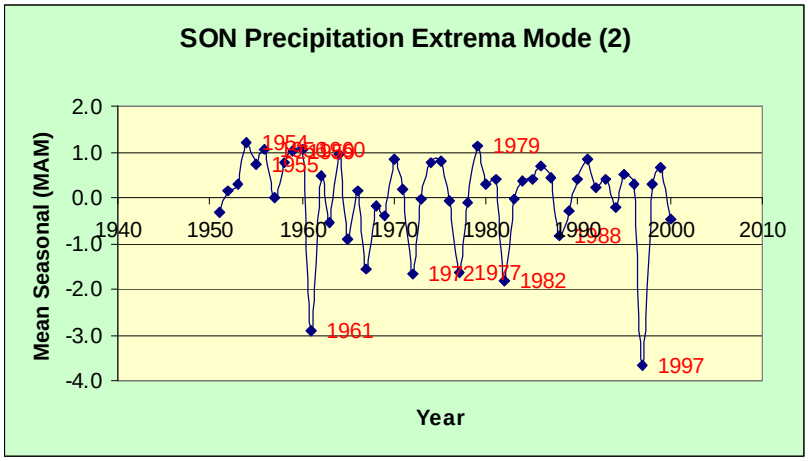

Fig.4.27 Precipitation time series showing extreme events

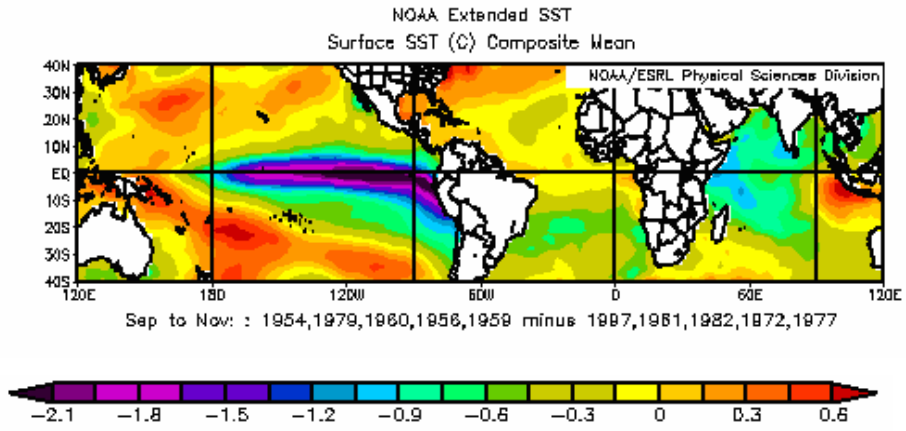

a) Composite SST patterns illustrating cold phase of ENSO, Atlantic dipole and IOD west (<0) and SE (>0)

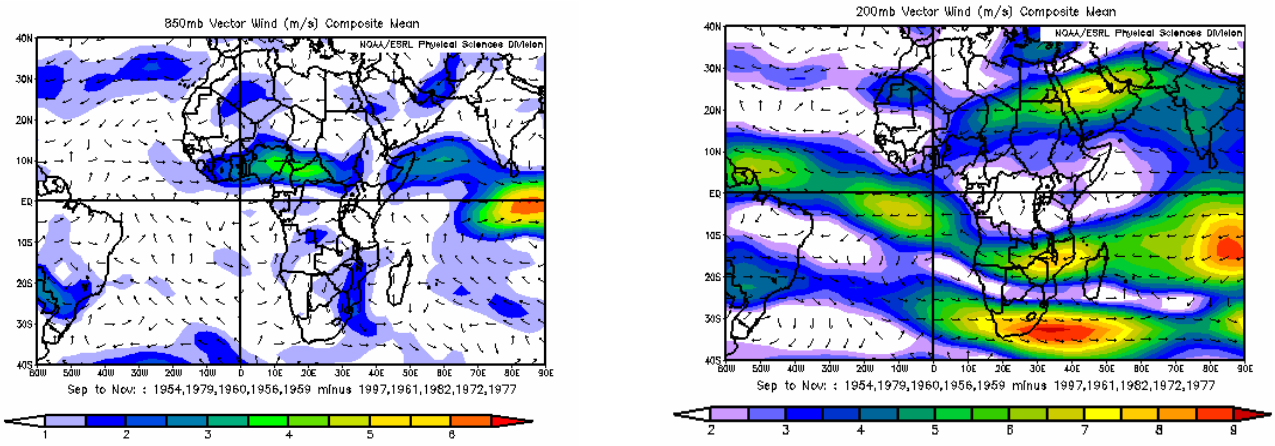

b) Wind vector at 850hp and 200hpillustrating anomalous westerly and easterly, respectively.

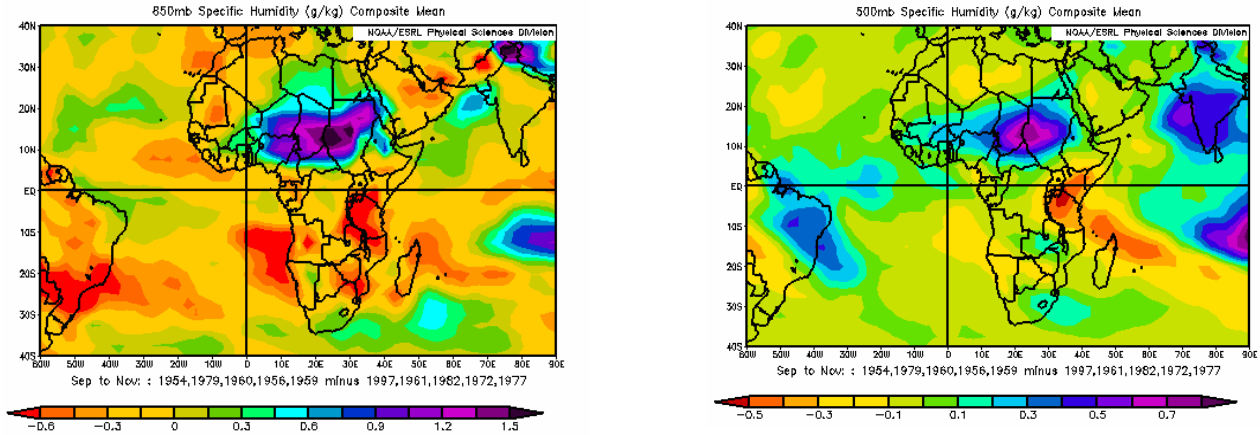

c) Specific humidity at 700hp and 500hp illustrating ample moisture over N.Ethiopia and deficient moisture over S.Ethiopia.

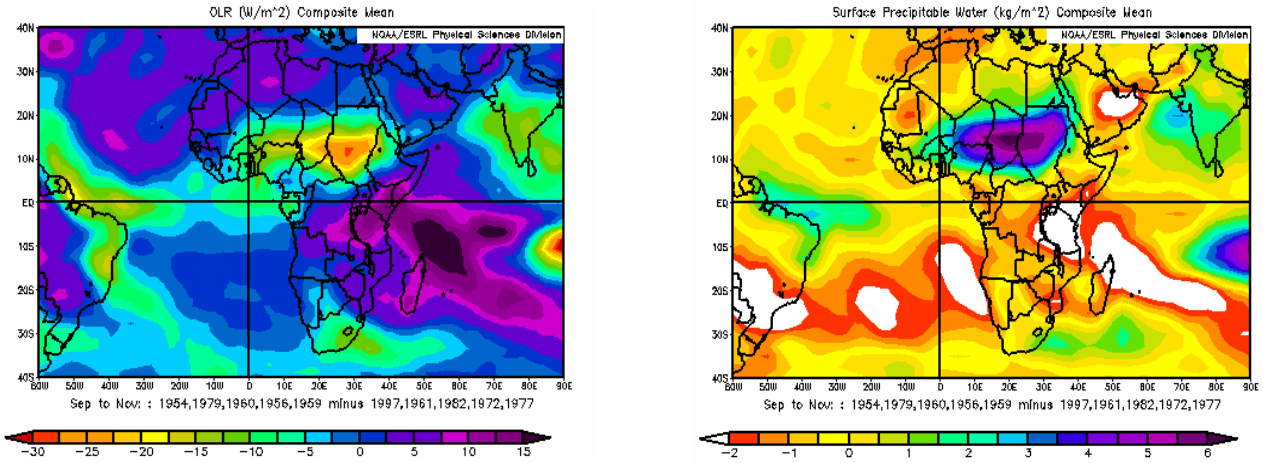

d) OLR illustrating enhanced and suppressed convective over South and North Ethiopia, respectively.

e) Rainfall illustrating wet over N.Ethiopia and dry over south Ethiopia

Fig.4.28 Atmospheric and oceanic causes for wet minus dry SON season precipitation

a) Composite SST pattern

The composite SST pattern shows a cold tongue anomaly ~-2.1^{0}C in the West Pacific which is consistent with La Niña condition shown in Fig.4.28a. A dipole structure over the Indian Ocean is reflecting in negative SST difference of ~0.9^{0}C around East Africa (Southern Ethiopia) and a positive SST difference ~0.6^{0}C around South East Indian Ocean). The N-S dipole pattern is shown in the Atlantic Ocean (positive north). These all together show the oceanic cause for wet minus SON season precipitation over Ethiopia.

b) Composite Wind Vector at 850hp and 200hp

The composite wind vector at 850-hPa and 200-hPa in fig 4.28b shows there is an eastward wind pumping moisture to Ethiopian highlands from Atlantic but because of the warm pool at the East Indian the moisture diverted to the warm pool taking away the moisture from country.

c) Composite Specific humidity

The composite specific humidity at 850-hp and 200-hPa show an ample moisture over north Ethiopia and deficient moisture around the southern part of Ethiopia (as a results of the diversion of moisture to eastern Indian (over the warmer sea). The north and south Ethiopia have two opposite specific humidity in responses to the atmosphere and ocean conditions.

d) Outgoing Long wave Radiation (OLR)

OLR fig.4.28d ,which is important to detect the tropical rainfall over composite wet minus dry field ,detects an suppressed convection over the southern part of Ethiopia and most part of Tropical North Africa including northern part of Ethiopia detected opposite which has an enhanced convective in agreement with Yeshanew and jury (2006b).

e) Precipitable water

The southern part of Ethiopian is seen dry while the northern part is wet. This precipitable water measures the water vapor content of a column of air. The dry condition of the south Ethiopia is as responses to La Nina, IOD negative phase and north-south dipole of Atlantic (positive north) Ocean. The Atlantic dipole pushed the ITCZ to the northern parts of Ethiopia far from the southern part. The cooling in eastern and central Pacific produces unfavorable conditions for rainfall through generating anti-cyclonic circulation at 850-hPa north of the country.

4.6.2 Atmospheric and oceanic causes for SON precipitation Mode (1)

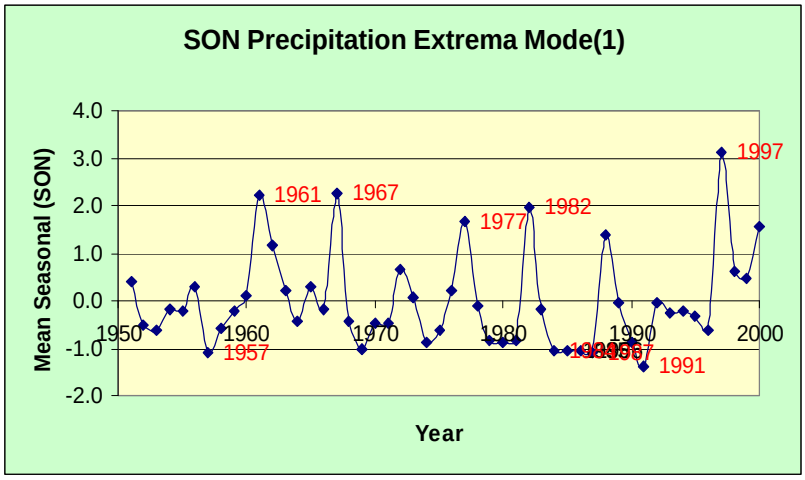

Fig.4.29 Precipitation time series showing extreme events

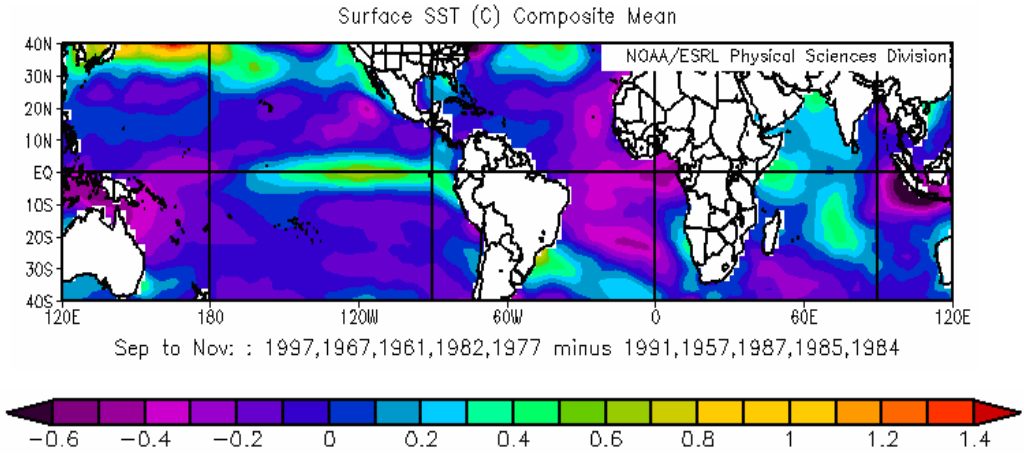

a) Composite SST pattern illustrating warm phase of ENSO, cold Atlantic and IOD East (>0) and SE (<0)

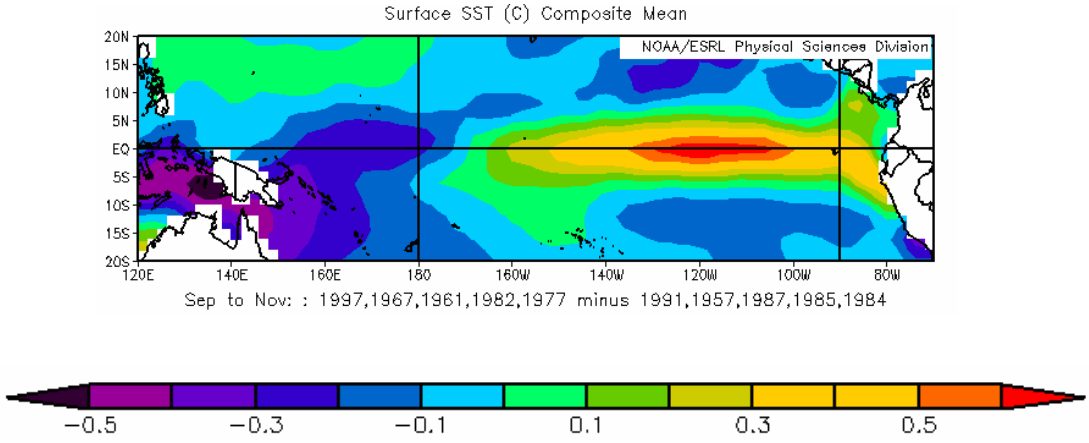

a-1) warm phase of ENSO over Pacific Ocean

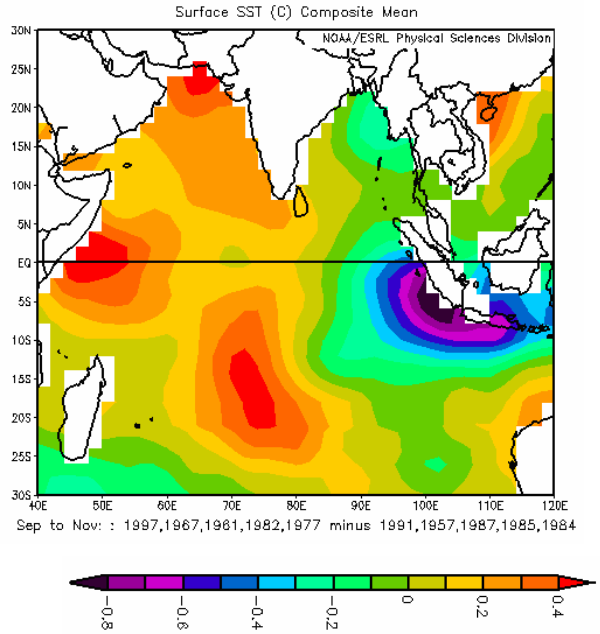

a-2) IOD east (>0) and SE (<0) mode

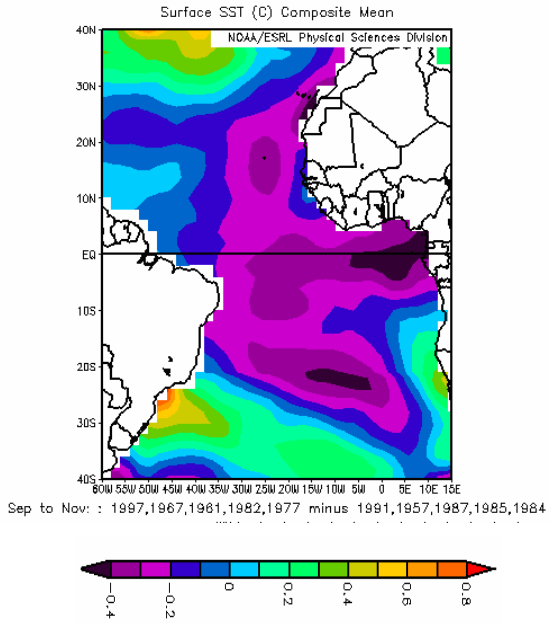

a-3) Cold Atlantic mode

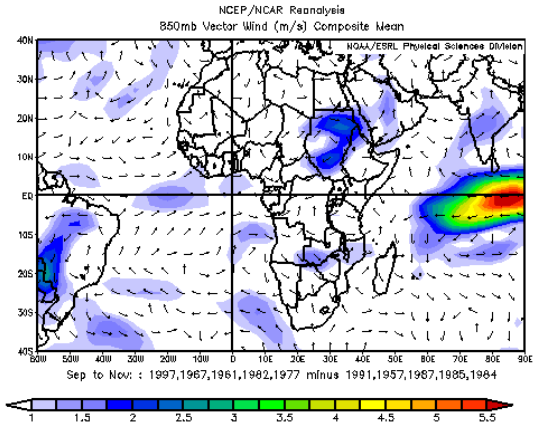

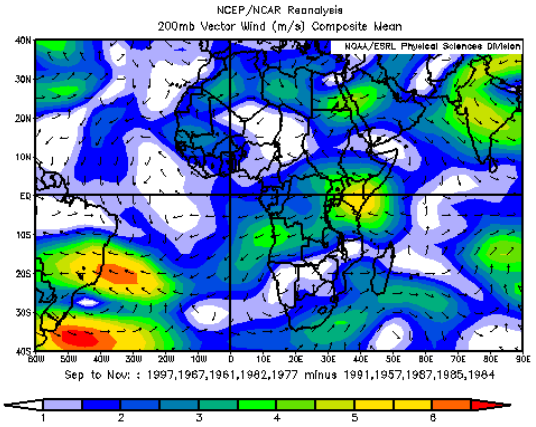

b) Composite wind vector at 850hp and 200hp illustrating Hadley cell

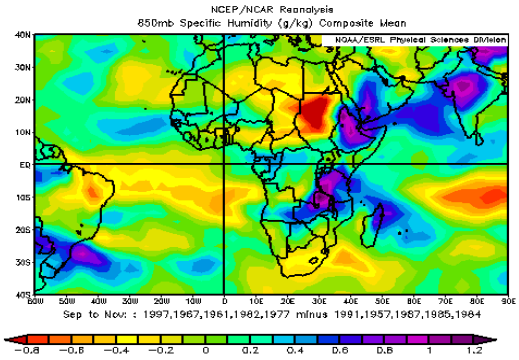

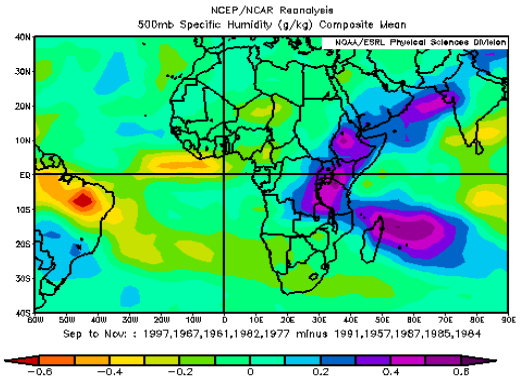

c) Composite specific Humidity illustrating ample moisture on Ethiopia

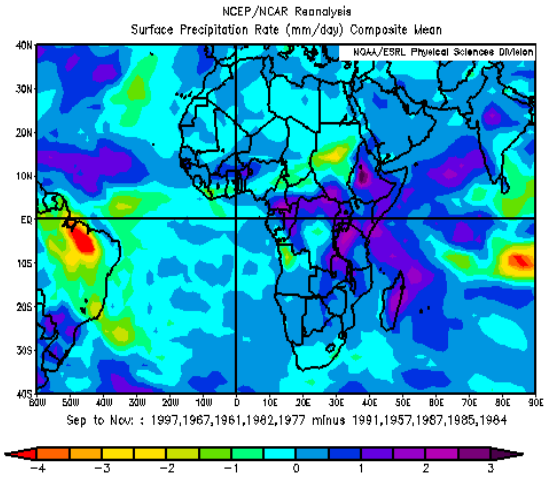

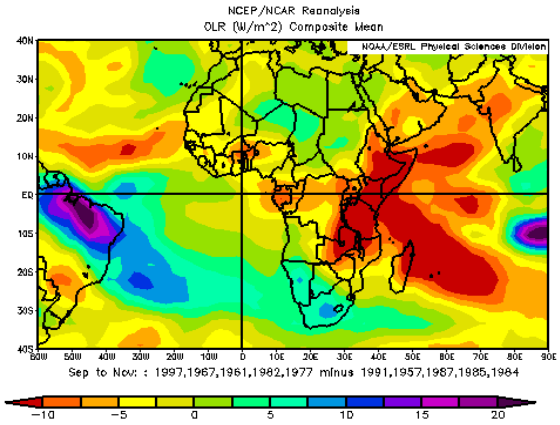

d) Composite Precipitation rate illustrating wet over Ethiopia

e) Composite OLR illustrating enhanced convective

Fig.4.30 Atmospheric and oceanic causes for wet minus dry SON season precipitation mode (1)

a) Composite SST pattern

The composite SST pattern exhibits a warm tongue in the central and east pacific which is consistent with the El Nino conitionfig.4.30a. A dipole pattern is shown over Indian Ocean which is consistent with a positive IOD exhibiting positive anomaly in the West Indian and cold anomaly around South-East Indian Ocean. A cold pool is shown in the tropical Atlantic Ocean. These all together the oceanic causes for the precipitation variability over Ethiopia.

b) Composite Wind Vector

The composite wind vector pattern shows the N-S circulation which is a Hadley type fig.4.30b.

The composite wind vector patterns at 850hp and 200hp illustrates anomalous westerly and easterly, respectively. These wind vectors coming from opposite-end converge around Ethiopia at 850hp and diverge at 200hpa.

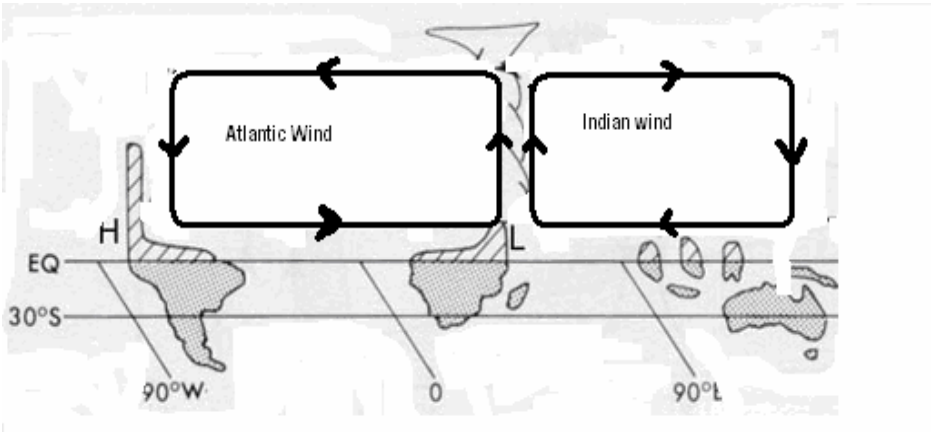

Fig.4.31 Schematic diagram for the two oppositely winds converge at 850hp and diverge 200hp of east Africa

From the equation of continuity

$$\vec{\nabla}_H \cdot \vec{V}_{\bar{H}} = \frac{\partial u}{\partial x} + \frac{\partial v}{\partial y} = -\frac{\partial w}{\partial p} \qquad (4.24)$$

Where u and v are surface winds along the x and y directions, and w is uplifting.

If $\nabla_H \cdot V_H < 0$ at 850-hPa, it represents convergence but if $\nabla_H \cdot V_H > 0$ at 200 h-Pa, divergence.

There is also a cell over the Indian Ocean which has a low level easterly wind that is extended to east Africa causing a convergence over Ethiopia. These all together with the positive dipole structure of SST over Indian Ocean ,the warm pool over central and east pacific related to El Nino and the cold mode of Atlantic oceans are the driving fore for ample moisture over Ethiopia. The OLR also shows an enhanced convective over the area in point fig.4.30d.

C) Composite Specific Humidity

The composite Specific humidity at 850hp and 200hp show ample moisture over Ethiopia.

d) Composite precipitation rate pattern

The composite precipitation rate shows wet over the whole region of Ethiopia fig 4.30d.

e) Composite OLR pattern

The composite OLR fig.4.30e exhibits <-10w/m^2 over the southern part of Ethiopia which implies enhanced convective over the area.

4.6.3 Atmospheric and oceanic causes for MAM precipitation Mode (3)

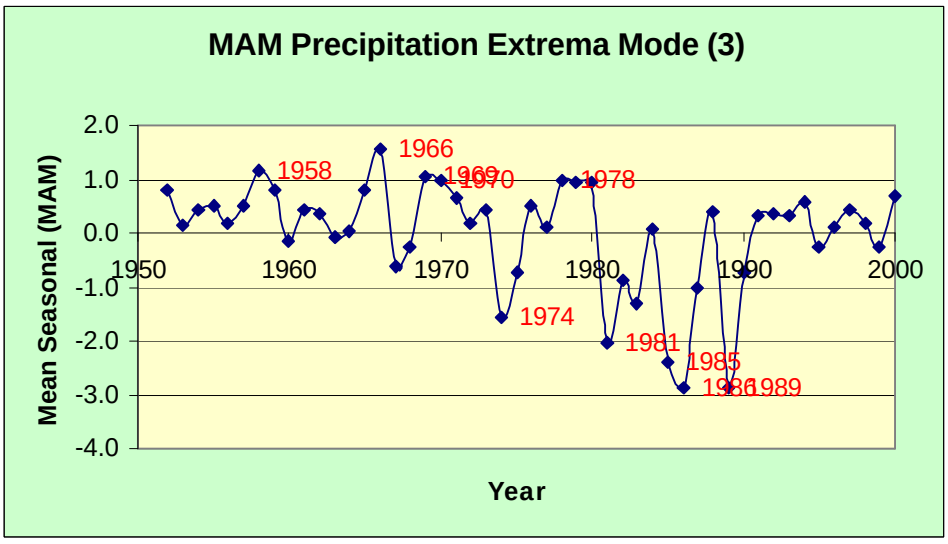

Fig.4.32 Precipitation time series showing extreme events

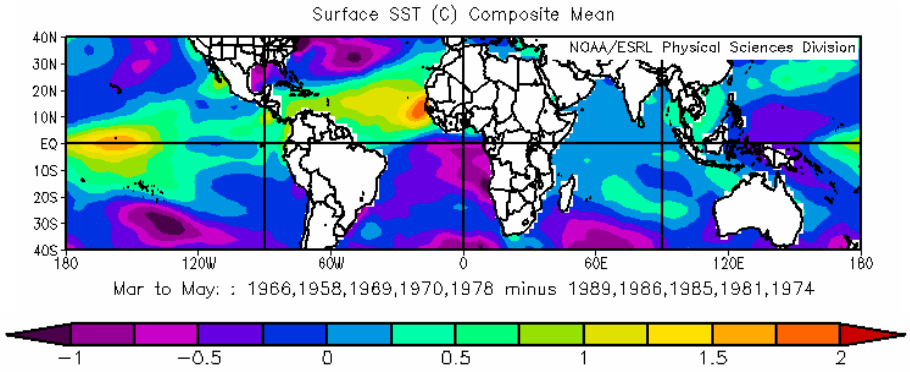

a) Composite SST pattern illustrating a warm phase of ENSO, N-S tropical dipole Atlantic (positive north) and trend Indian Ocean

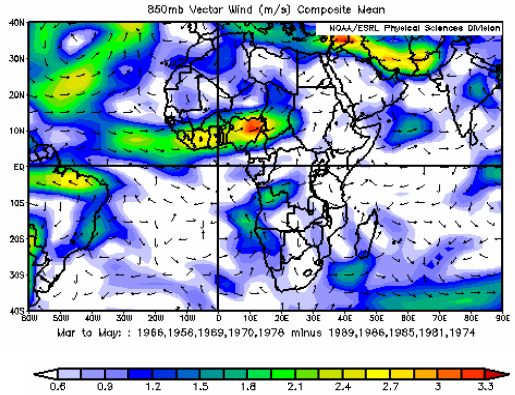

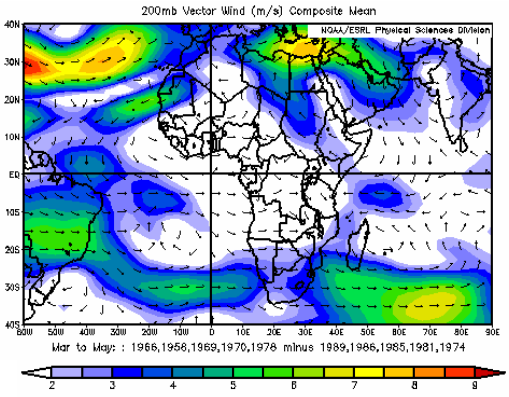

b) Composite wind vector at 850hp and 200hp illustrating Atlantic enhancing and opposing Indian

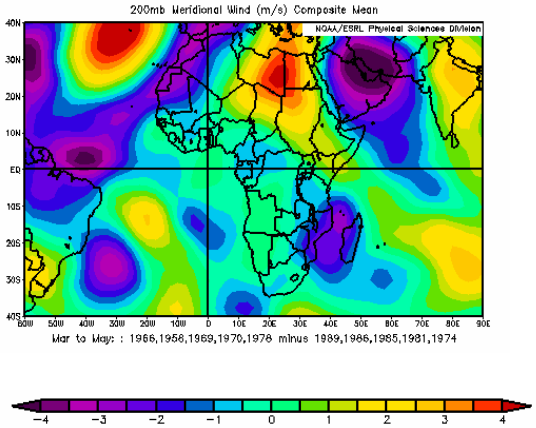

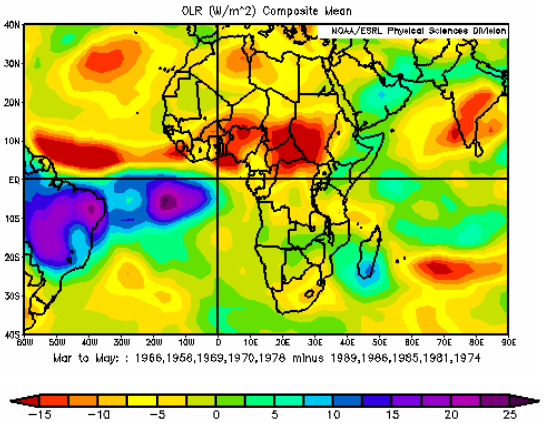

c) Composite OLR illustrating enhanced convective south and suppressed convective north (right) and composite meridional at 200hp showing Rossby waves (left)

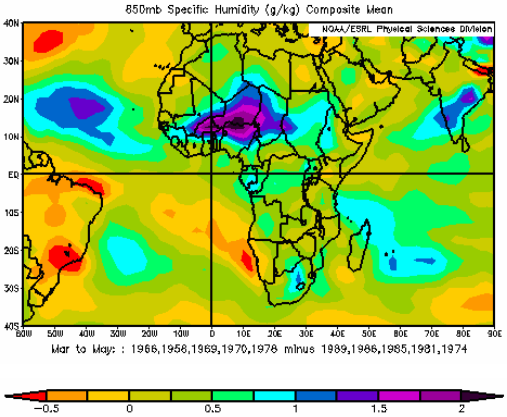

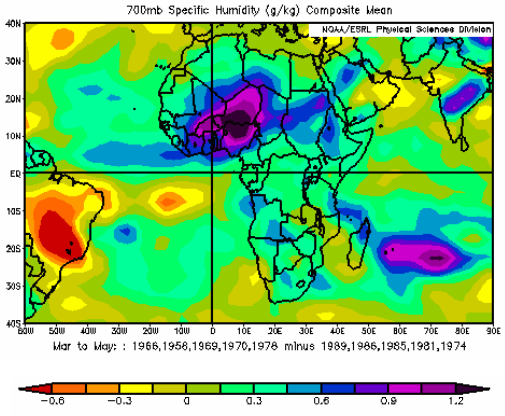

d) Composite specific humidity illustrating ample moisture over north-west Ethiopia and deficient moisture over south and south-east Ethiopia

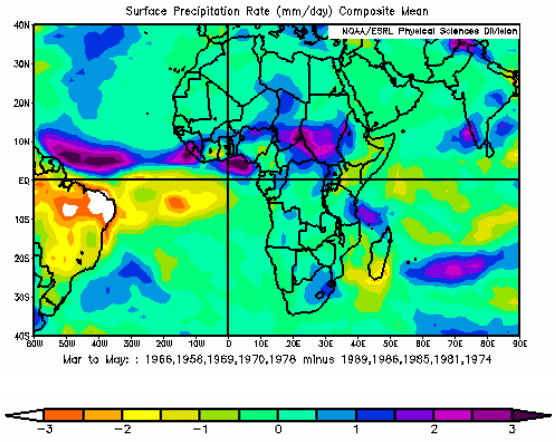

e) Composite precipitation illustrating normal condition in most part of Ethiopia

Fig.4.33 Atmospheric and oceanic causes for wet minus dry MAM season precipitation mode (3)

a) Composite SST pattern

The composite SST pattern shows a central warm pool in Pacific Ocean and N-S tropical mode over Atlantic (positive north).But the Indian Ocean exhibits a trend mode.

b) Composite wind vector

The composite wind vector at 850hp and 200hp show an enhanced easterly Atlantic and opposing Indian wind fields shown in fig.4.33b.The composite meridional pattern shows the Rossby waves

c) Composite OLR pattern

The composite OLR pattern ,which is important for detecting tropical rainfall, of fig.4.33c shows enhanced convective over the north-west Ethiopia and an suppressed convective over the south-east Ethiopia.

d) Composite specific humidity

The composite specific humidity at 850hp and 200hp fig.4.33d show ample moisture over north-west Ethiopia and deficient moisture over S-E Ethiopia.

e) Composite precipitation

The normal warm condition is exhibited over most part of Ethiopia except a small N-W part of it which gets wetter than the other part of the country.

4.6.4 Atmospheric and oceanic causes for MAM precipitation Mode (2)

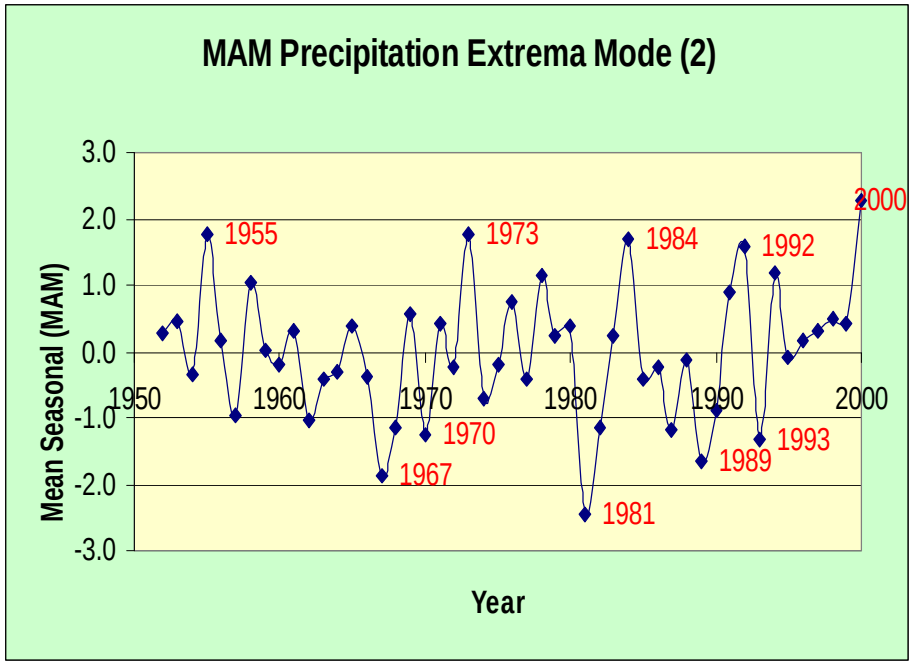

Fig.4.34 Precipitation time series showing extreme events

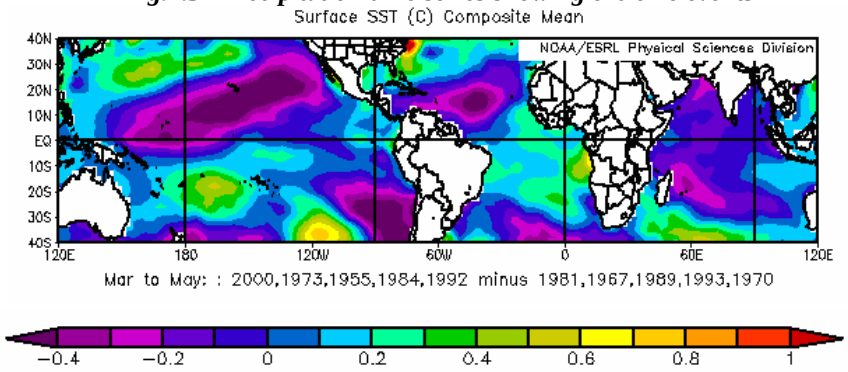

a) Composite SST pattern illustrating

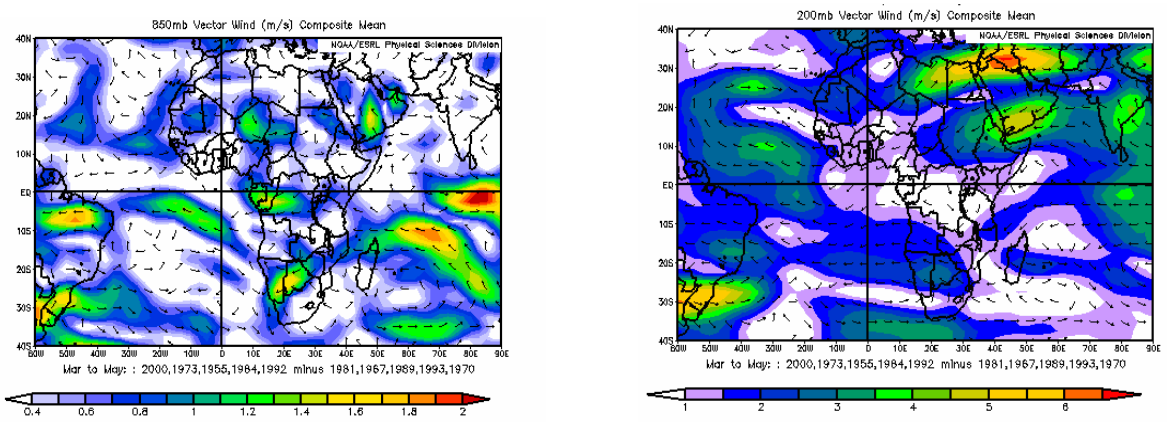

b) Composite wind Vector at 850hp and 200hp

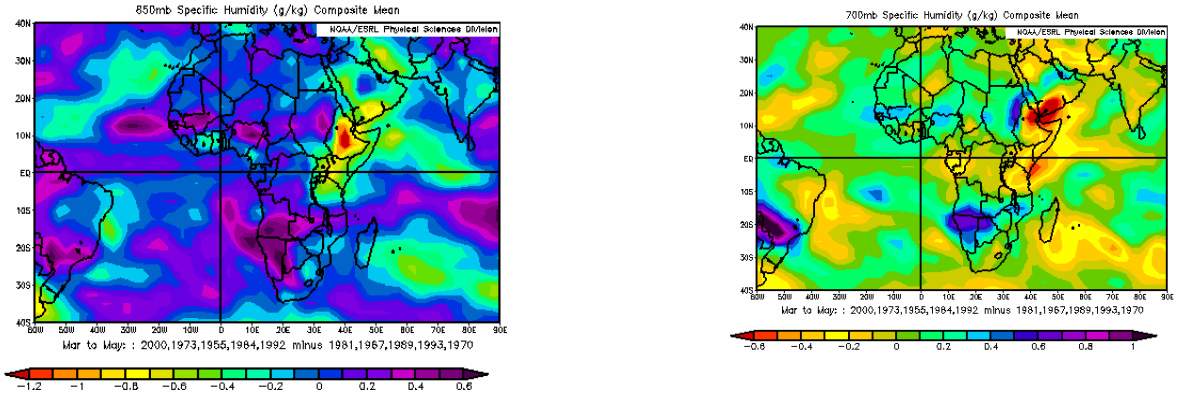

c) Composite specific humidity at 850hp (left) and 700hp (right)

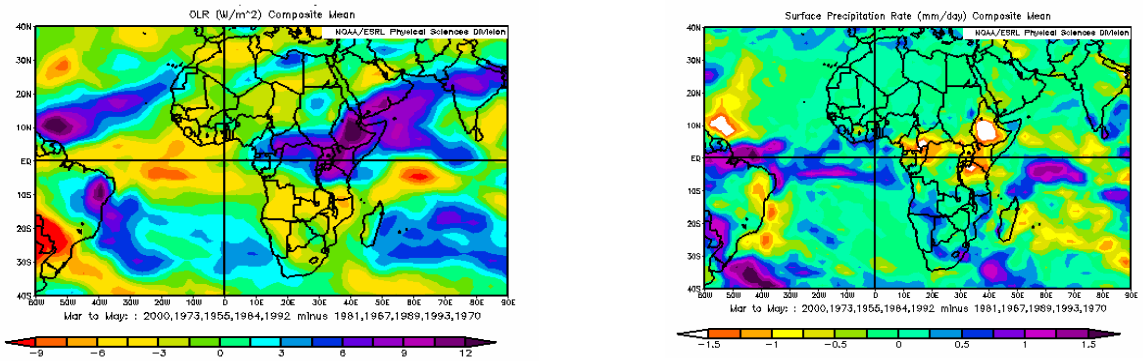

d) Composite OLR *e) Composite Precipitation rate*

Fig.4.35 Atmospheric and oceanic causes for wet minus dry MAM season precipitation mode (2)

a) Composite SST pattern

The composite SST pattern fig. 4.35a illustrates N-S tropical modes of Pacific and Atlantic Ocean with a trend mode of Indian Ocean.

b) Composite wind vector

The composite wind vector pattern at 850hp and 200hp show there is a low-level easterly wind extended to the east Africa but there is also a circulation cell over the Indian Ocean that brings the moisture to the East Indian Ocean. An anticyclone circulation is exhibited at high level around Ethiopia fig.4.35b.

c) Composite Specific humidity

The composite specific humidity at 850hp and 200hp shows deficient moisture over Ethiopia fig .4.35c, while most of the neighborhoods have ample moisture.

d) Composite OLR

The composite OLR pattern of fig.4.35d shows suppressed convective over Ethiopia.

e) Composite precipitation rate

The composite precipitation rate exhibits dry over Ethiopia fig 4.35d.

4.6.5 Atmospheric and oceanic causes for MAM precipitation Mode (1)

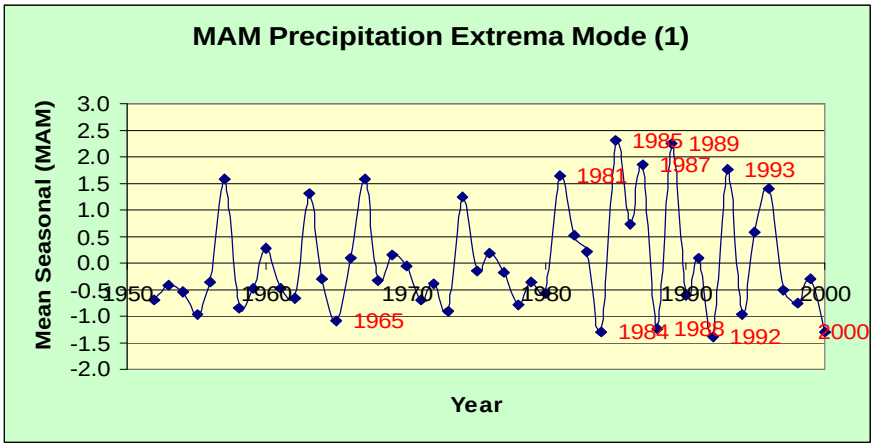

Fig. 4.36 Precipitation time series showing extreme events

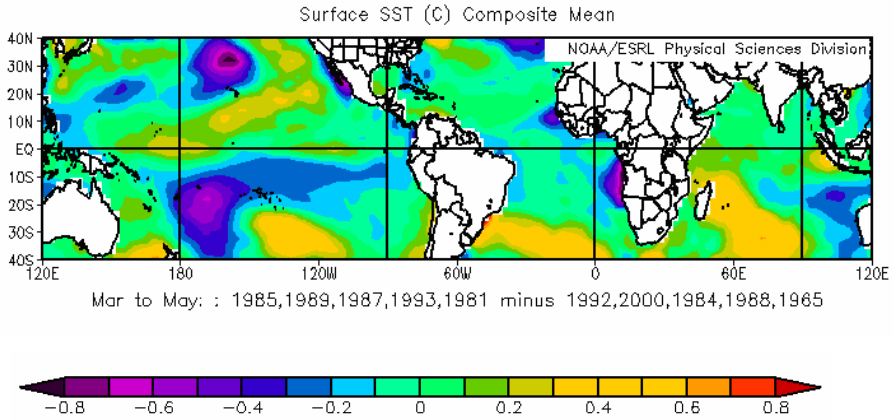

a) Composite SST pattern

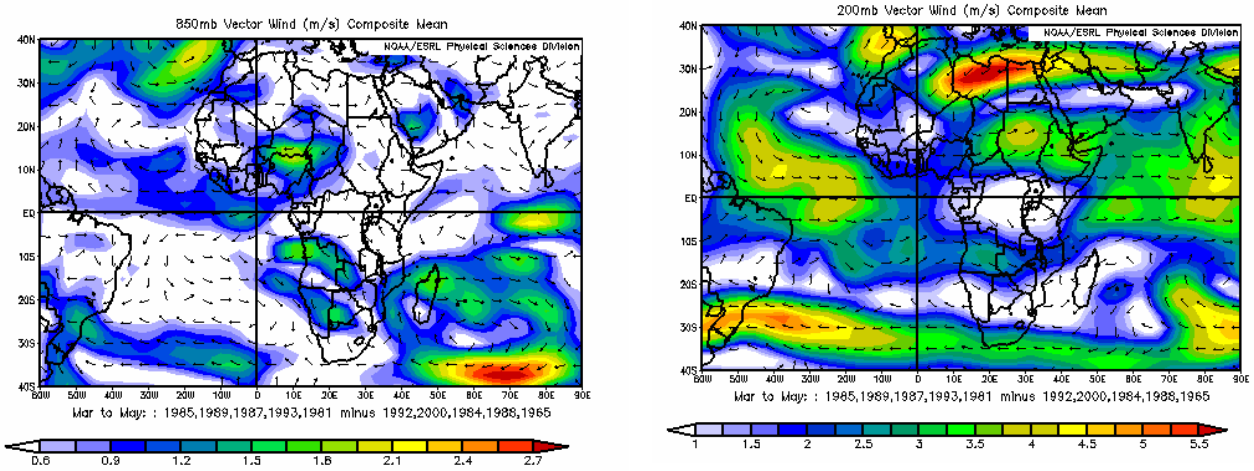

b) Composite wind vector at 850 h-Pa and 200 h-Pa

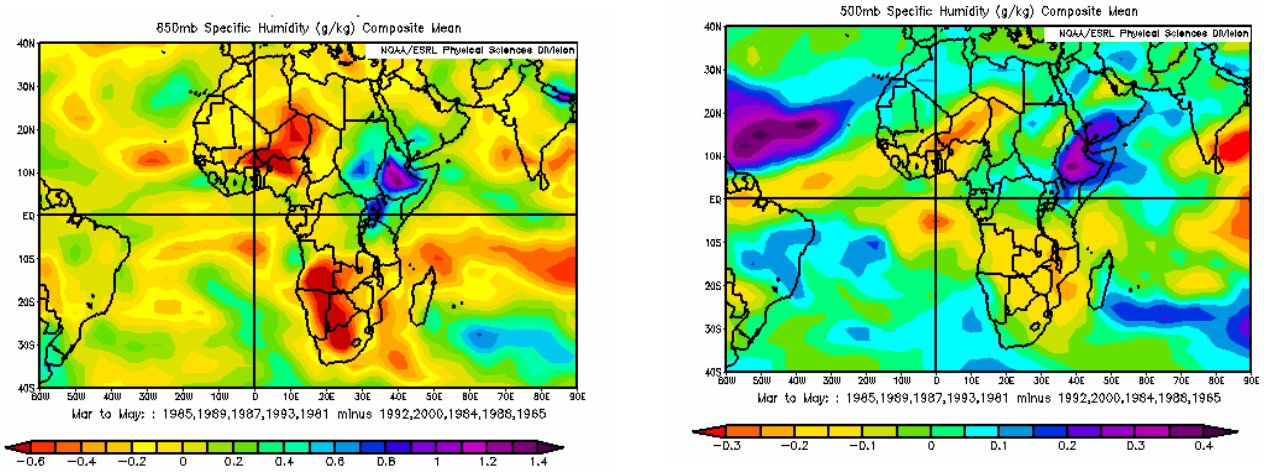

c) Specific humidity at 850 h-Pa and 500 h-Pa

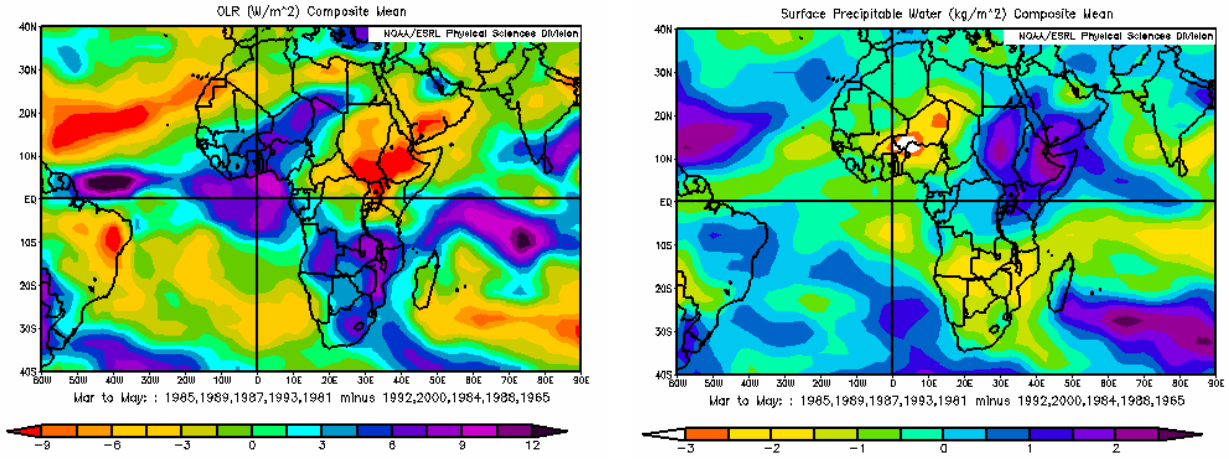

d) Composite OLR ***e) composite precipitable water***

Fig.4.37 Atmospheric and oceanic causes for wet minus dry MAM season precipitation mode (1)

a) Composite SST pattern

The composite SST pattern shown in fig.4.37a exhibits an N-S tropical dipole mode in the Pacific Ocean a dipole which is warm in the wets and cold in the SE Indian Ocean which is consistent with the positive IOD.A tropical warm pool is also exhibited in the Atlantic Ocean.

b) Composite wind vector

The 850hp and 200hp composite structures exhibit there are two way descending motions (N-S and E-W) over Ethiopia. There is a field over the Indian which has a low level easterly wind that is extended to east Africa fig 4.37b.

c) Composite specific humidity

The 850hp and 500hp composite pattern shows ample moisture over Ethiopia fig 4.37c.

d) Composite OLR

The composite OLR pattern of fig 4.37d shows negative implying an enhanced convective over Ethiopia.

e) Composite Precipitable water

The composite precipitable water pattern exhibits wet over Ethiopia fig 4.37e.

Chapter Five
Conclusions and Recommendation

5.1 Conclusions of the study

The southern part of Ethiopia has two main rainfall seasons that are the big rainfall season March through May (MAM) and short rainfall season September through November(SON).From this study we can conclude that the SON rainfall season of the area is positively affected by the tropical oceans SST anomalies and the atmospheric circulation between 850hp and 200hp.During the warm phase of ENSO (El Nino) condition southern part of Ethiopia gets a large amount of rainfall which may also cause one of the extremes of the climate variability which is flood during the SON season of the region. Not only during the El Niño condition does the area of study experience large amount of rainfall but also during the positive IOD, which is when warm around West Indian Ocean and cold around south-east. When the equatorial Atlantic is cold, the SON season of south Ethiopia also experiences ample rainfall. Therefore, the SST anomalies of the tropical oceans drive the climate variability over the southern Ethiopia. This is also shown from the detection of suppressed convective by the OLR.The composite specific humidity pattern also confirms this with its ample moisture over the area and also the wetness of the area shown by the composite precipitation rate together depict the modulation of tropical oceans SST and atmospheric circulation over the southern part of Ethiopia fig 4.33. This is in agreement with several studies for example; Nicholson and Kim (1997) find a strong connection between ENSO and rainfall over much of the African continent and suggest a linkage through ENSO-induced SST anomalies in the Indian Ocean, which in turn modulate interannual variability of rainfall over Africa. An atmospheric general circulation model suggests that the Indian ocean sea surface temperature (SST) exerts a greater influence over the East African short rains than the pacific (Goddard and Graham 1999).Empirical studies also find that the short rains correlate strongly with SST in the western Indian ocean (Mutai et al.1998; Nicholson 1997; Ogallo et el.1988), suggesting that Indian Ocean SST is a major contributor to the variability of the short rains. A potential candidate for short rain variability is the Indian ocean zonal mode (IOZM), sometimes referred to as the Indian ocean dipole (Saji et el).It is preferred to use the term IOZM as it matches the out-of-phase development of the SST extrema in the east and west Indian ocean, consistent with the physics

suggested by Webster et el. (1999).The term dipole, on the other hand, suggests simultaneous variation in the east and west. The positive IOZM is characterized by a reversal of the east-west equatorial gradient in SST across the Indian Ocean, with warmer than normal water along the equatorial east coast of Africa and cool water near Sumatra. The negative anomalies in the east tend to lead the positive western anomalies. This mode appears to have a complicated relationship with ENSO, occurring at times of ENSO extrema and at other times when the Pacific Ocean was not anomalous (Reason et al.2000; Webster et al.1999; Saji et al.1999).

We conclude from Mode (2) and (3) (sub sections 4.6.1 During the cold phase of ENSO (La Niña) condition, positive IOD and N-S contrast of the Atlantic oceans, the southern part of Ethiopia didn't not receive ample rainfall during its short rainfall season (SON). However, SON is one of the main rainfall season of the region, it faces problem of abnormal rain during the same season. This below normal rainfall may also cause drought over the area Fig. 4.28a .The composite wind vectors that showed divergence over south Ethiopia fig 4.28b, the deficient moisture of the composite specific humidity patterns, the positive (suppressed convective) of the composite OLR pattern and the dry condition of the precipitation together show how the conditions of the tropical oceans SST modulation affect the climate variability of the southern part of Ethiopia fig. 4.28.

From sub-section 4.6.3 the central warm phase of the Pacific Ocean and the N-S tropical mode of Atlantic Ocean together with enhanced Atlantic and opposing Indian cause the N-W part of Ethiopia to have above normal MAM rainfall.

We can conclude from sub-section 4.6.4 that the main big rainfall season of the southern part of Ethiopia is challenged by the N-S tropical modes of pacific and Atlantic oceans. During the N-S tropical modes of the Atlantic and pacific oceans the southern part of Ethiopia did not receive much rainfall fig 4.35e.

The wet minus dry composite MAM season precipitation are used to plot the composite structures of atmospheric circulation and tropical oceans SSTs as shown in fig 4.37.The composite SST structures of fig 4.37a for MAM precipitation Mode (1) show the positive IOD pattern of the Indian ocean and the tropical N-S mode of the pacific ocean together with the atmospheric circulation cause South Ethiopia to receive over normal MAM rainfall fig 4.37.Therefore during the positive IOD condition, the Ethiopia MAM climate affected positively (ample rainfall is received by the region) which may also cause flood. The ample moisture of the specific humidity pattern, the enhanced convective of the OLR and the wet precipitable water pattern together with the negative IOD and the N-S tropical mode of the Pacific Ocean are the cause for the above normal condition of rainfall over south Ethiopia. During this condition the Atlantic Ocean exhibits

a normal warm pool. The overturning atmospheric circulations and Atlantic SST North-south dipole are the causes for the ample rainfall over Southern Ethiopia.

Tropical oceans are shown contributing to climate, hydrology and vegetation variability. Tropical oceans SST anomalies contribute 50%, 51.6% and 53.5% to precipitation, vegetation and Awassa lake level variability respectively during SON season and 24.2% and 41.9% to precipitation and vegetation, respectively during MAM season but have no significant contribution to MAM season of Awassa Lake level. And tropical oceans heat content contributes 59% and 85.6% to precipitation and vegetation variability over southern Ethiopia during SON season with small significance during MAM season.

6.2 Recommendation

The findings of this research are the spring board in monitoring and predicting the extremes of climate, vegetation and hydrological variability. The people at large, environmental, hydrological and atmospheric institutes can be benefited from appropriate use of the knowledge obtained from this research finding in controlling the impacts of extreme variability such as drought and flood in the area in point. On top of this we would like to recommend that the future research in physics should solve social, economic, development hindering systems and all of us should put our finger prints on these issues.

References

1. Anyah R.O. and F.H.M.Semazzi; 2005: Climate Variability over the Greater Horn of Africa based on NCAR AGCM ensemble. *Theor. Appl.Climatol*.000.1-24

2. Atheru, Z.K.K. and C.Mutai; 2002: Climate Variability in Eastern Africa; its causes and relationship to ENSO. *Drought Monitoring Centre, Nairobi* (DMCN)

3. Black E.; 2003: The impact of Indian and Pacific Ocean processes on the East African Short rains.*Clivar-Exchanges* 27:1-4

4. Black E., J.Slingo, and K.R.Sperber; 2003: An observational study of the Relationship between Excessively Strong Short Rains in Coastal East Africa and Indian Ocean SST.*Mon. Wea. Rev*., 131, 74-94

5. Barth, A.; 2004: Assimilation of Sea surface temperature and sea surface height in a two-way nested primitive equation model of the Ligurian Sea. PhD Thesis.

6. Behera, S.K., R.Krishnan and T.Yamagata, 1999: Unusual Ocean-Atmosphere conditions in the tropical Indian Ocean during 1994.*Geophy.Res.Lett*.26, 3003-3004

7. Behera, S.K., and T.Yamagata, 2002: Impacts of the Indian Ocean Dipole on the Southern Oscillation. *Accepted by J.Met.Soc.Japan*.

8.Behera S.K.,J.Luo,S.Masson,T.Yamagata,P.Deleclise,S.Gualdi,A.Navarra;2003:Impact of the Indian ocean on the East African short rains. CGCM study.*CLIVAR-Exchanges*. 27:1-4

9. Bekele, F., 1992: The Effect of Southwest Indian Ocean Cyclones on Belg and Kiremt. NMSA mimeo. *Addis Ababa, Ethiopia*: NMSA.

10. Bekele, F., 1993: *Probability of Drought Occurrence under Different Events.* NMSA mimeo. Addis Ababa, Ethiopia: NMSA

11. Bekele, F. 1997: Ethiopian Use of ENSO Information in Its Seasonal Forecasts, Internet Journal of African Studies. No. 2. March.

12. Bigg, G.R, T.D.Jikells, P.S.Liss and T.J.Osborn; 2003: The role of the oceans in climate.*Int.j.Climatol*.23:1127-1159.

13. Clark, C.O., P.J.Webster and J.E.Cole; 2003: Interdecadal changes in the relationship between Indian ocean SST and East African Coastal rainfall.J.Clim.16:548

14. Chang P.; 1998: The Atlantic Ocean: Unusual tropical Atlantic Ocean temperatures cause climate swings in Brazil and West Africa. *The ocean and global climate*.6:2

15. Disaster Prevention and Preparedness Commission (DPPC).Early System Report.1998 Belg Production and Food Prospects, August, 1998.

16. Donlon, C.J., 2002: GHRSST-PP Data Product Specifications v2.0.Technical report, GODEA Height Resolution Sea Surface Temperature Pilot Project, GHRSST-PP Reference Document GHRSST/10, http:ghrsst-pp.org.

17. Goddard, L., and N.E.Graham; 1999: Importance of the Indian Ocean for simulating Rainfall anomalies over eastern and southern Africa.*J.Geo.Res. 104, 19099-19116*

18. Haile, T., 1988: Causes and characteristics of drought in Ethiopia. *Ethiopian Journal of Agricultural Science*, 10, 85-97.

19. Han W.Q., P.J.Webster; 2002: Forcing mechanisms of sea level interannual variability in the Bay of Bengal *Phys Oeanogr* 32:21239.

20. International Research Institute of Climate system; 2006: IRI climate Digest.

21. Indeje M., F.H.M. Semazzi, L.J.Ogallo; 2000: ENSO signals in East African Rainfall Seasons.*Int.J.Climatol*.20:19-46.

22. IRI report to USAID, 2005

23. Krishnamurti, T.N., and M.Kanamitsu; 1981: Northern summer planetary-scale monsoons during drought and normal rainfall months. Monsoon Dynamics, 19-48.

24. Latif M, D.Dommenget, M. Dima, and A.Grotzner A, (1999): The Role of Indian Ocean Sea surface temperature in forecasting East African Rainfall anomalies during December-January 1997/98. *J climate* 12:3497-3505

25. Latif M., A.Grotzner; 2000: The equatorial Atlantic Oscillation and its response to ENSO.Climate *Dynamics* 16:213-218.

26. Li T., Y.Zhang, E.Lu, D.Wang; 2002: Relative role of dynamic and thermodynamic processes in the development of the Indian Ocean dipole: an OGCM diagnosis.*Geophys Res Lett* 29(DOI: 10.1029/2002 GL 015789)

27. Marshall J., Y.Kushnir, D.Battisti, P.Chang, A.Czaja, R.Dikson, J.Hurrel, M. McCartney, R.Saravanan and M.Visbeck; 2001: North Atlantic variability; Phenomena, Impacts andMechanisms.*Int.J.climatol*.21; 1863-1898.

28. McCrery J.P., D.T.Anderson; 1984: Simple models of the El Nino and Southern Oscillation. *Mon. Weather. Rev* 112:934-946.

29. Murtugudde R.G., J.P.McCreary, A.J.Busalchi; 2000: Oceanic processes associated with anomalies events in the Indian Ocean with relevance to 1997-1998. *J Geophys Res* 105:295-3306.

30. Mutai C.C. and M.N.Ward, and A.W.Coman; 2000: East African rainfall and the tropical circulation/convention on intra-seasonal to interannual time scales. *J Climate*3:3915-3939

31. Nicholson S.E. 1996: A review of climate dynamics and climate variability in Eastern Africa. In: the limnology, Climatology and Pale climatology of the East African Lakes (Eds T.C.JOHNSON and E.ODADA).*Gordon and Breack, pp.25-56.*

32. Nicholson, S. E., and J. Kim, 1997: The Relationship of the El Nino Southern Oscillation to African Rainfall. *Int. J. Climatol.*, 17, 117-135

33. NMSA. Early Warning System Report, November 1997.The impact of Abnormal Weather in 1997.

34. NOAA a, (National Oceanic and Atmospheric Association), 2004, ENSO background and Description, Retrieved October 10, 2004 from http://www.cdc.noaa.gov/ENSO/enso.description.html

35. NOAA b, (National Oceanic and Atmospheric Association), 2004, El Nino theme Page, Retrieved October 10,2004from http://www.pmel.noaa.gov/tao/elnino/el-nino-story.html

36. Ogallo, L.J., 1988: Relationship between seasonal rainfall in East Africa and Southern Oscillation.*J.Climatol*., 8, 34-43

37. Okumura Y., S.-P.Xie, A.Namaguti, and Y Tanimoto; 2001: Tropical Atlantic air-sea interaction and its influence on the NAO.*Geophys, Res.Lett.28, 1507*-1510.

38.Orlove B.S.,J.L.Tostesone;1996:The application of seasonal to interannual climate forecasts based on El Niño-Southern Oscillation(ENSO) events: Lessons from Australia,Brazil,Ethiopia,Peru,and Zimbabwe.

39. Philander, S.G.H.., 1990.El Niño, La Nina and Southern Oscillation. *Academic Press, San Diago*, CA, 289pp.

40. Rajagolapan B., Y.Kushinir, and Y.M.Toure; 1998: Observed decadal midlatitude and tropical Atlantic climate variability.*Geophys.Res.Lett.* 25:3967-3970

41. Rao A.S., S.K.Behera, Y.Masumoto, T.Yamagata; 2002: Interannual Variability in the subsurface tropical Indian Ocean. *Deep-Sea Res II* 49:1549-1572.

42. Reason, C.J.C., R.I.Allan, J.A.Lindesay, and T.J.Ansell, 2000: ENSO and Climatic signals across the Indian Ocean basin in the global context: part I, Interannual composite patterns.*Int.J.Climatol*. 20, 1285-1327.

43. Robertson A.W., C.R.Mechoso, and Y.-J.Kim; 2000: The influence of Atlantic sea surface temperature anomalies on the North Atlantic Oscillation.*J.Clim*., 13:122-138.

44. Robertson, A.W., C.Farara, and C.R.Mechoso; 2003: Simulations of the Atmospheric response to South Atlantic Sea surface temperature anomalies.*J.clim*. 16:2540-2551.

45. Rowland, J., A.Nadeau, J.Brock, R.Klaver, and D.Moore; 1996: Vegetation Index foe Characterizing Drought Patterns. Raster Imagery in Geographic Information Systems. *Santa Fe, New Mexico, Onward Press, pp.247-254.*

46. Saji N.H., B.N. Goswami; 1996: An improved linear model of tropical surface wind variability *J R Metreorol Soc* 122:23-54

47.Saji,N.H.,B.N.Goswami,P.N.Vinyachandra and T.Yamagata,1999:A dipole mode in the tropical Indian Ocean,*Nature,401,360-363*.

48. Saji N.H., and T.Yamagata; 2003: Indian Ocean dipole mode events and African rain variability.*CLIVAR-Exchanges* 27:1-4

49. Saji, N.H., and T. Yamagata; 2003.Possible impacts of Indian Ocean dipole mode events on global climate.*Clim.Res*.25, 151-169.

50. Saji N.H., Yamagata T ;(2003): Structure of SST and surface wind variability during Indian Ocean Dipole Mode years: COADS observations.*J Clim* 16:2735-2751.

51. TsegayeWolde-Georgis.1997.El Nino and Drought Early Warning in Ethiopia. *Internet Journal of African Studies,* No 2.march. http://www.brad.ac.uk/research/ijas/ijasno2/ijasno2.html

52. Tsegaye Wolde-Georgis: The impacts of cold events on Ethiopia. A la Nina Summit

53. Vinyachandrin P., N.Iizuka, and T.Yamagata, 2002: Indian Ocean Dipole mode events in an ocean general circulation model.*Deep.Sea Res*.49B:1573-1596

54. Vinayachandran P.N., N.H. Saji, T.Yamagata; 1999: Response of the Equatorial Indian Ocean to an unusual wind event during 1994.*Geophys Res Lett* 26:1613-1616

55. Wallace J.M.and P.V.Hobbs; 1977: Atmospheric science 'An Introductory Survey'. By *Academic Press.*

56. Ward, M, and A.Yeshanew; 1990: World wide sea surface temperature and kiremt rains in Ethiopia.NMSA momo.Addis Ababa, Ethiopia: NMSA

57. Watanable, M., and M.Kimato; 1999: Tropical-extra tropical connection in the Atlantic atmosphere-ocean variability.*Geophys.Res.Lett*. 26:2247-2250.

58. WCRP; 1999.A strategy for climate research in Africa .World climate Research Programme, CLIVAR.WRCP. Report 16/1999P. ICPO publication series 29.

59. Webster P.J., Moore A.M., Loschnigg P.J., Leben R.R.; 1999: Coupled ocean-atmosphere dynamics in the Indian Ocean during 1997-1998.*Nature*, 401,356-360.

60. Wick, G.A., 2002: Infrared and microwave remote sensing of sea surface temperature. Seminar at the University of Colorado at Boulder "Remote Sensing Seminar" graduate course.

61. Wold-Georgis; 2000: The case of Ethiopia "Reducing the Impacts of Environmental Emergencies through Early Warning and Preparedness: The case of the 1997-97 El Nino"

62. Xie, S.-P., and A.Tanimoto; 1998: A pan-Atlantic decadal climate oscillation.*Geophys.Res.Lett*. 25:2185-2188.

63. Yamagata T., S.K.Behera, S.A.Rao, Z.Guan, K.Asok, and H.Saji.2002a: The Indian Ocean Dipole: a physical entity *Clivar Exchanges* 24, pp 15-18, 20-22.

64. Yamagata T., S.K.Behera, S.A.Rao, Z.Guan, K.Asok, and H.Saji.2002b: Comments on the Indian Ocean Dipole (*submitted to Bull.Amer.Met.Soc.)*

65. Yamagata T, S.K.Beherai, J.Luo, S. Masson, M.R.Jury, and S.A.Rao, 2004: Coupled Ocean-Atmosphere Variability in the Tropical Indian Ocean *Am. Geophys. Union* 10.1029

66. Yeshanew A (2003) Mechanisms and prediction of climate variability in tropical North African. PhD thesis, University of Zululand (South Africa), pp 546

67. Yeshanew A and M.R.Jury, 2006: North African Climate Variability. Part 1: Tropical thermo cline coupling. *Theor. Appl. Climatol.*

68. Yeshanew A and M.R.Jury, 2006: North African Climate Variability: Part 2: Tropical circulation system. *Theor Appl. Climatol*.

69. Yeshanew A and M.R.Jury, 2006: North African Climate Variability: Part 3: Resource prediction. *Theor Appl. Climatol*

70. IRI Climate Digest: 2006: Climate Impacts-August.

DECLARATION

I the underlined declare that this Thesis is my original work and has not been presented for any degree in any University and all the resources of materials used for the Thesis have been duly acknowledged.

Name: Mesfin Tadewos Dubale

Signature: _____

This Thesis has been submitted for examination with my approval as University advisor.

Name: Abebe Yeshanew (PhD)
(Advisor)

Signature: _____

Name: Gizaw Mengistu (PhD)
(Co-Advisor)

Signature: _____

Date and place of submission: Physics Department

Addis Ababa University

24 July 2007